



# 宇宙线的起源 LHAASO的核心科学目标之一



刘四明  
西南交通大学

LHAASO合作组

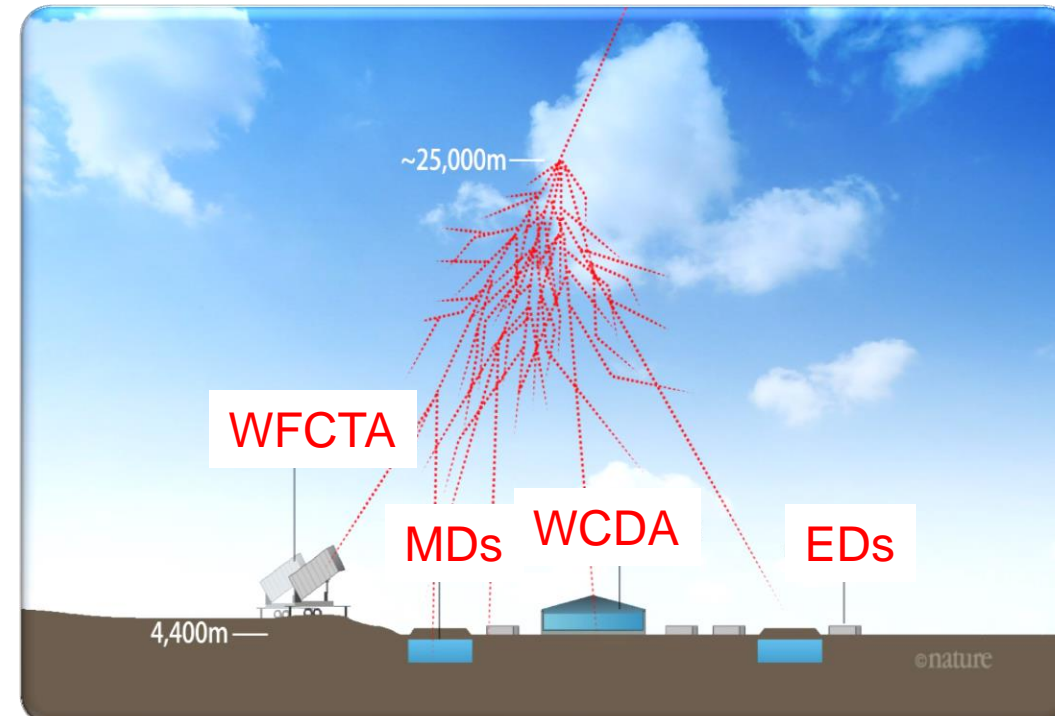


# Large High Altitude Air Shower Observatory

Electromagnetic Detectors (EDs)  
Muon Detectors (MDs)  
Water Cherenkov Detector Array (WCDA)  
Wide Field of view Cherenkov Telescope Arrays (WFCTA)

## Scientific Goals

- γ-ray astronomy
- Survey for sources (above 500 GeV)
- PeVatrons (above 100 TeV)
- All kind of sources: SNR, PWN, MYC, binary, pulsar
- AGN, GRB etc.
- Cosmic Ray Physics
- The knees
- Compositions : individual species H, He and Fe
- Anisotropy: (1 TeV to 10 PeV)
- New Physics Front: DM, LIV, etc.



# 什么是宇宙线？胡红波

**能量：导致空气电离（必要条件）**

进入大气的宇宙线和空气中的原子核很快的反应，产生大量短寿命的粒子并最后都衰变到稳定的粒子。

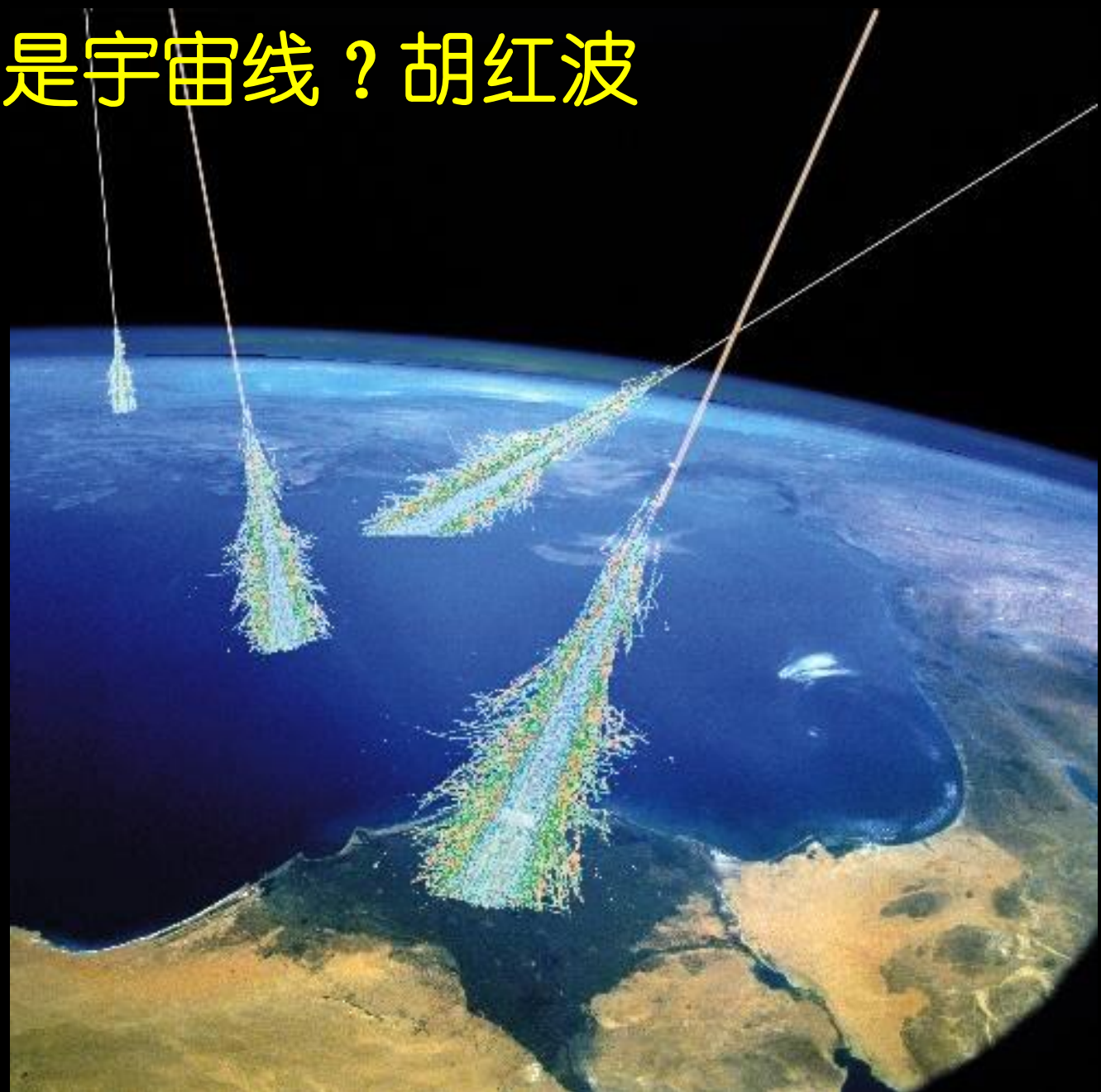
**起源：和核衰变对应产生的高能辐射对应来自大气层之外**

**物质粒子：引力波与电磁波对应**

宇宙线是来自宇宙空间的高能粒子流，是自动送上门来的宇宙深处的高能物质样品。

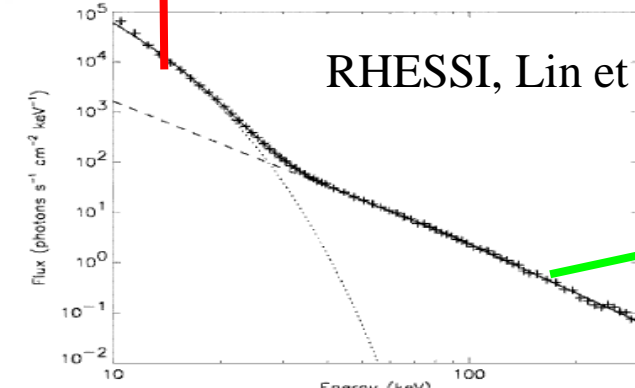
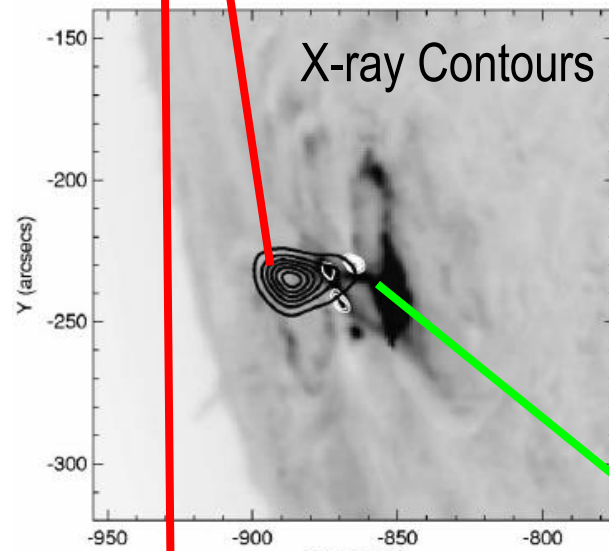
宇宙线中大部分是带电粒子，如：质子， $\alpha$ 粒子、铁核等等；还有少量的中性粒子如： $\gamma$ 光子、中微子等等。

宇宙线无处不在，我们人类浸泡在大量的宇宙线粒子中，例如每秒有数以万亿的中微子穿过我们的身体。暗物质粒子？



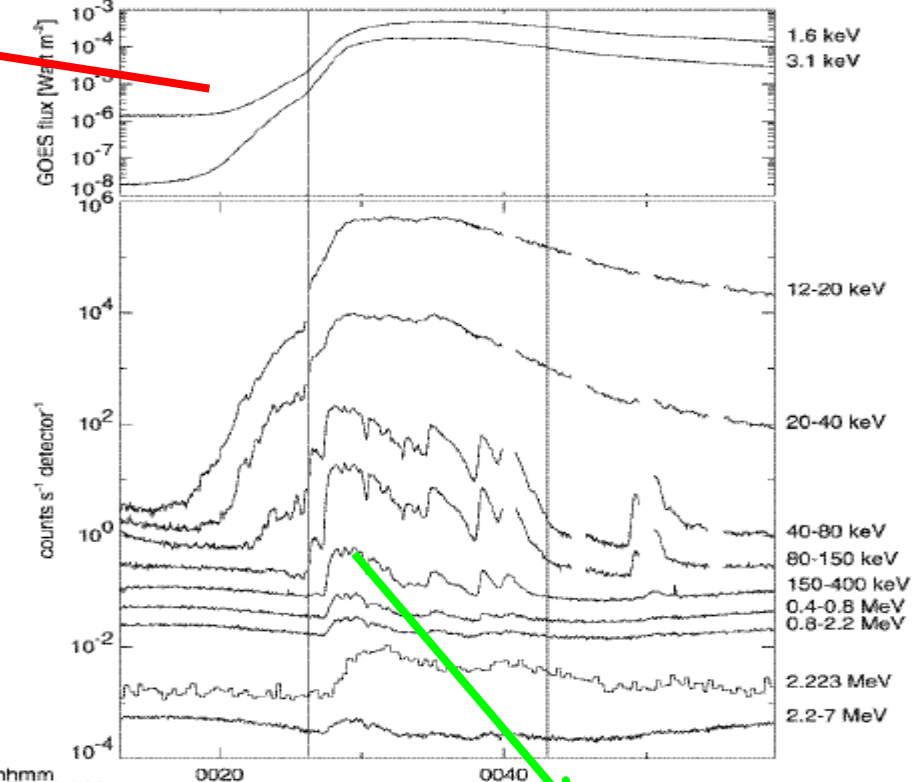
# 太阳耀斑

Low-energy: Gradual Thermal  
Coronal Source



X-ray Spectrum

X-ray Light curves



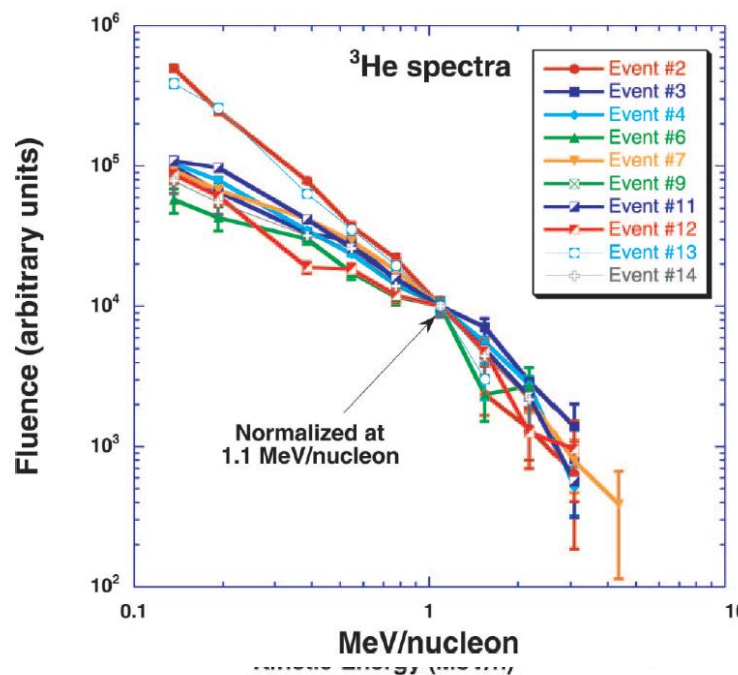
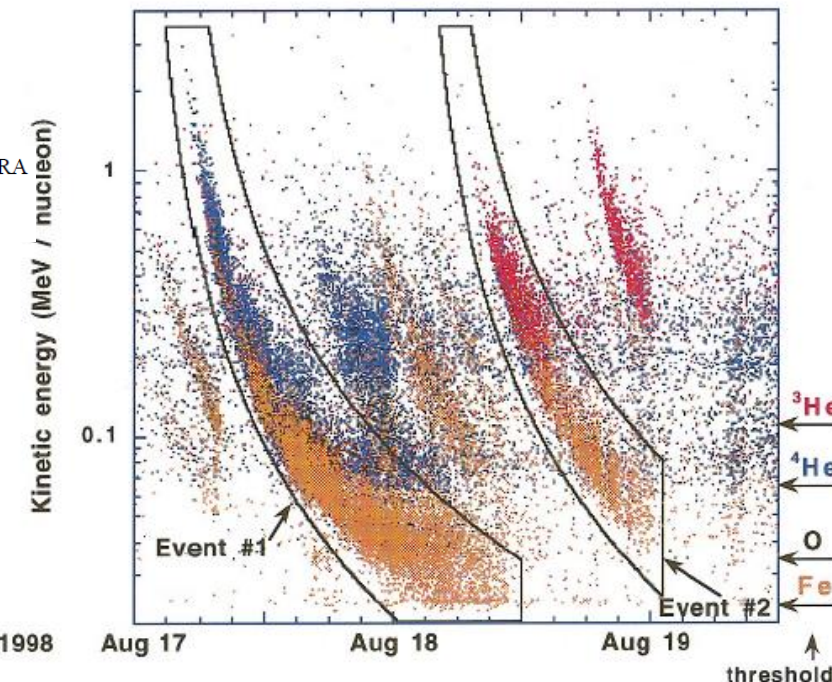
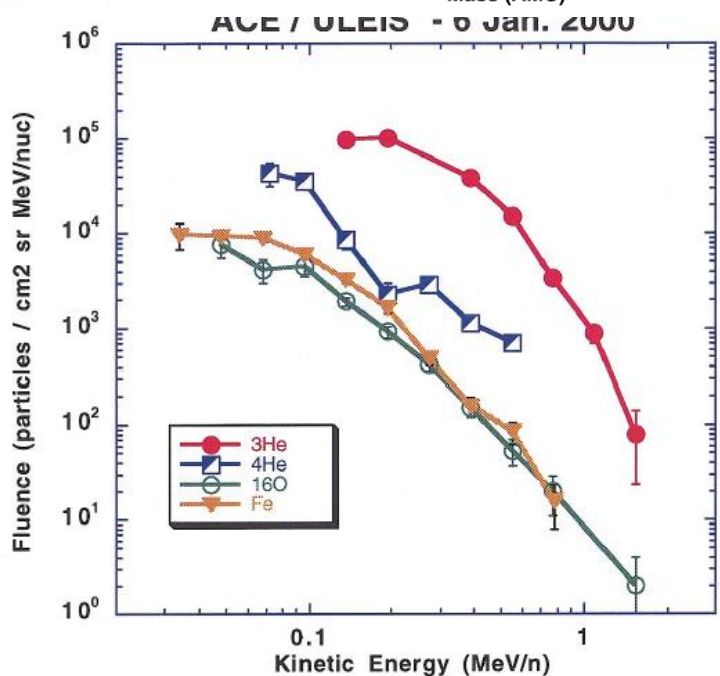
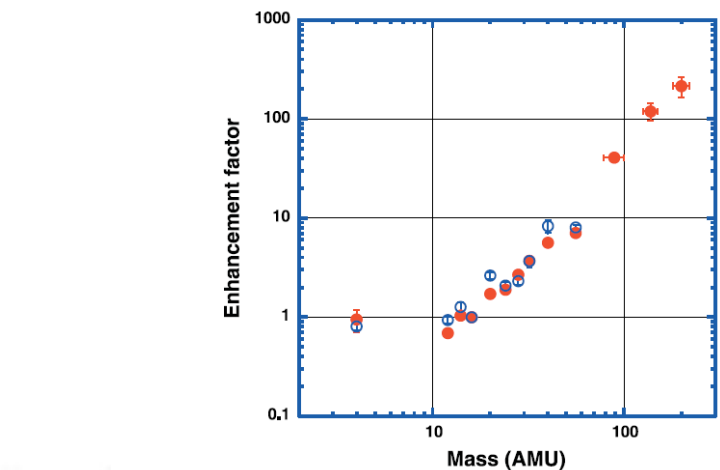
High-energy: Impulsive  
Non-thermal  
Chromospheric  
Footpoints

# 太阳高能粒子

NEW PROPERTIES OF  $^3\text{He}$ -RICH SOLAR FLARES DEDUCED FROM LOW-ENERGY PARTICLE SPECTRA

G. M. MASON,<sup>1,2</sup> J. R. DWYER,<sup>1,3</sup> AND J. E. MAZUR<sup>4</sup>

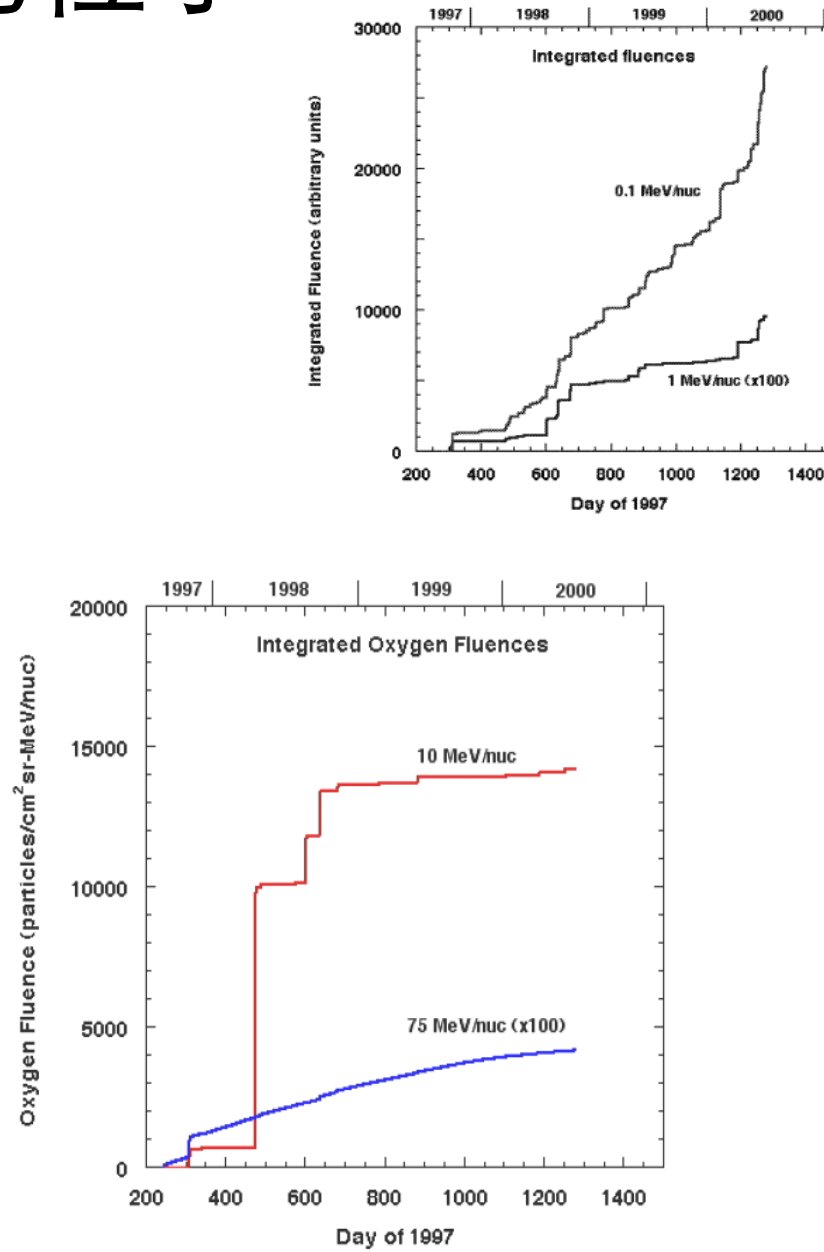
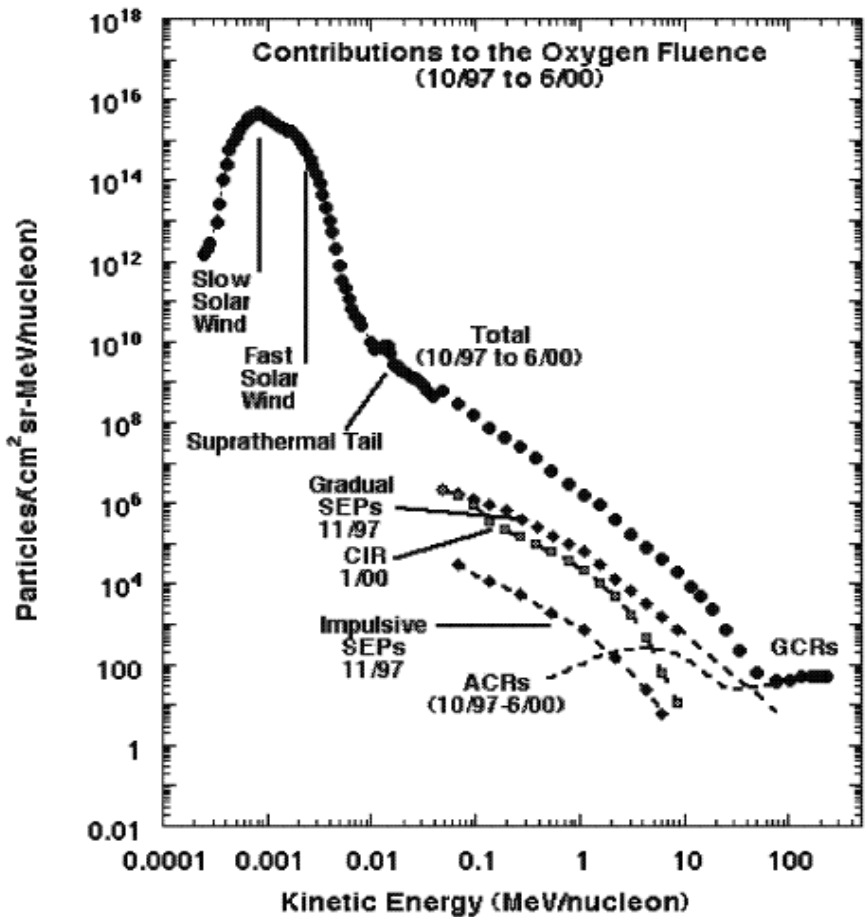
Received 2000 August 10; accepted 2000 October 16; published 2000 December 7

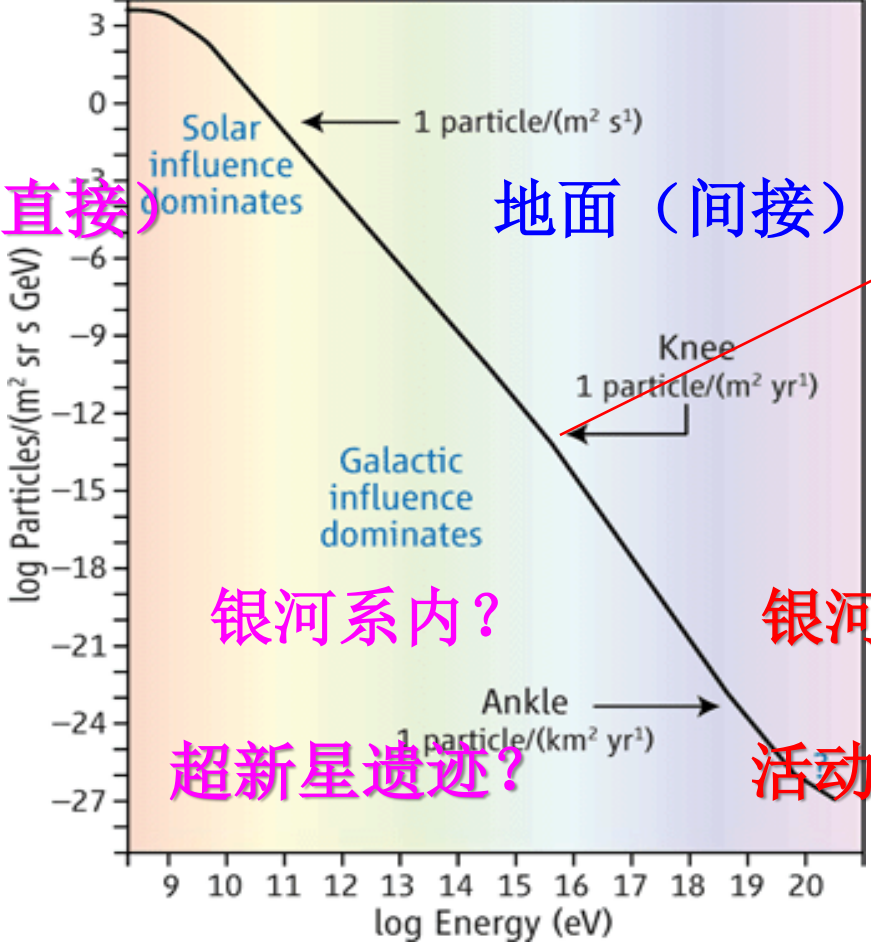
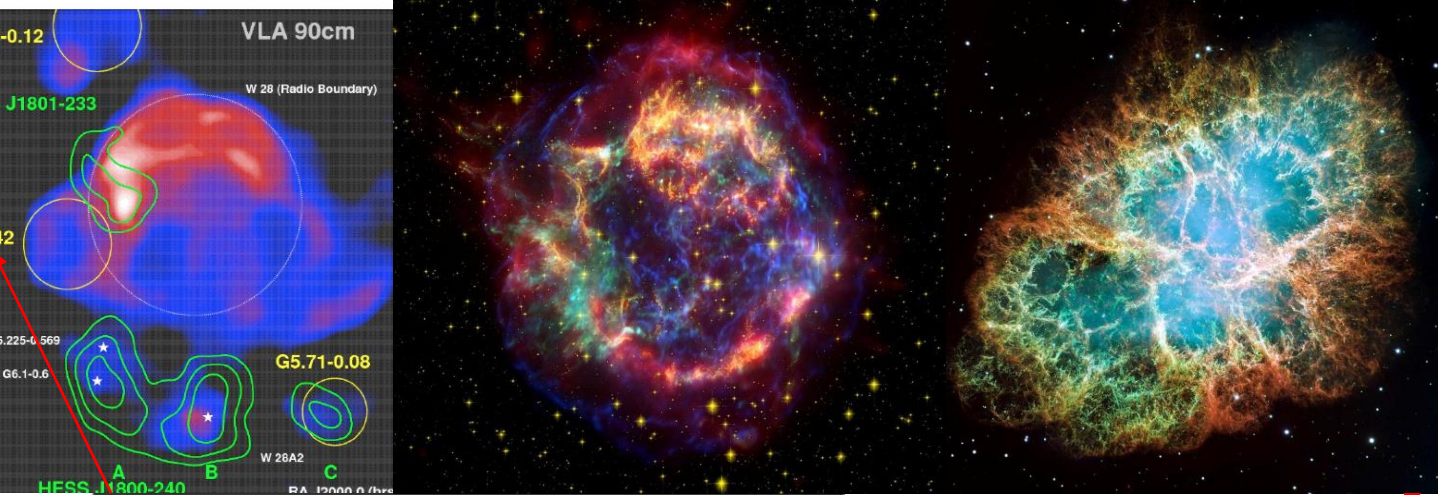
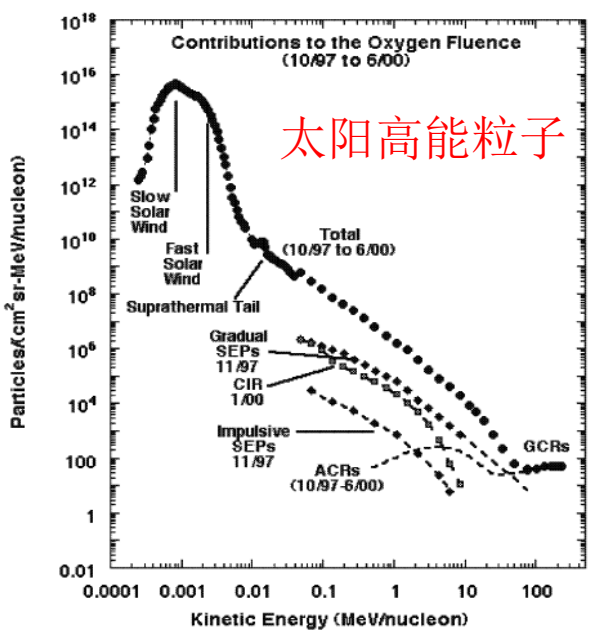


# 太阳高能粒子

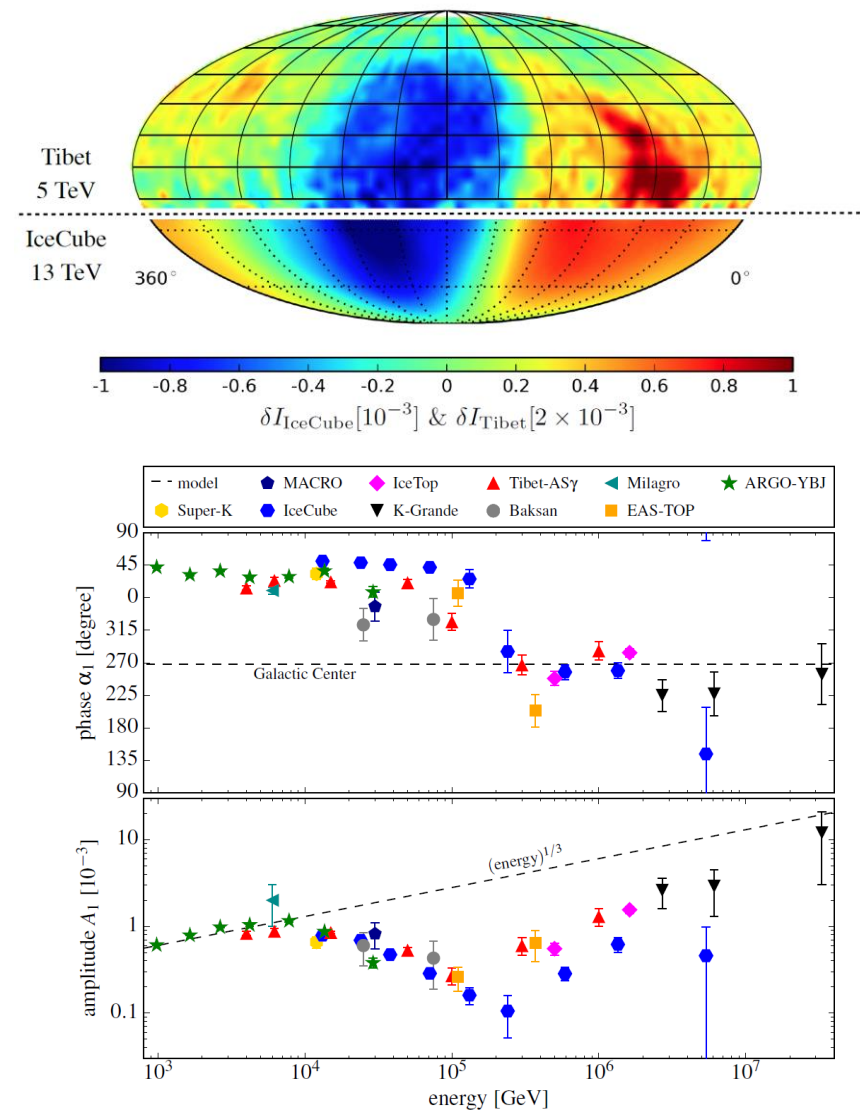
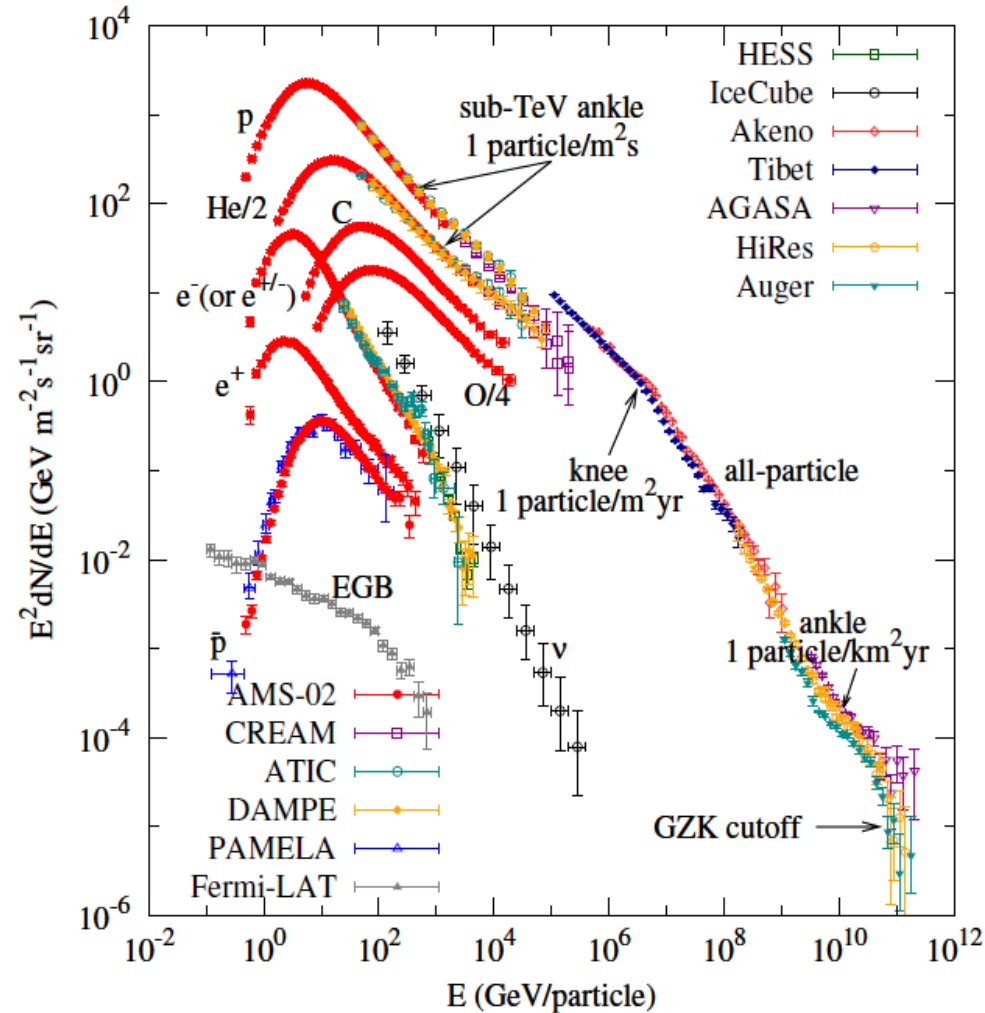
## Long-Term Fluences of Solar Energetic Particles from H to Fe

R.A. Mewaldt · C.M.S. Cohen · G.M. Mason ·  
D.K. Haggerty · M.I. Desai

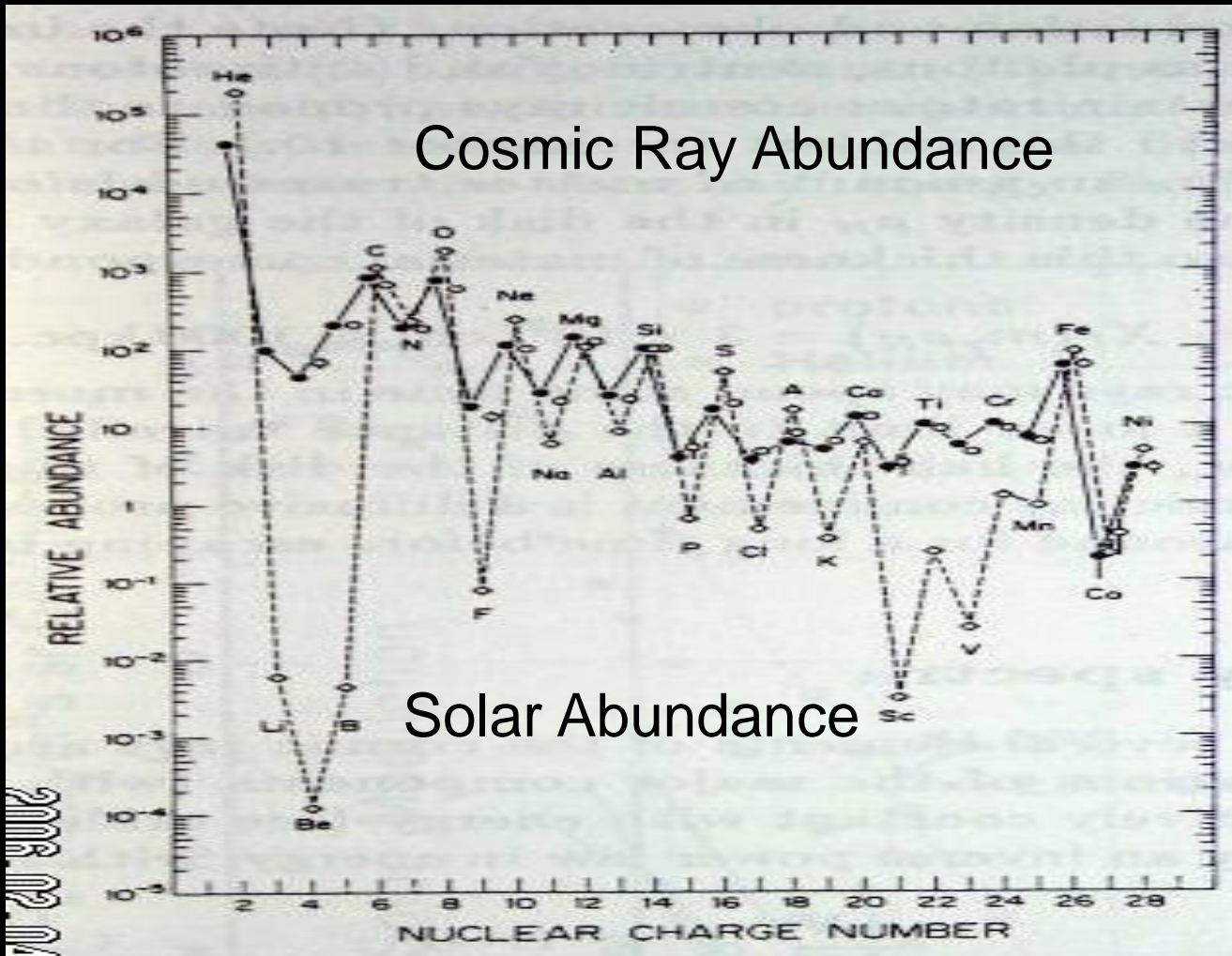




# 宇宙线的能谱和流量各向异性



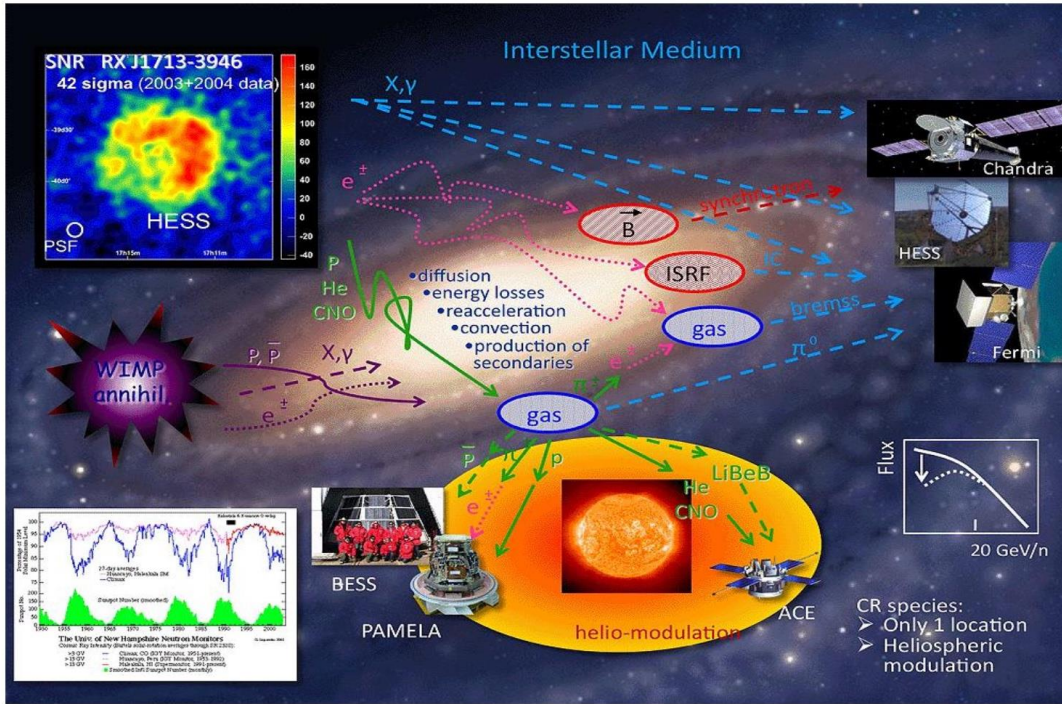
# Cosmic Ray Composition



From B/C flux ratio one has a grammage of  $\sim 10 \text{ g/cm}^2$ . For an ISM density of 1 per cc, the distance travelled by CR is about 10000kpc, corresponding to an age of  $\sim 10$  million years.

# General picture of Galactic cosmic rays

© I. V. Moskalenko



Acceleration at source

Diffusion and Interaction

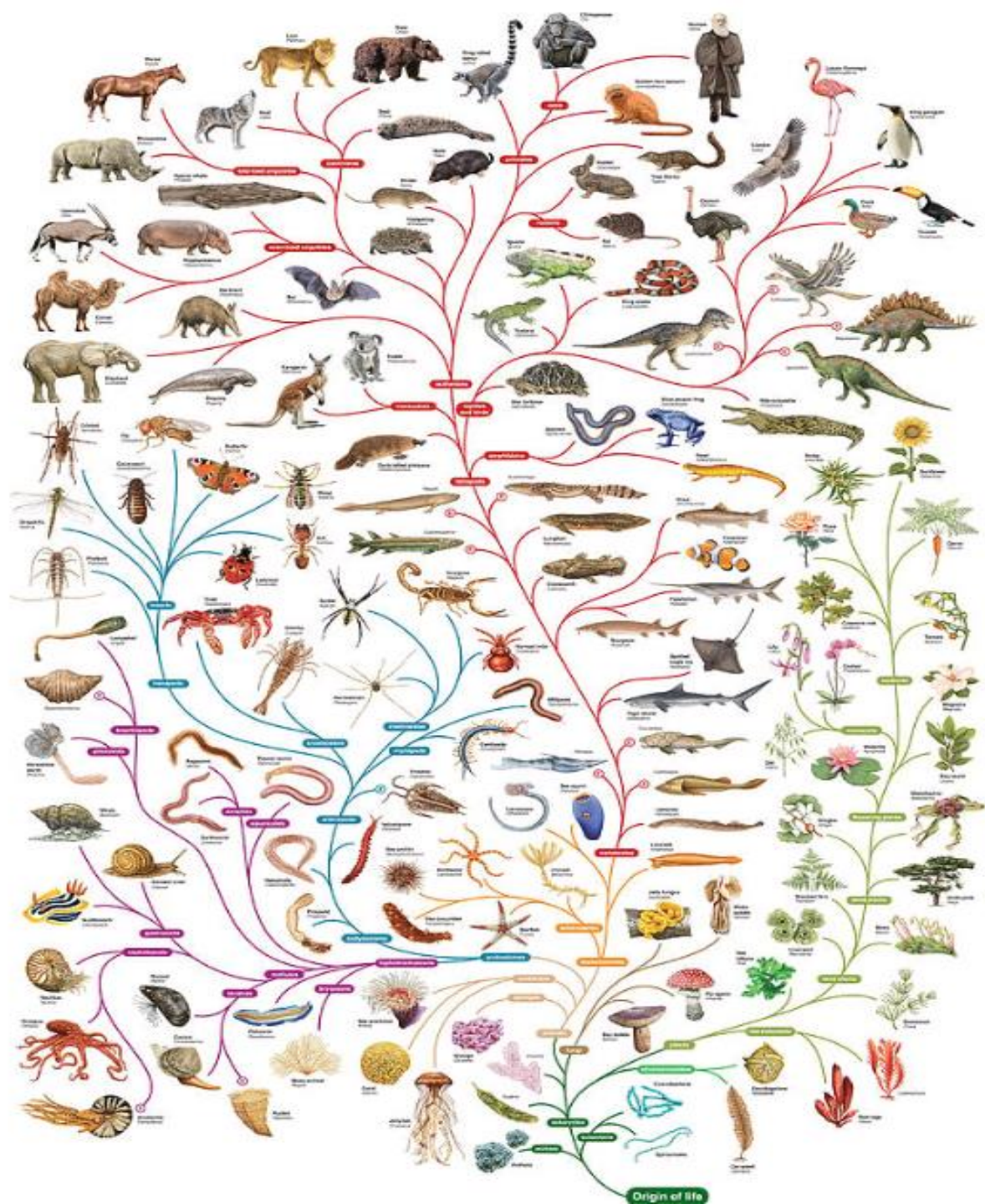
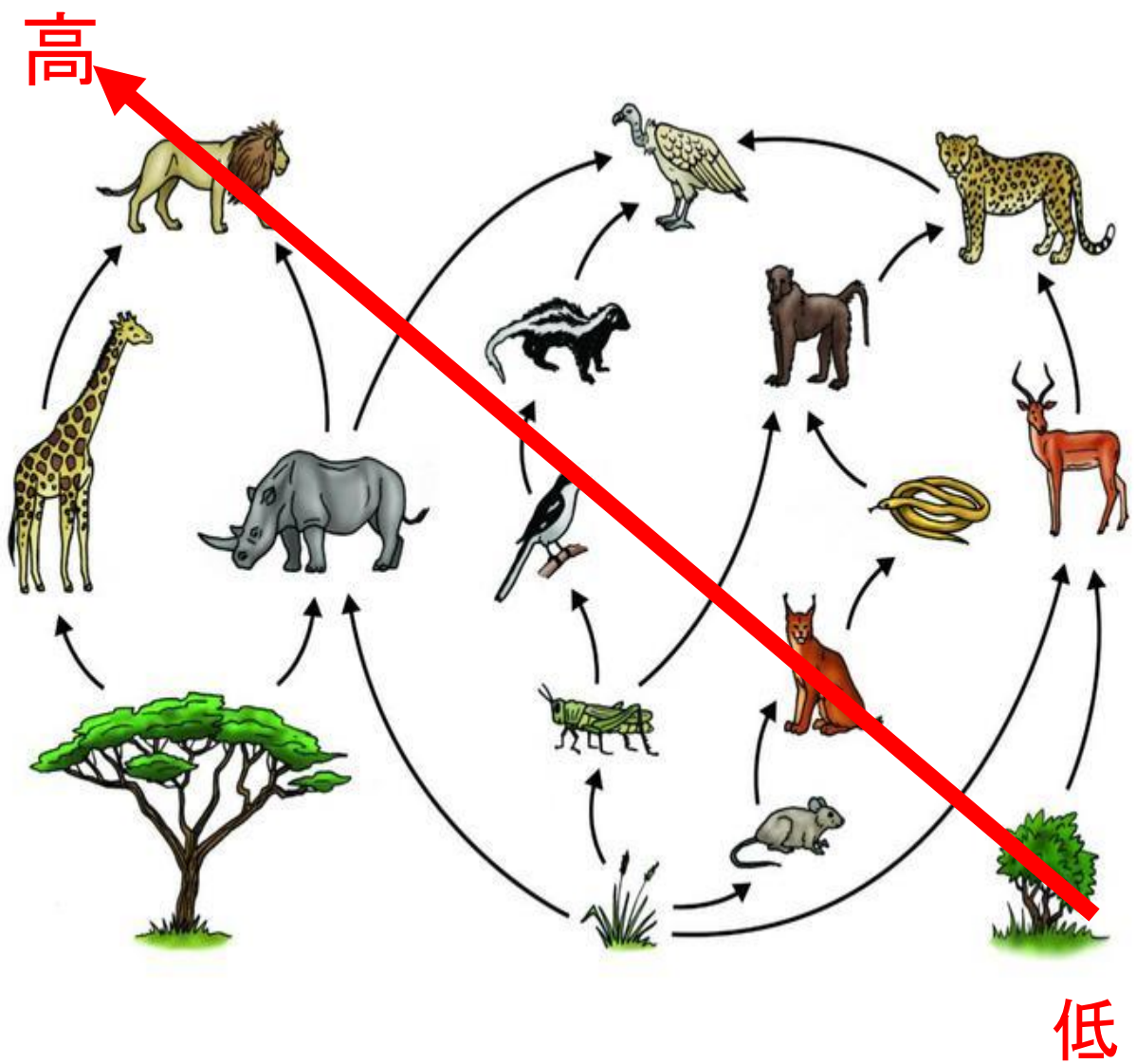
Helio-sphere propagation

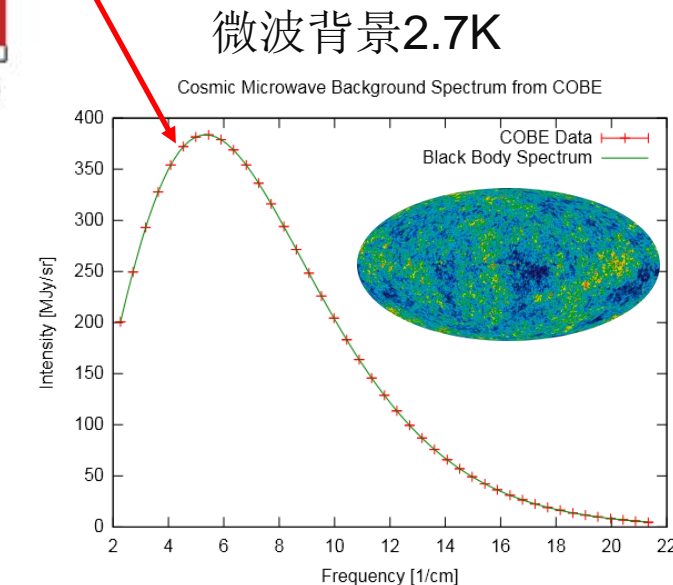
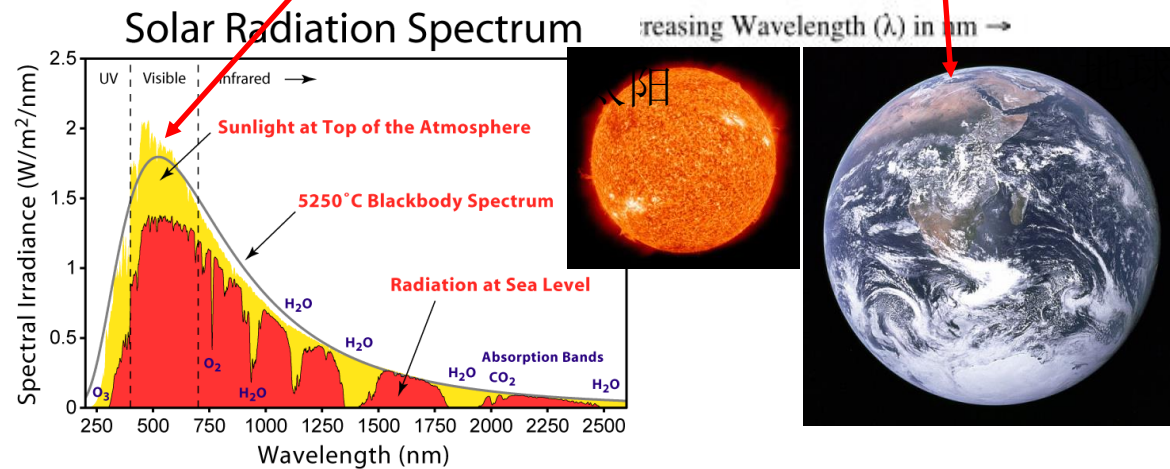
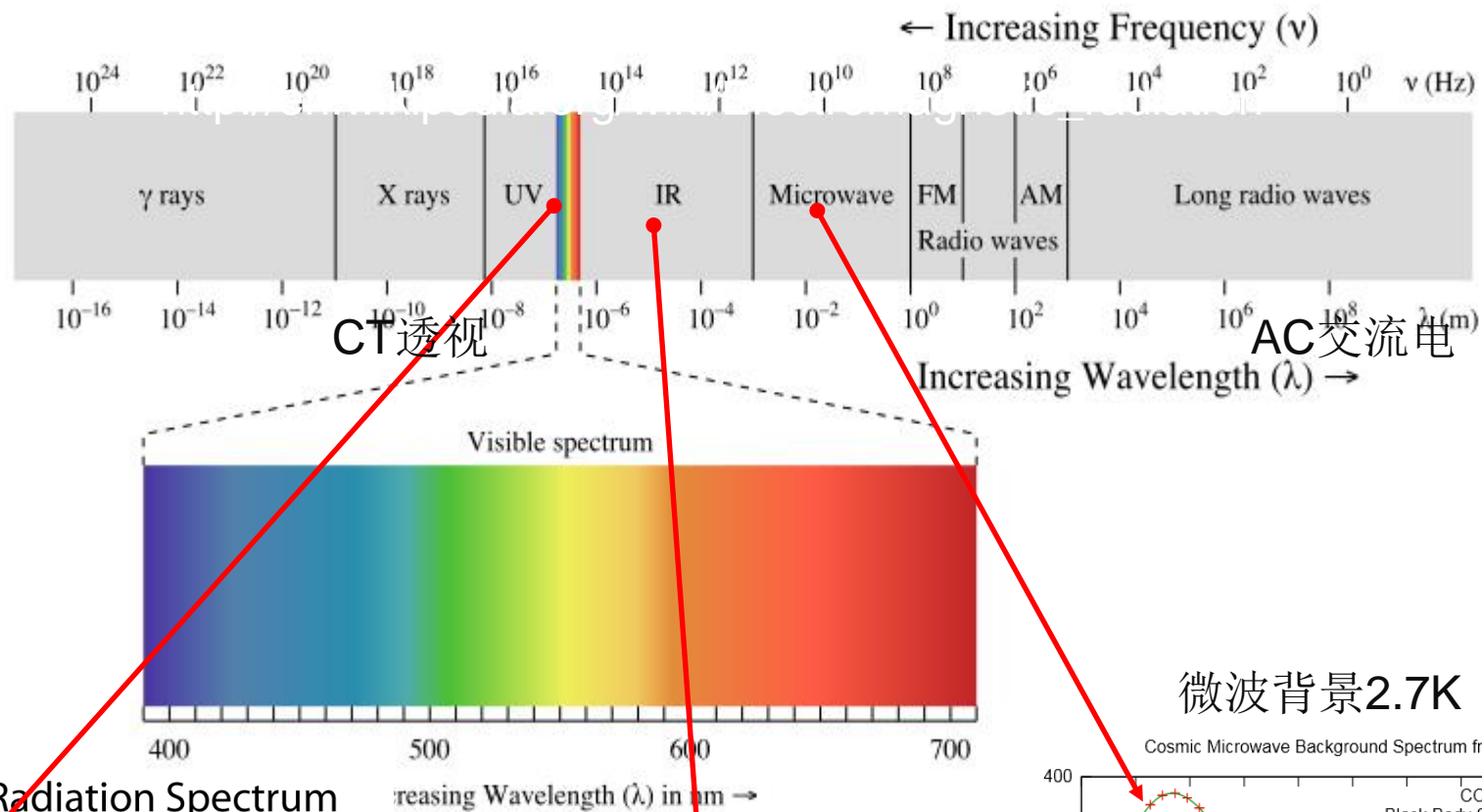
Detection at the Earth

Diffuse  $\gamma$  rays are expected *a priori* to be produced by CR interactions during the propagation, and are thus powerful probe of CR propagation

宇宙线的起源

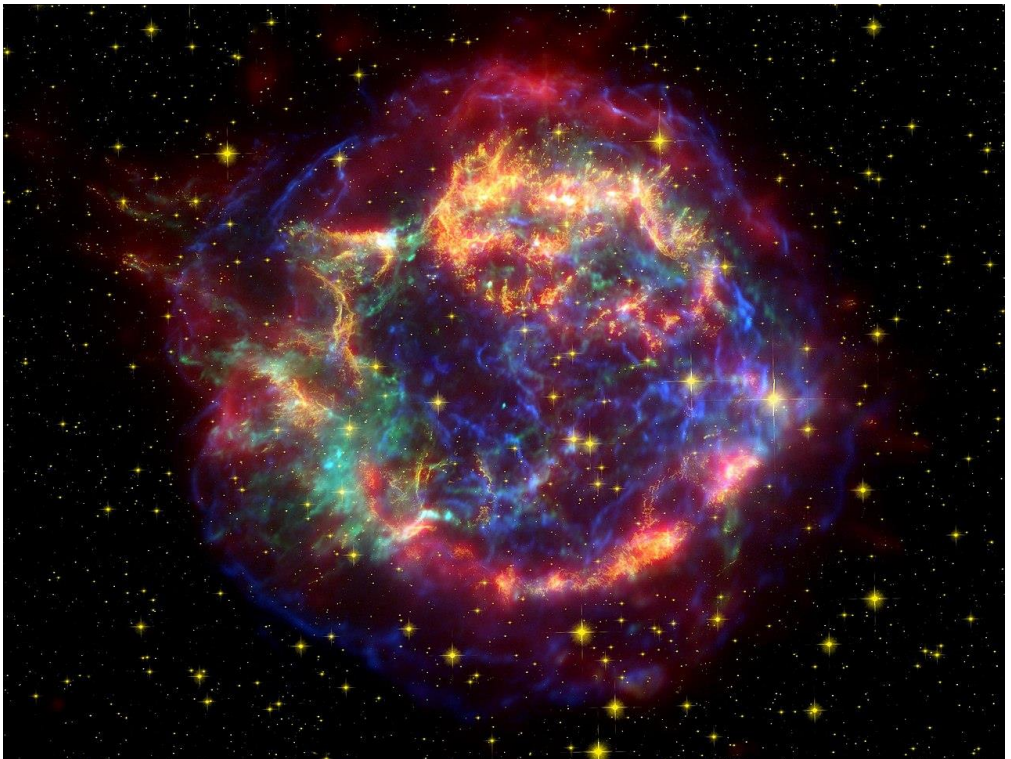
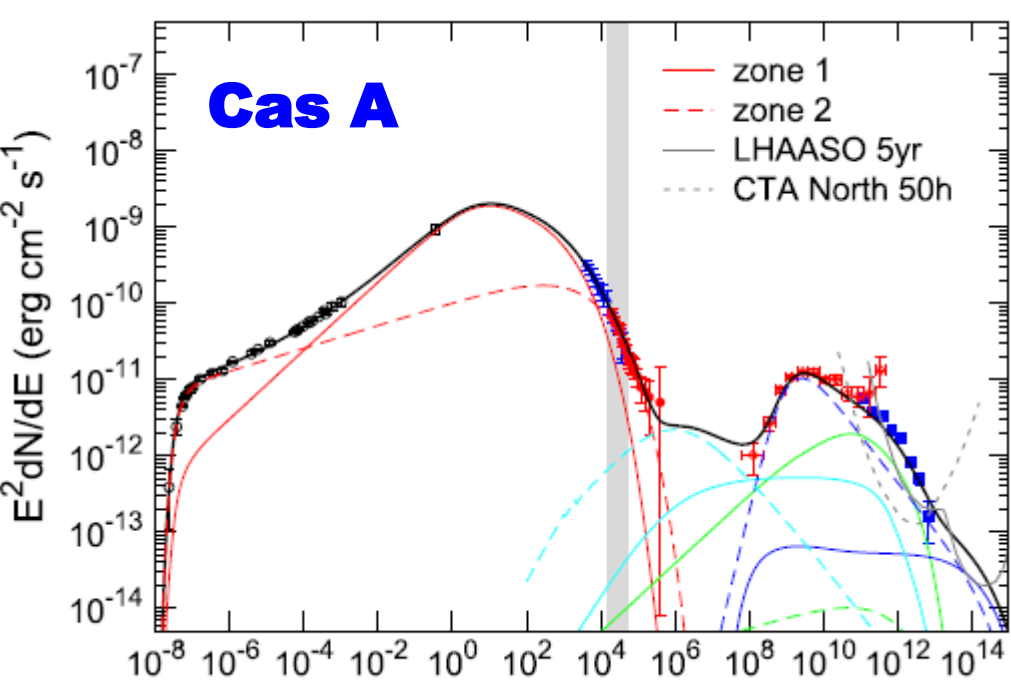
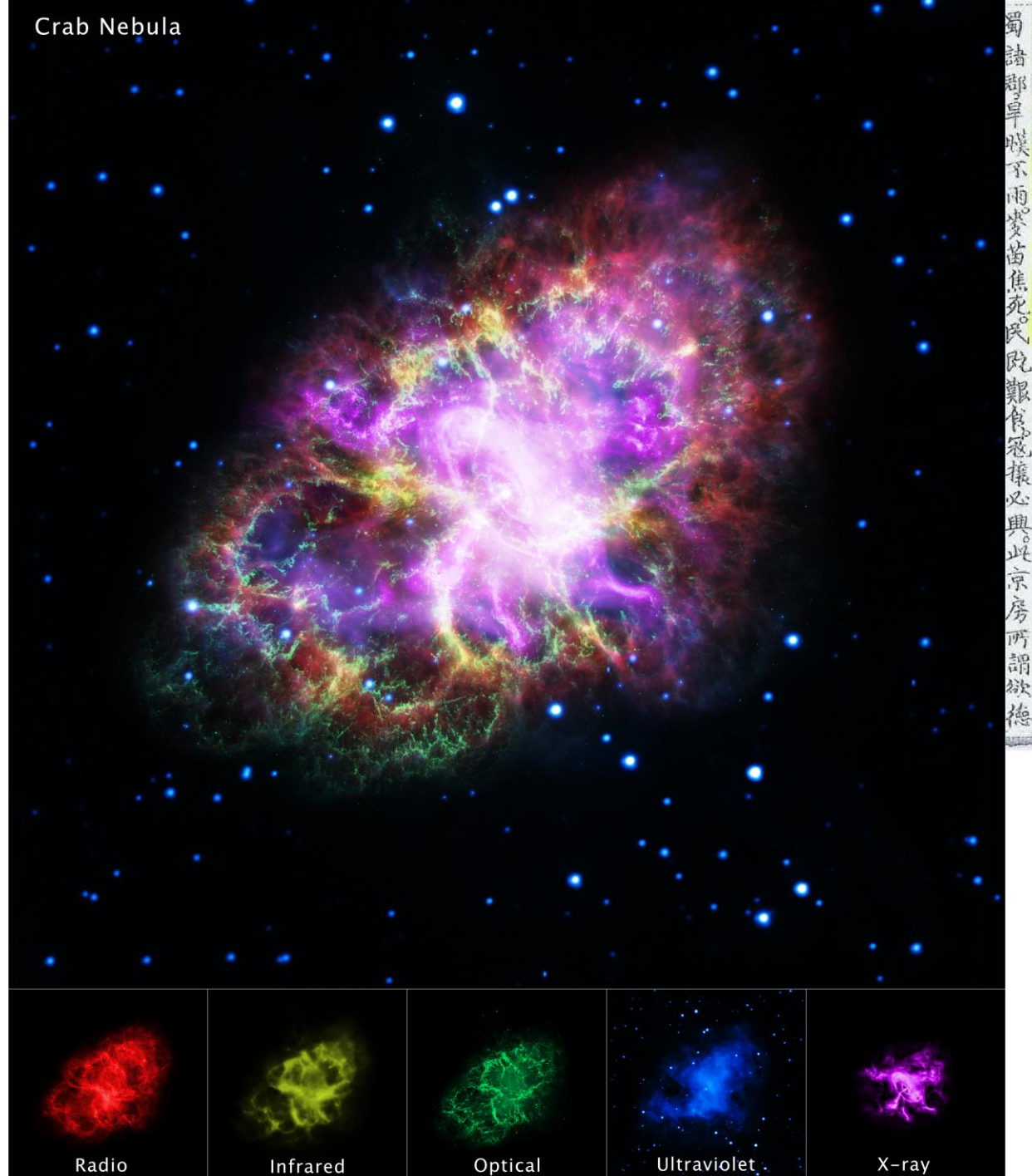
# 物种起源与食物链



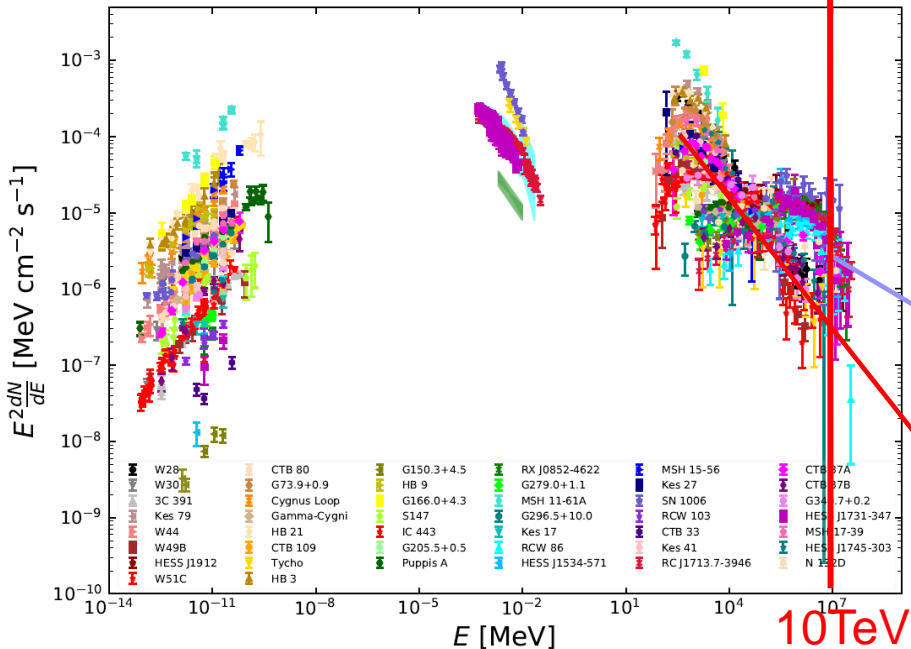


宋仁宗至和二年侍御史趙抃上言曰臣伏見自去年五月已來妖星遂見僅及周稔至今光耀未退此谷永所謂駢駢驟步芒炎長焰所懲奸犯其為譎變甚可畏也又去冬連今春京東西路及陝右川蜀諸郡旱曠不雨麥苗焦死民既艱食寇攘必興此京房所謂微德

蟹狀星云



# Origin of Cosmic Rays

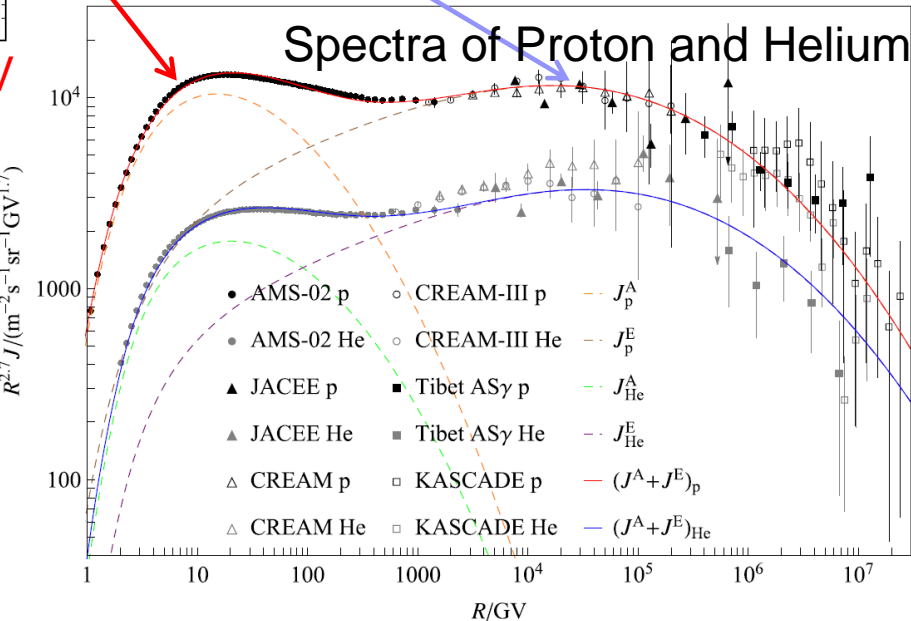
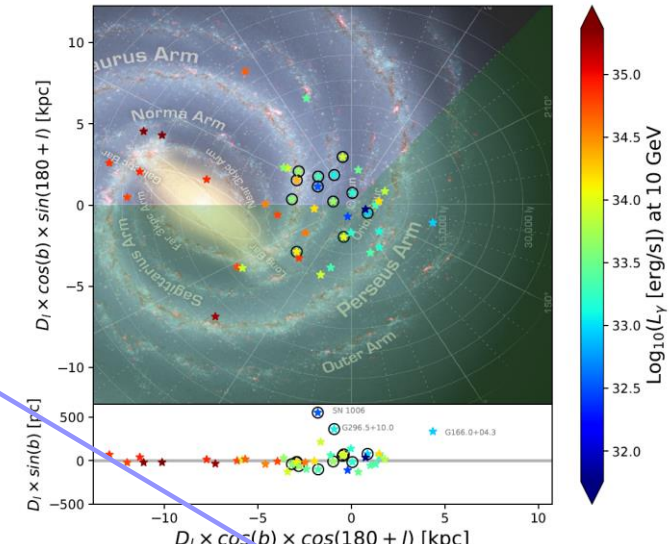


Multiwavelength spectra of 44  
SNRs normalized at 100 GeV  
and their distribution in the

Reviews of Modern Plasma Physics  
(2022) 6:19  
<https://doi.org/10.1007/s41614-022-00080-6>

REVIEW PAPER

The origin of galactic cosmic rays



# Gamma-ray detectors

高能

Space-based  
**EGRET, AGILE,  
Fermi, DAMPE**



**HE: >0.1 GeV**  
**Large FOV**  
**80% duty cycle**  
 **$0.1^\circ \sim 5^\circ$**   
**resolution**  
 **$1 \text{ m}^2$  area**

甚高能

IACTs:  
**H.E.S.S., MAGIC, VERITAS,  
CTA**



**VHE: >0.1 TeV**  
 **$3^\circ \sim 5^\circ$  FOV**  
**15% duty cycle**  
 **$0.06^\circ \sim 0.17^\circ$**   
**resolution**  
 **$10^5 \text{ m}^2$  area**

超高能

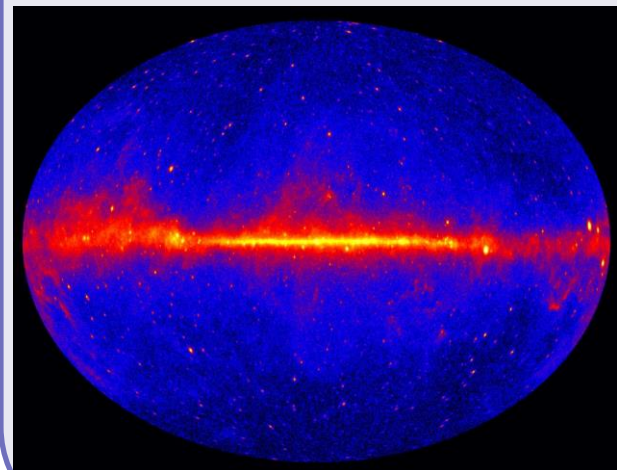
EAS arrays:  
**Milagro, ARGO-YBJ**  
**Tibet Asγ, HAWC,  
LHAASO**



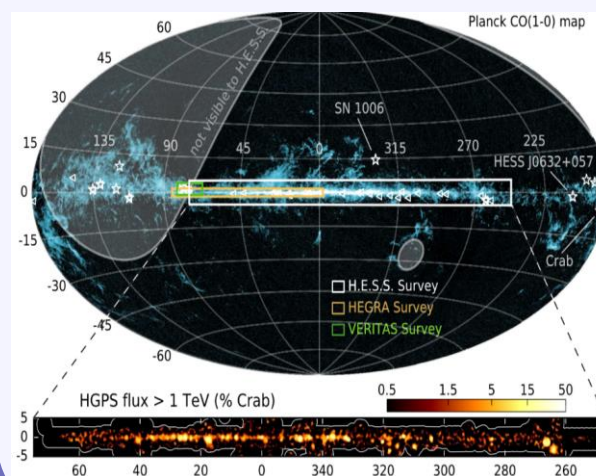
**VHE: >0.1 TeV**  
**UHE: >0.1 PeV**  
**Large FOV**  
**100% duty cycle**  
 **$0.1^\circ \sim 1^\circ$  resolution**  
 **$10^{3-6} \text{ m}^2$  area**

# Impressive Gamma-ray Source Catalogs

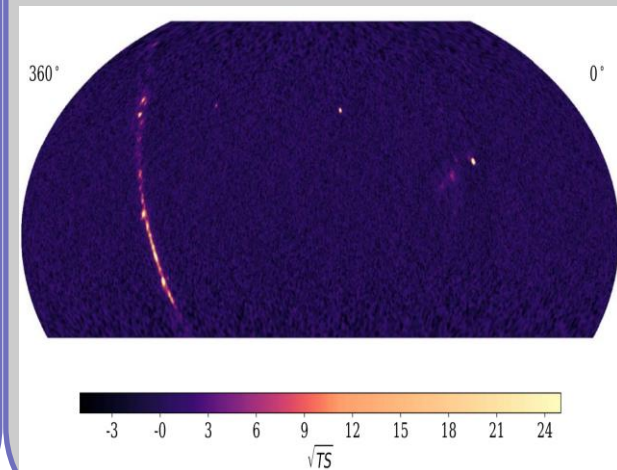
Fermi-LAT  
12ys data  
6658 sources  
50 MeV to 1 TeV



H.E.S.S.  
10ys data  
78 sources  
0.2-100 TeV

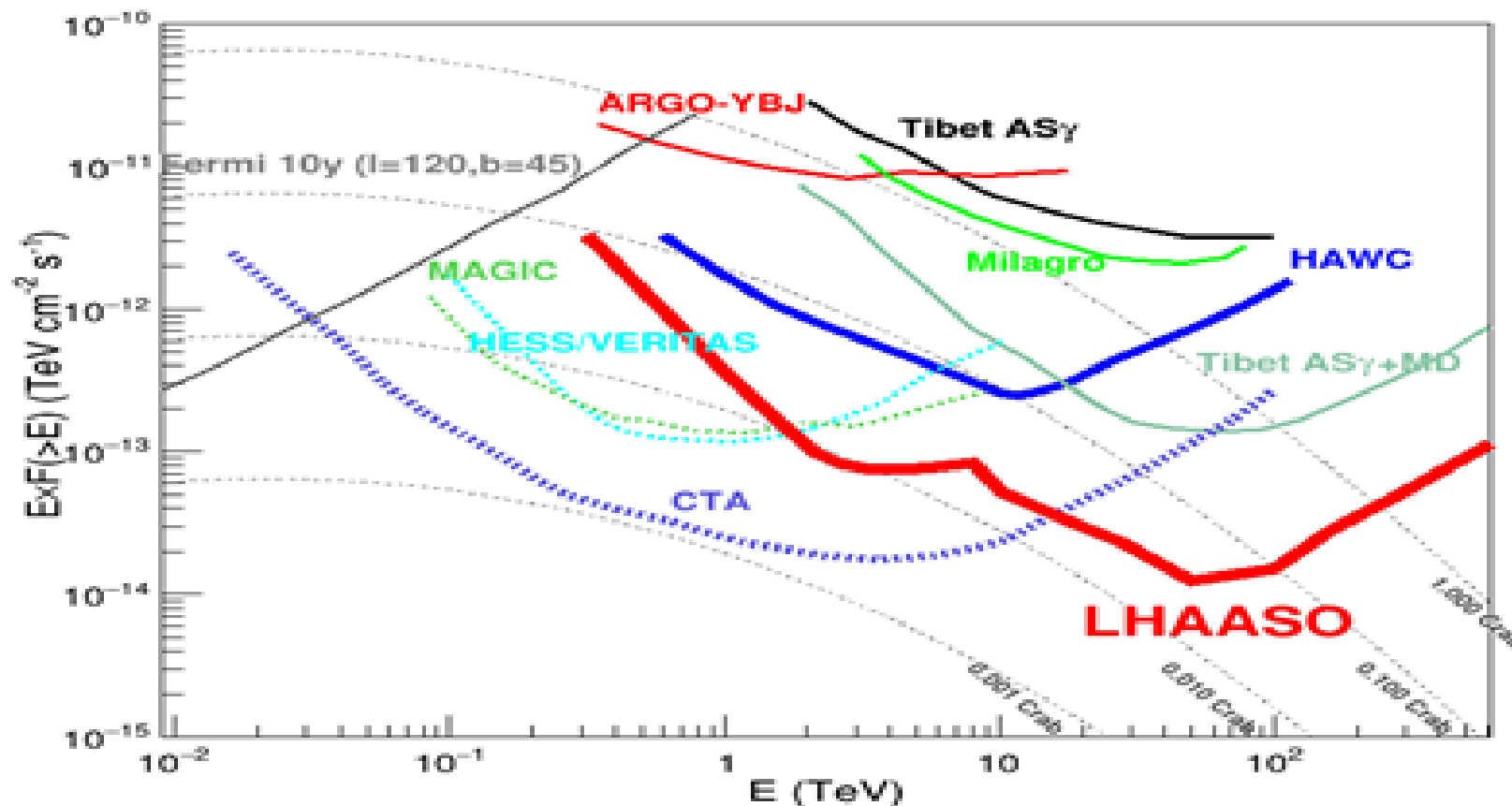


HAWC  
5ys data  
65 sources  
1~100 TeV



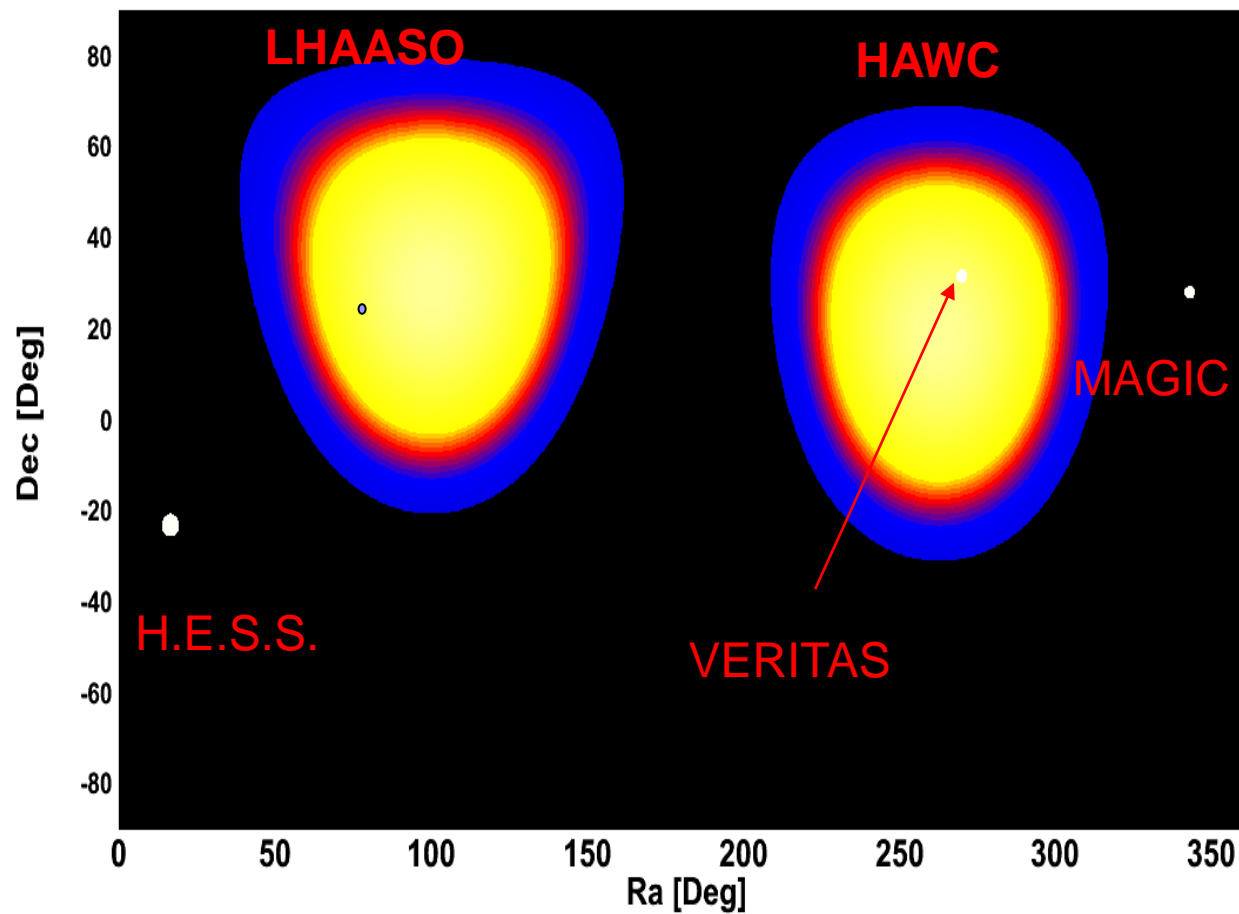
# LHAASO sensitivity

**With large FOV and high sensitivity, LHAASO is an ideal detector for sky survey to search VHE and UHE sources!**



# Field of view for GRB/TOO

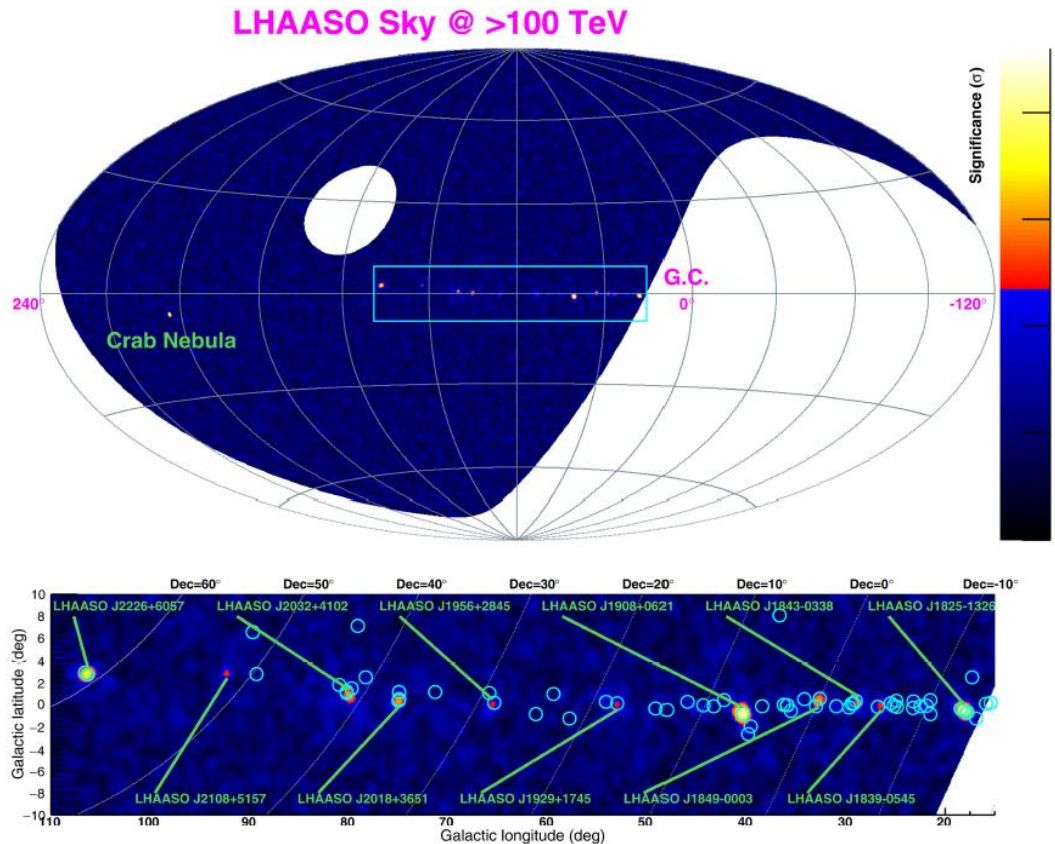
1/7 of the sky at any time



# Ultrahigh-energy photons up to 1.4 petaelectronvolts from 12 $\gamma$ -ray Galactic sources

<https://doi.org/10.1038/s41586-021-03498-z>

A list of authors and affiliations appears at the end of the paper.



# Ultrahigh-energy photons up to 1.4 petaelectronvolts from 12 $\gamma$ -ray Galactic sources

<https://doi.org/10.1038/s41586-021-03498-z>

A list of authors and affiliations appears at the end of the paper.

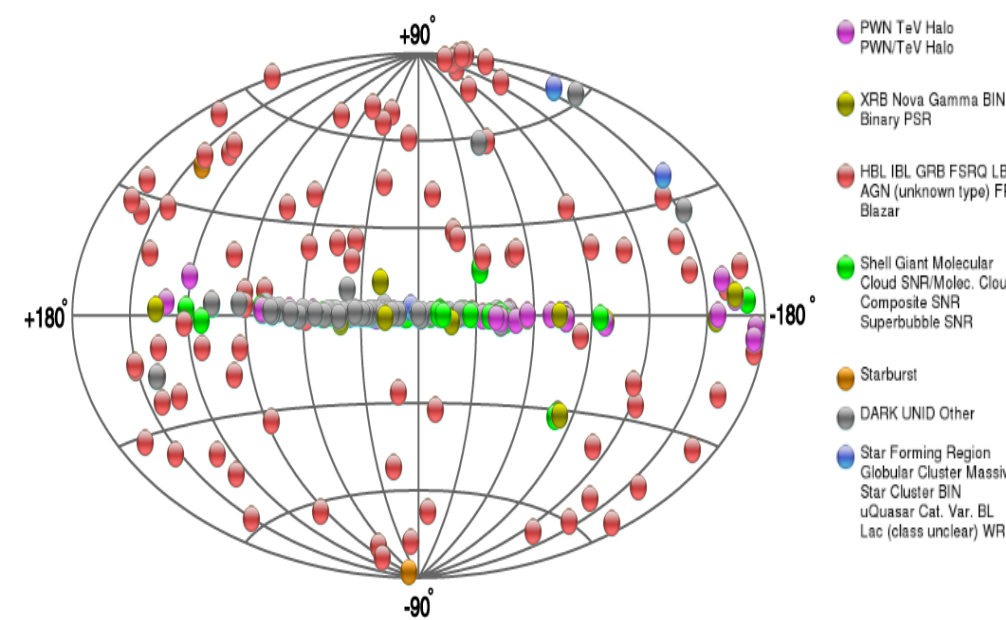
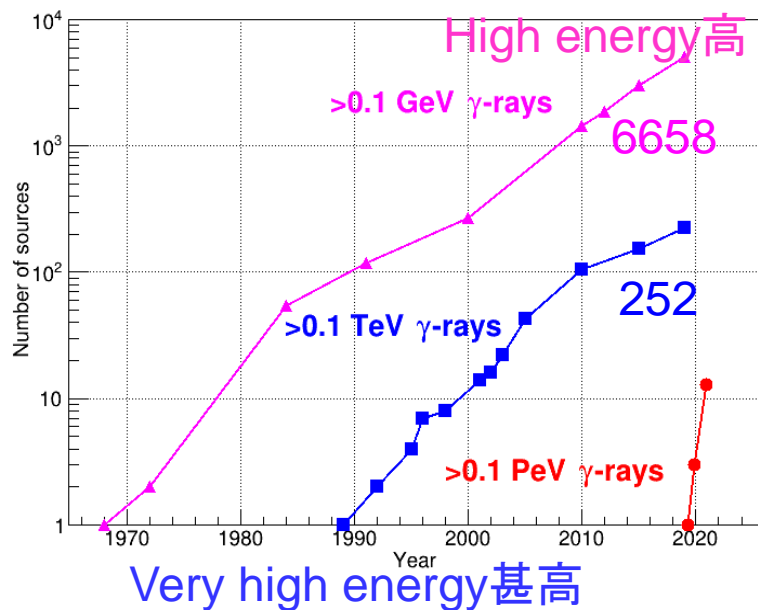
**Table 1 | UHE  $\gamma$ -ray sources**

Source name	RA ( $^{\circ}$ )	dec. ( $^{\circ}$ )	Significance above 100 TeV ( $\times\sigma$ )	$E_{\max}$ (PeV)	Flux at 100 TeV (CU)
LHAASO J0534+2202	83.55	22.05	17.8	$0.88 \pm 0.11$	1.00(0.14)
LHAASO J1825-1326	276.45	-13.45	16.4	$0.42 \pm 0.16$	3.57(0.52)
LHAASO J1839-0545	279.95	-5.75	7.7	$0.21 \pm 0.05$	0.70(0.18)
LHAASO J1843-0338	280.75	-3.65	8.5	$0.26 - 0.10^{+0.16}$	0.73(0.17)
LHAASO J1849-0003	282.35	-0.05	10.4	$0.35 \pm 0.07$	0.74(0.15)
LHAASO J1908+0621	287.05	6.35	17.2	$0.44 \pm 0.05$	1.36(0.18)
LHAASO J1929+1745	292.25	17.75	7.4	$0.71 - 0.07^{+0.16}$	0.38(0.09)
LHAASO J1956+2845	299.05	28.75	7.4	$0.42 \pm 0.03$	0.41(0.09)
LHAASO J2018+3651	304.75	36.85	10.4	$0.27 \pm 0.02$	0.50(0.10)
LHAASO J2032+4102	308.05	41.05	10.5	$1.42 \pm 0.13$	0.54(0.10)
LHAASO J2108+5157	317.15	51.95	8.3	$0.43 \pm 0.05$	0.38(0.09)
LHAASO J2226+6057	336.75	60.95	13.6	$0.57 \pm 0.19$	1.05(0.16)

Celestial coordinates (RA, dec.); statistical significance of detection above 100 TeV (calculated using a point-like template for the Crab Nebula and LHAASO J2108+5157 and 0.3° extension templates for the other sources); the corresponding differential photon fluxes at 100 TeV; and detected highest photon energies. Errors are estimated as the boundary values of the area that contains  $\pm 34.14\%$  of events with respect to the most probable value of the event distribution. In most cases, the distribution is a Gaussian and the error is  $1\sigma$ .

# LHAASO开启了超高能伽马射线天文学!

Great progresses are achieved in ground-based VHE gamma-ray astronomy!

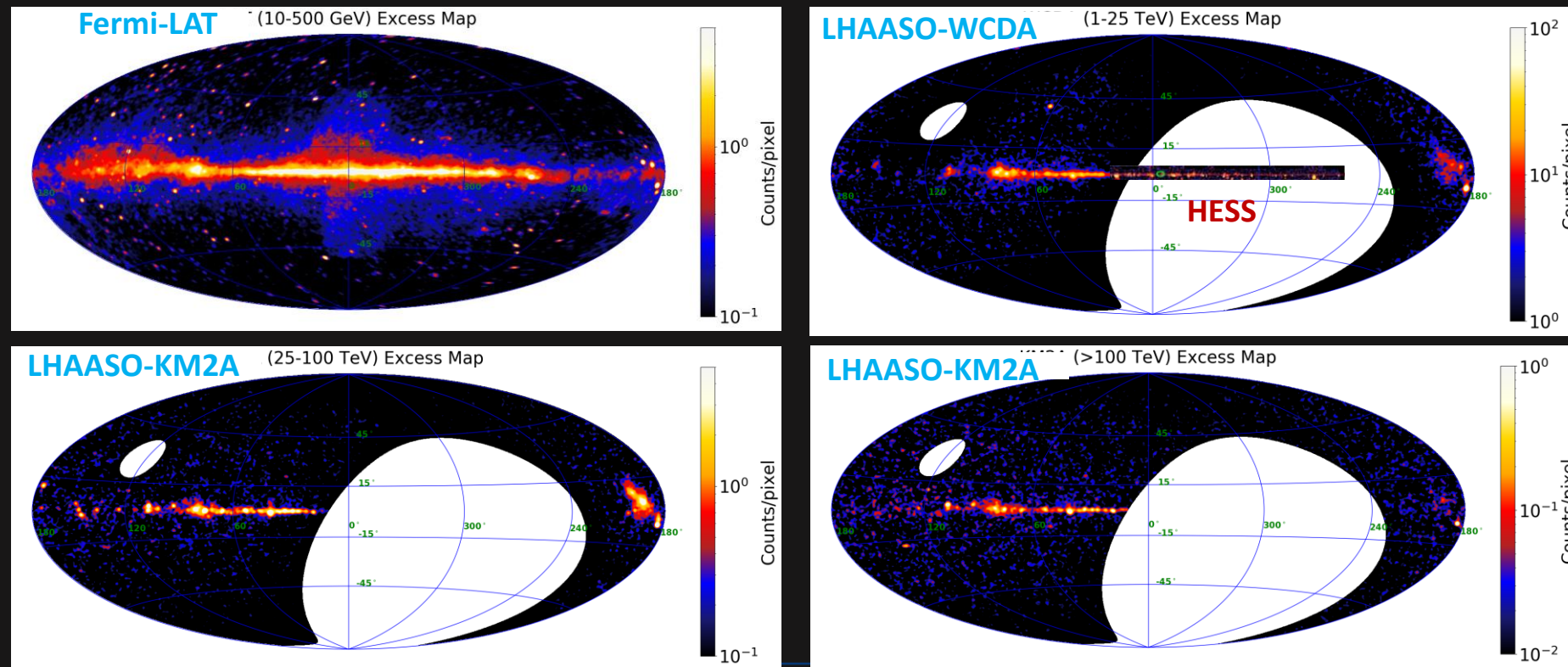


Ultra-high energy 超高

# Ultra-High-Energy $\gamma$ -ray Astronomy

arXiv:2305.17030v1

- Survey discovered 30+ new sources, 40+ PeVatrons and diffuse  $\gamma$ -ray emission

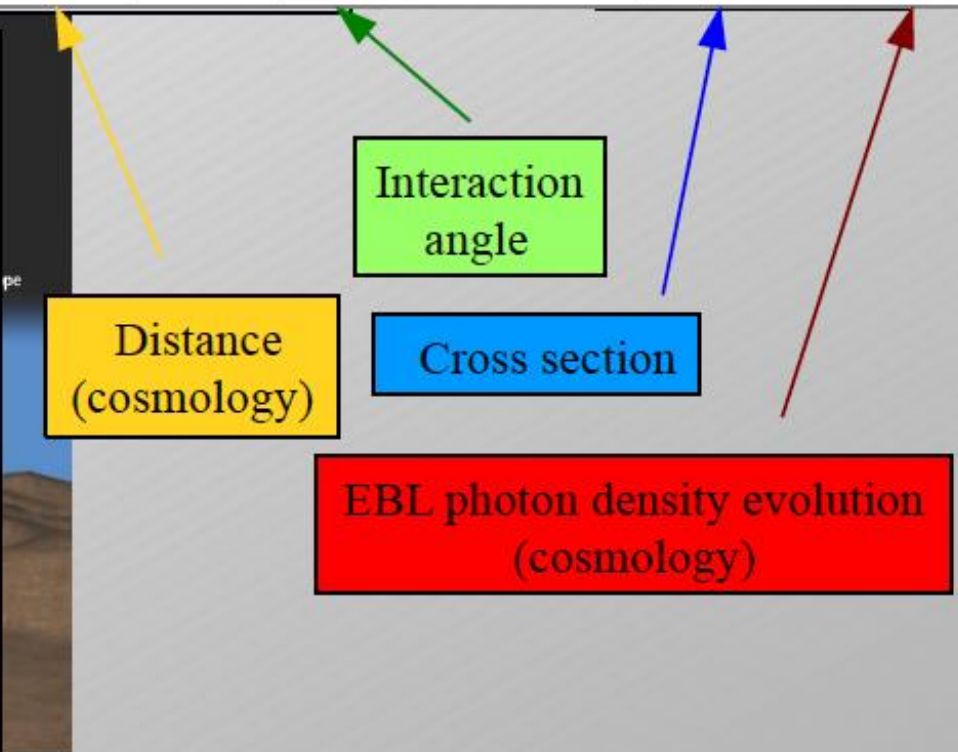
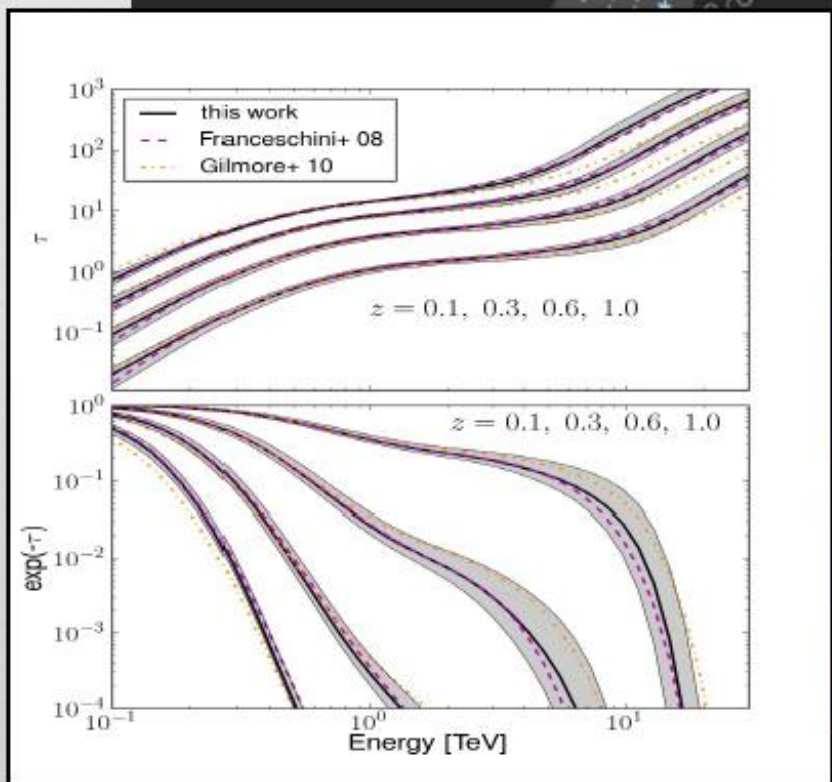


# Gamma-Ray Attenuation

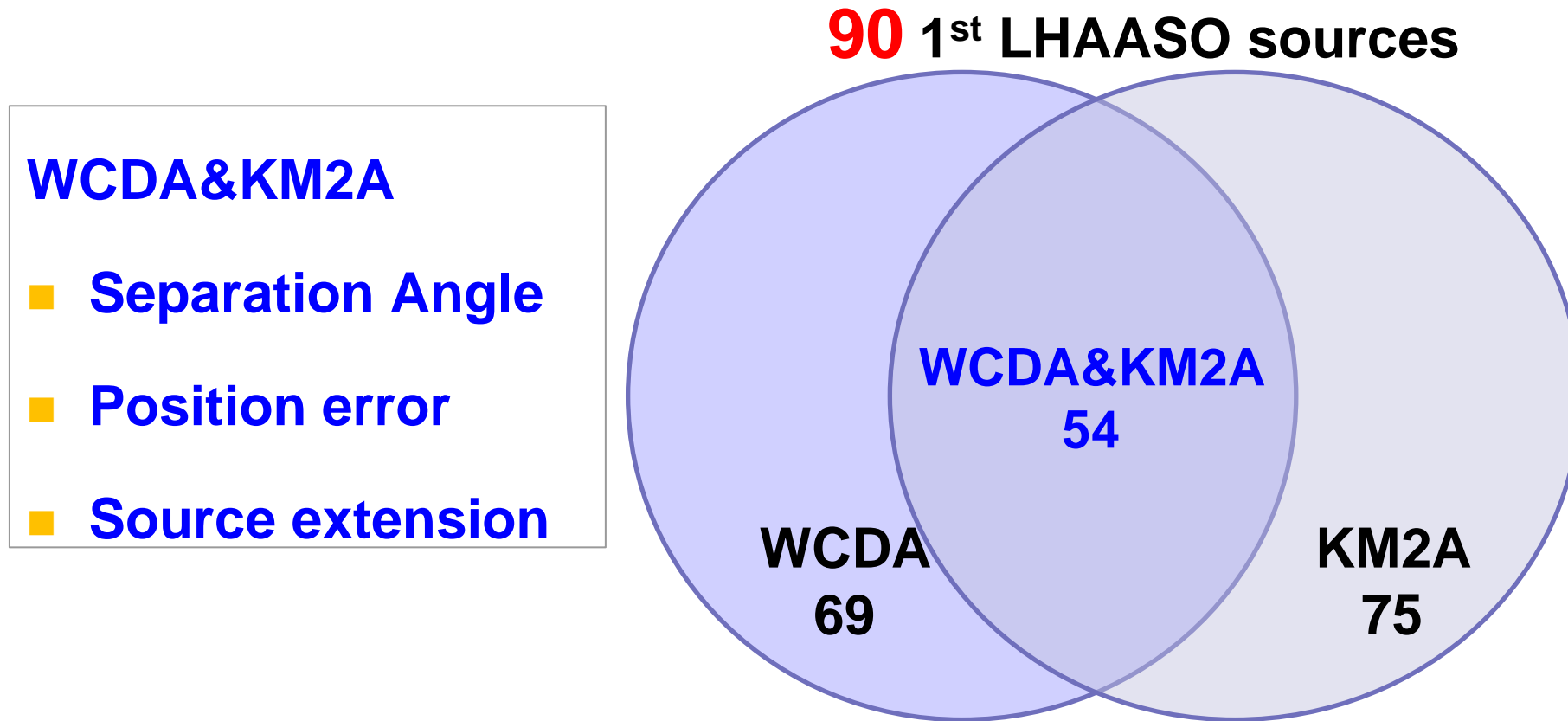


$$\left. \frac{dN}{dE} \right|_{obs} = \left. \frac{dN}{dE} \right|_{int} \exp [-\tau(E, z)]$$

$$\tau(E, z) = \int_0^z \left( \frac{dl'}{dz'} \right) dz' \int_0^2 d\mu \frac{\mu}{2} \int_{\varepsilon_{min}}^{\infty} d\varepsilon' \sigma_{\gamma\gamma}(\beta') n(\varepsilon', z')$$



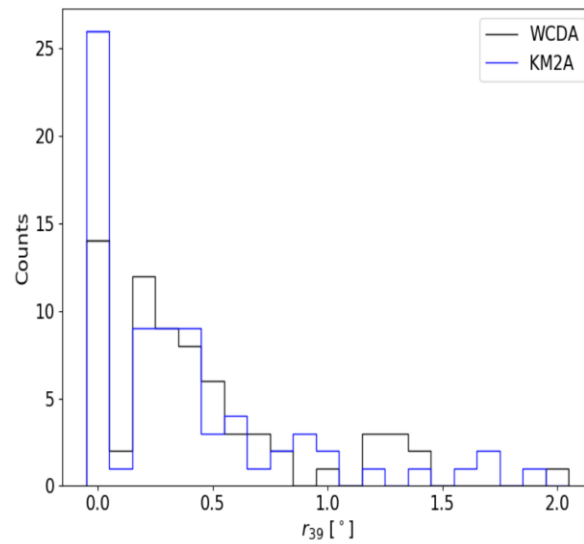
# **Construction of the 1<sup>st</sup> LHAASO sources**



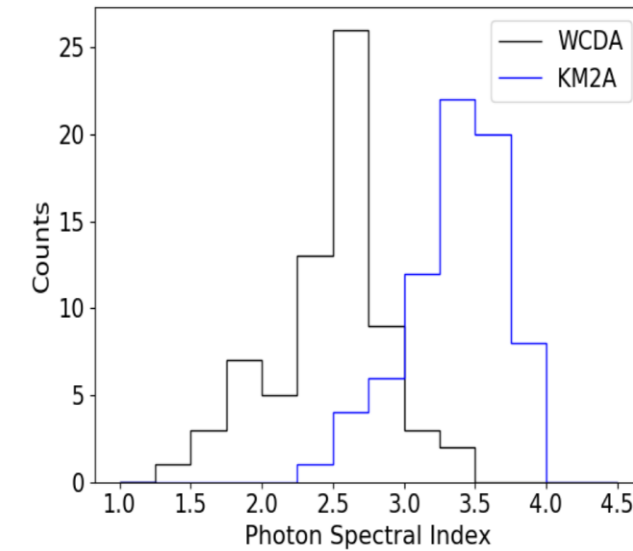
# Features of WCDA and KM2A sources

- WCDA detected 69 sources at  $>5\sigma$  (TS>37) and extension  $<2^0$
- KM2A detected 75 sources at  $>5\sigma$  (TS>37) and extension  $<2^0$

Source extension

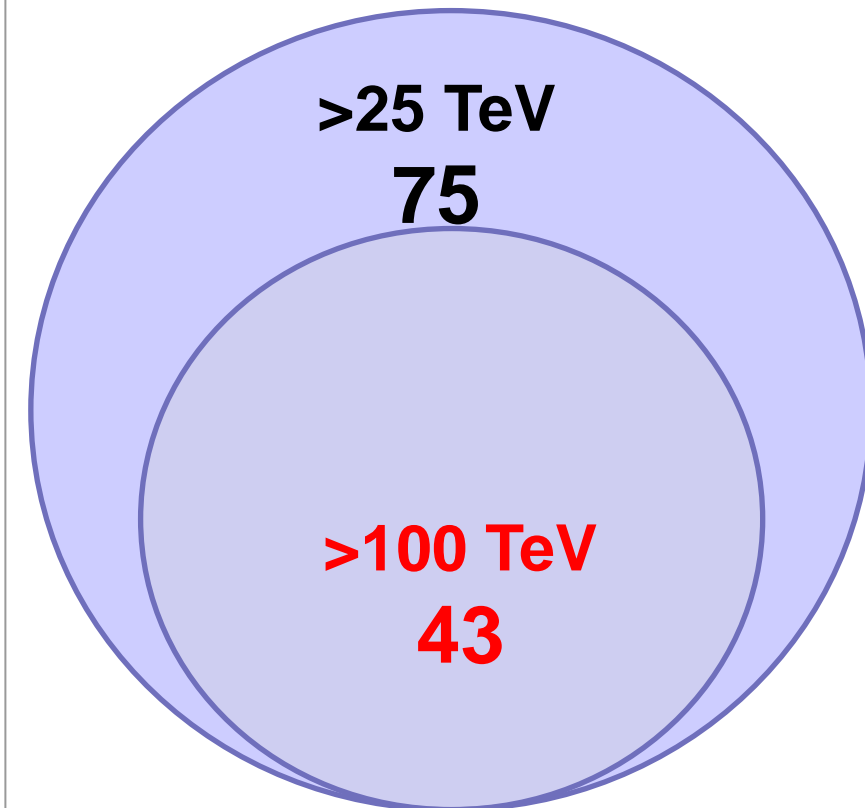


Spectral index

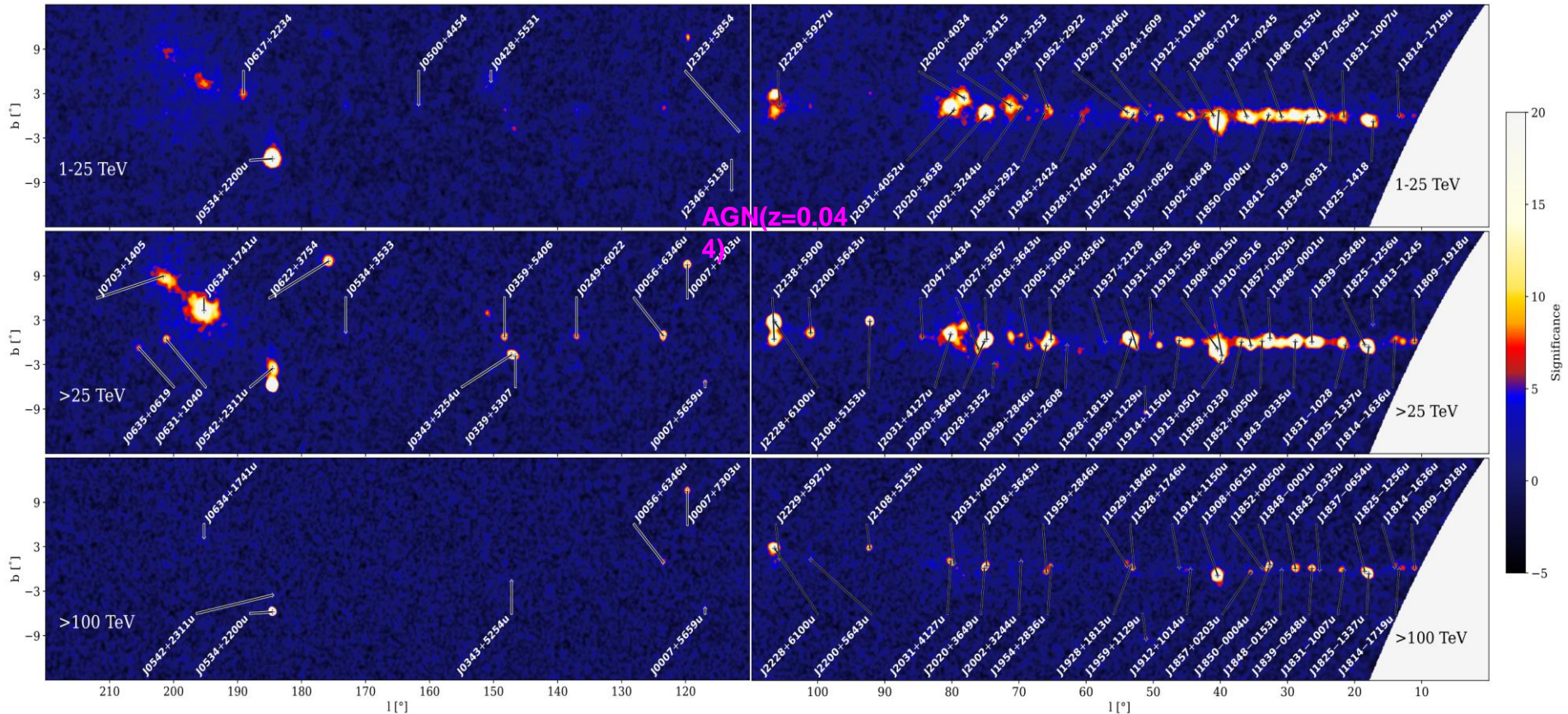


# **UHE gamma-ray sources**

- The position and extension achieved by KM2A at >25 TeV are used.
- Sources with significance  $>4\sigma$  at >100 TeV are labeled as UHE sources

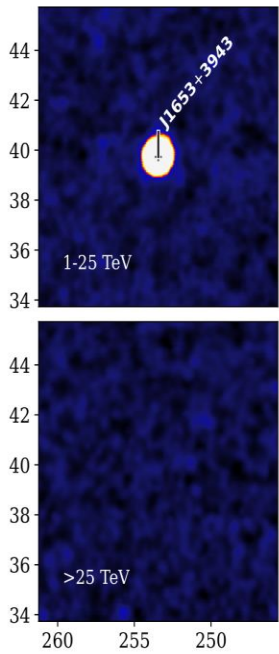


# 82 sources with the Galactic latitude $|b| < 12^\circ$

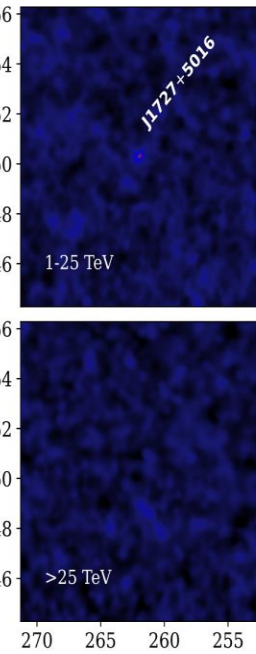


# **8 sources with the Galactic latitude $|b|>12^\circ$**

**Mrk 421**  
 **$z=0.031$**

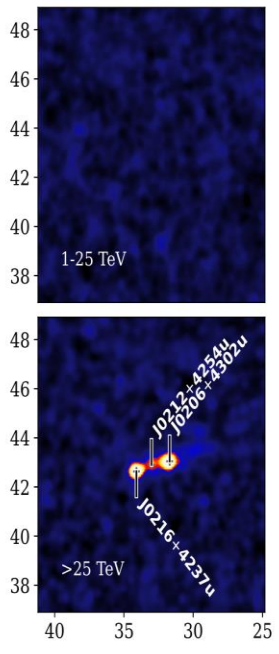


**1ES 1727+502**  
 **$z=0.055$**

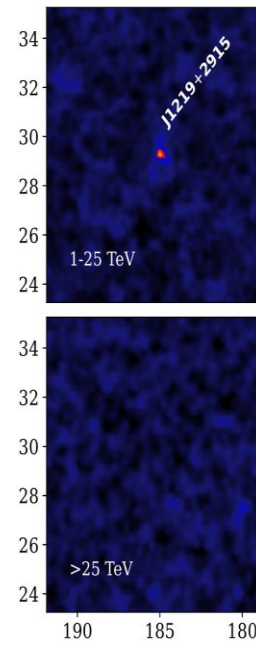


**4  
AGNs**

**Mrk 501**  
 **$z=0.034$**



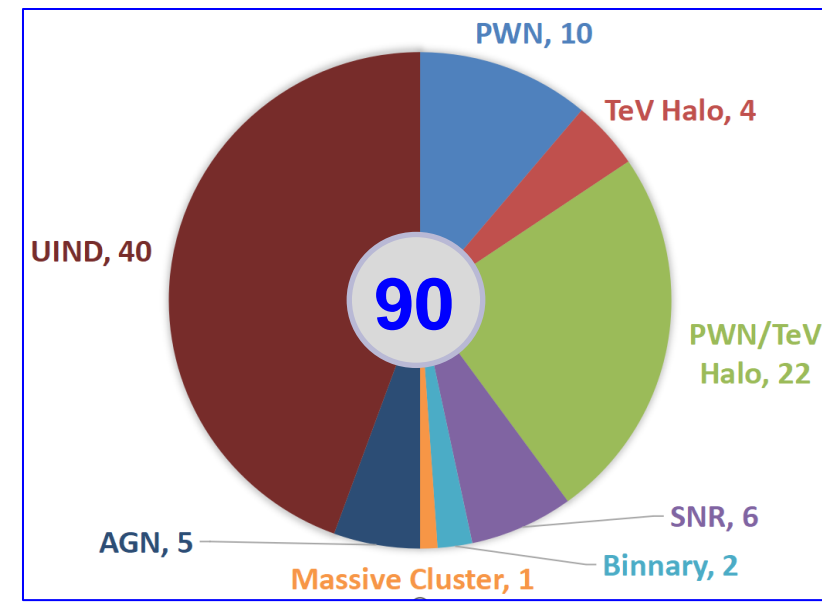
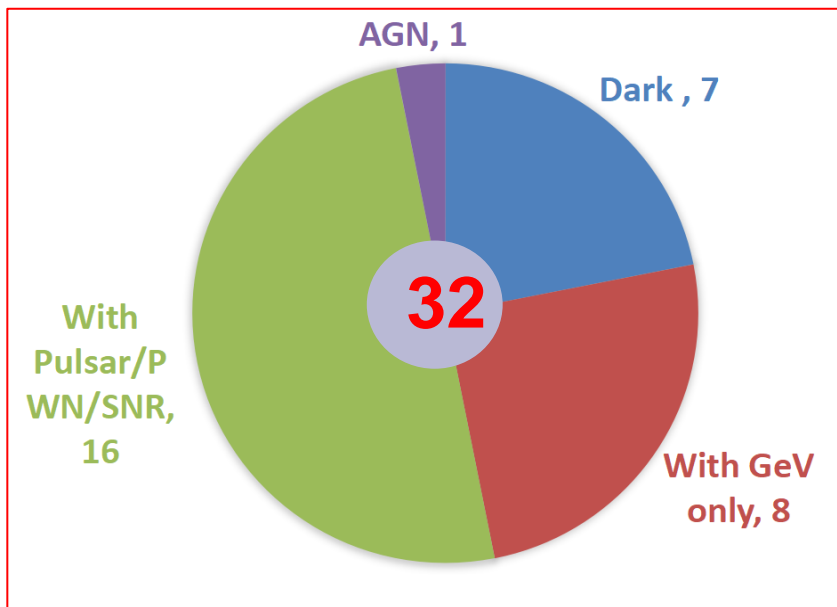
**NGC 4278**  
 **$z=0.002$**



$\alpha_{2000} [^\circ]$

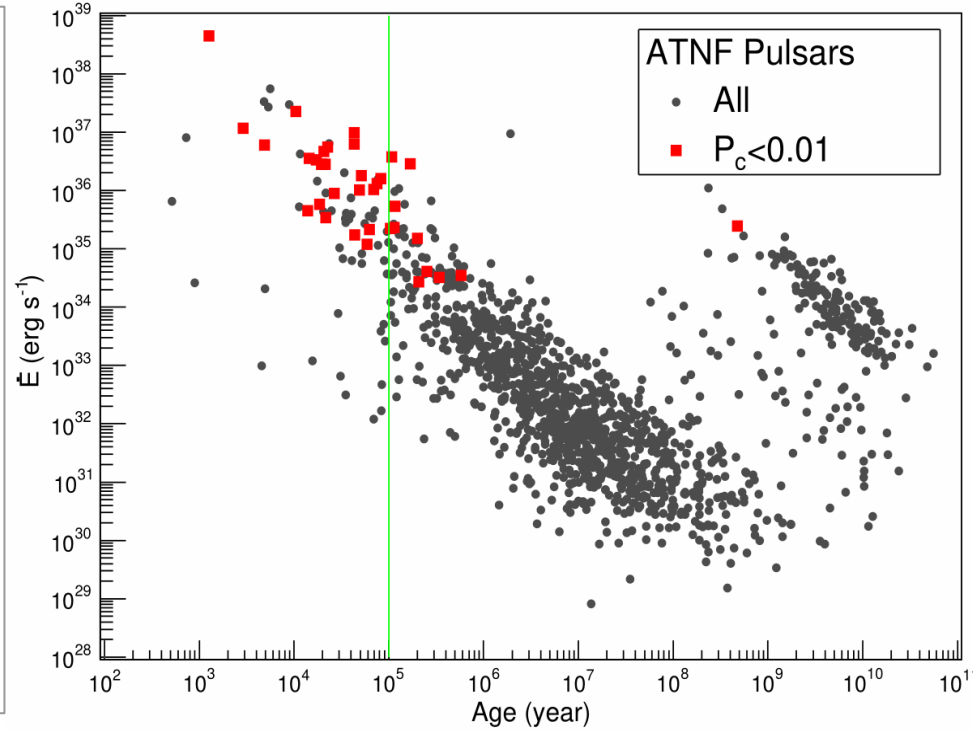
# Association with known TeV Sources

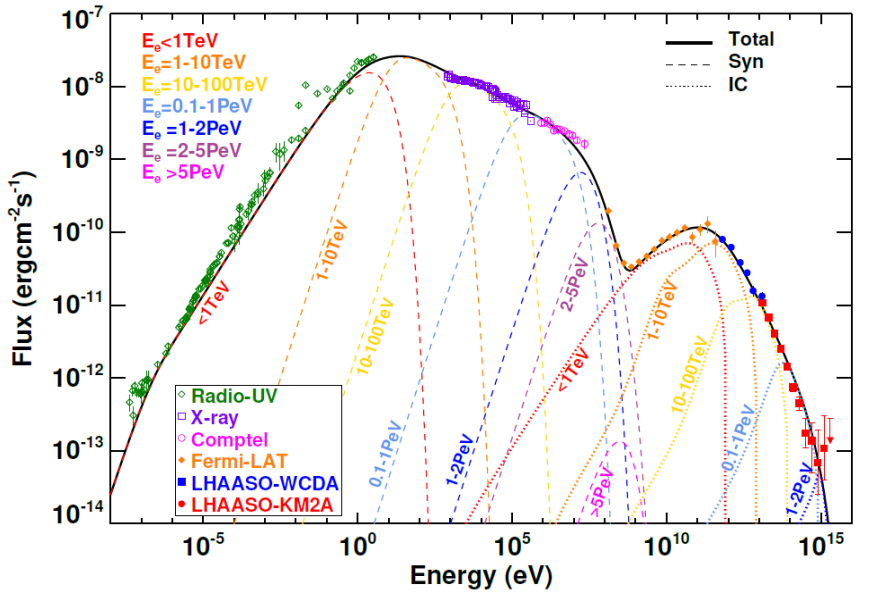
- 58 sources with TeVCat+3HAWC association
- 32 new sources (25+7)



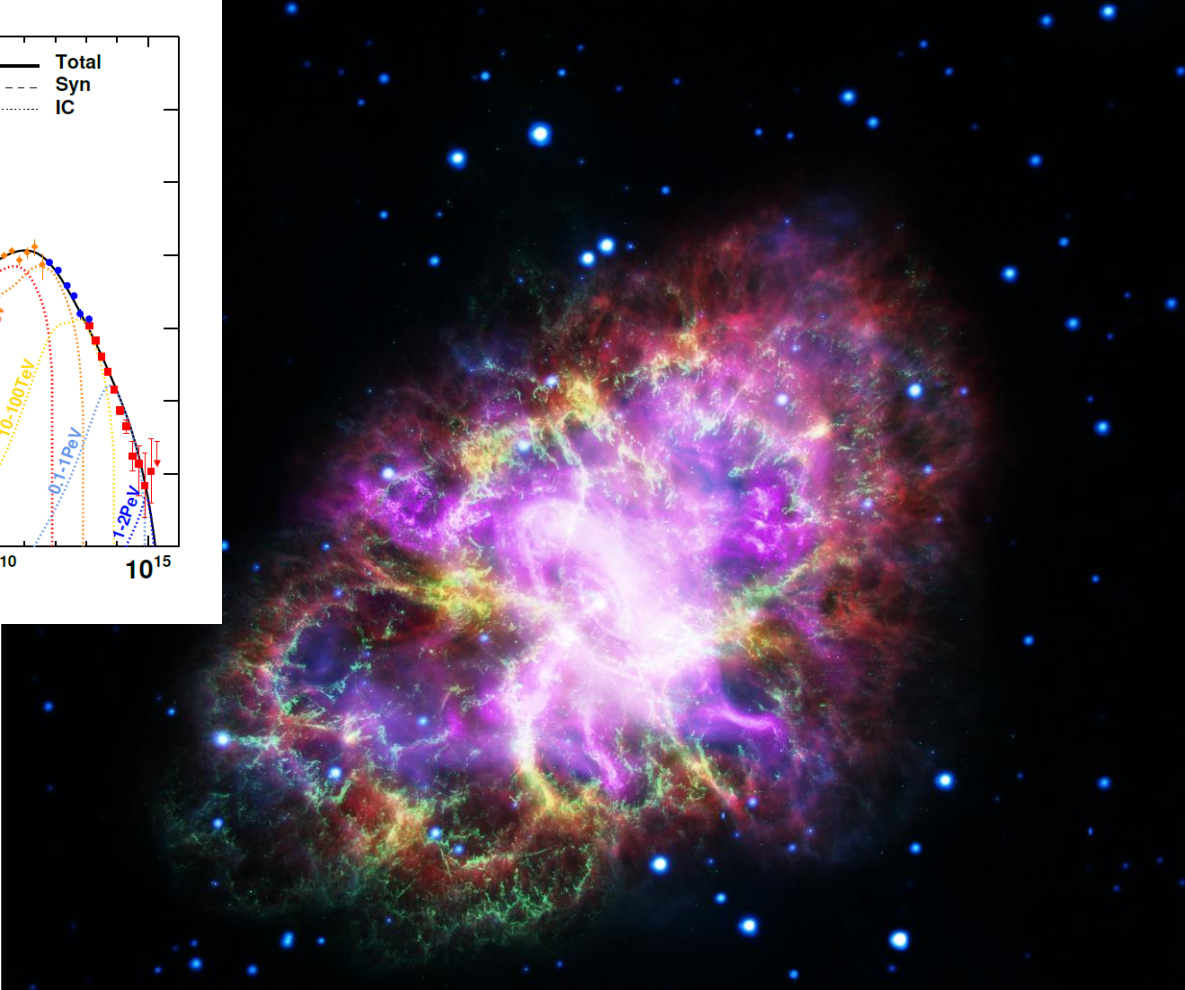
# Association with ATNF pulsars

- **65 1LHAASO sources with pulsar nearby  $<0.5^{\circ}$ .**
- **35 associations with chance coincide probability  $<1\%$ . (13 labeled as PWN or Halo in TeVCat)**
- **22 new possible PWN/TeV Halo**

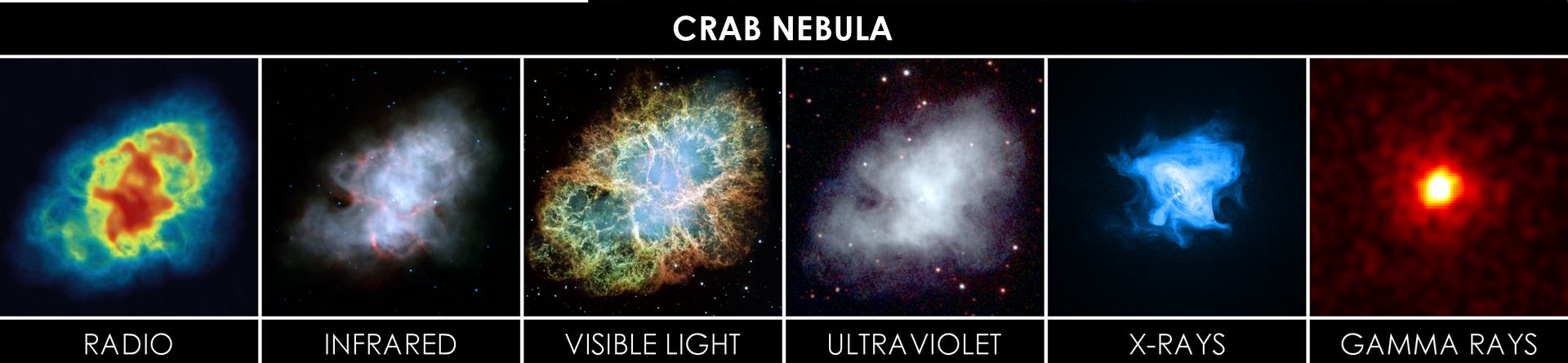


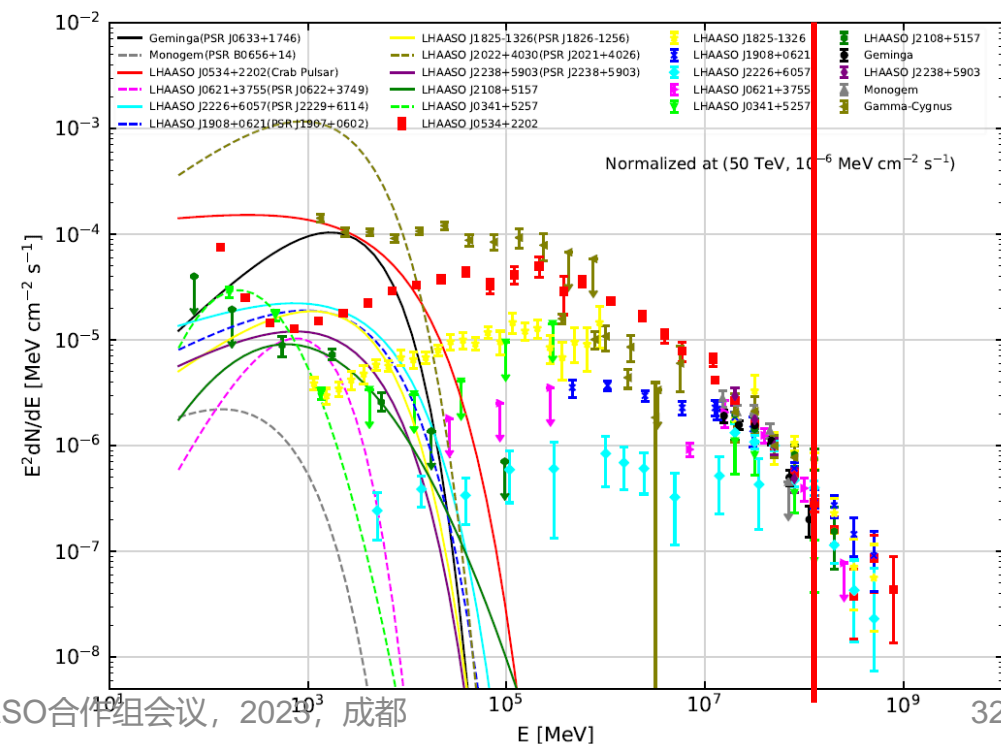
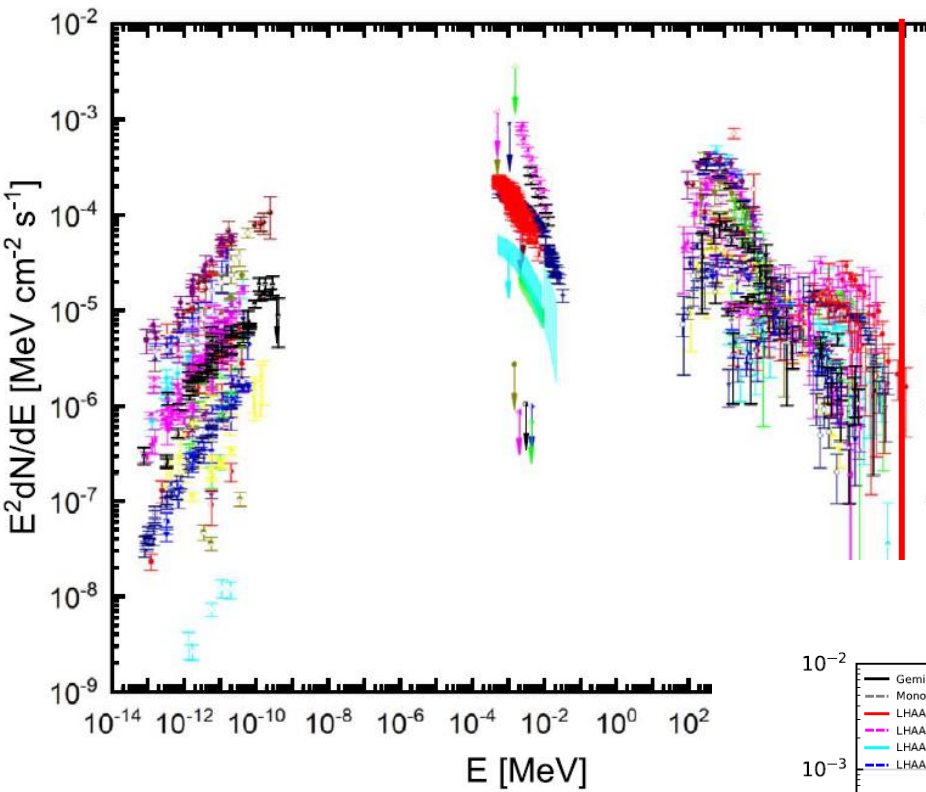


# 蟹状星云

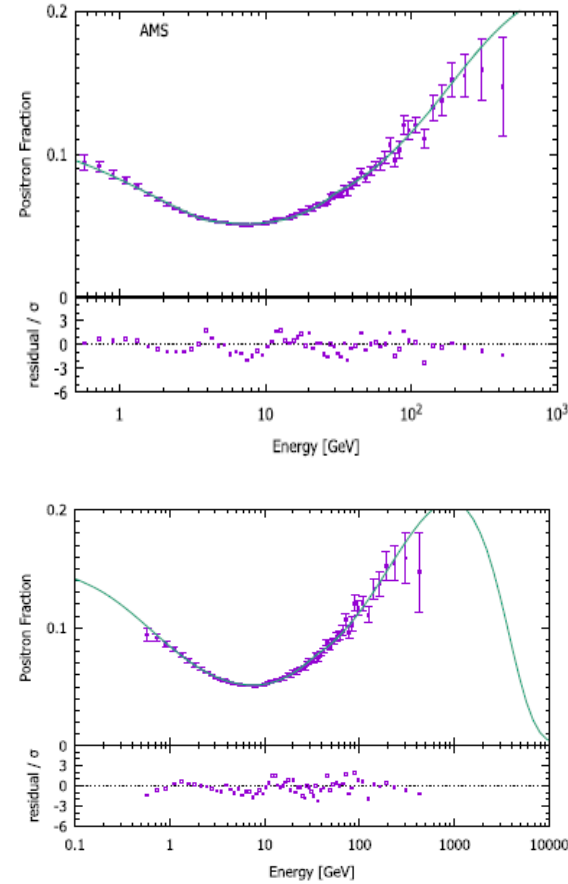
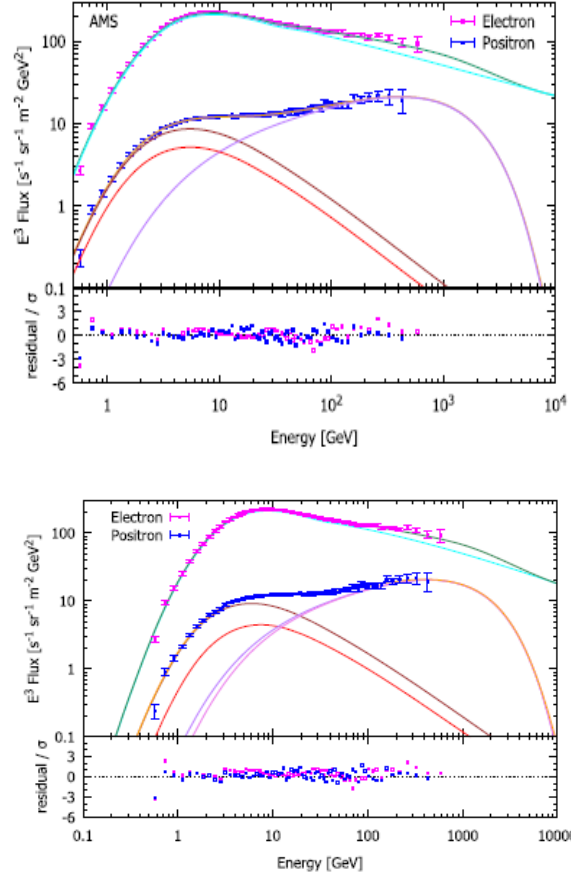
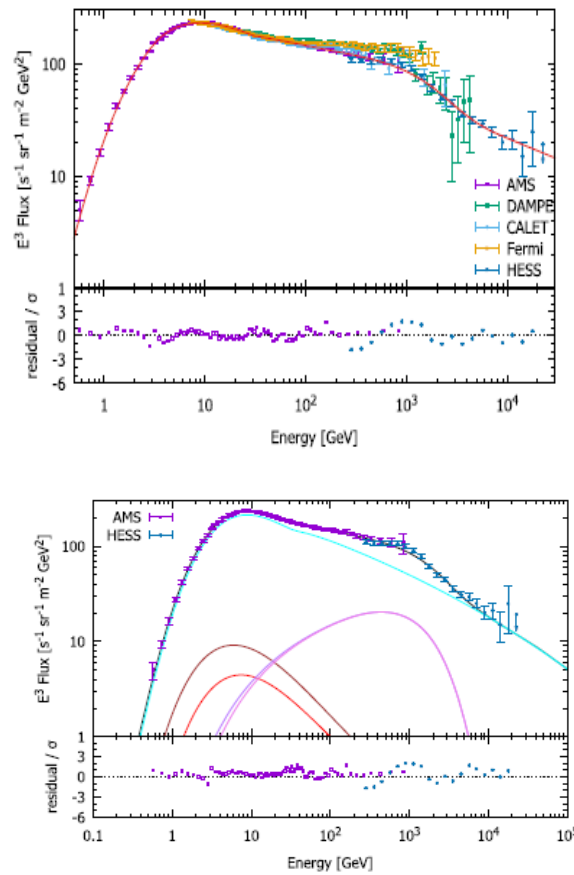


CRAB NEBULA





# 宇宙线正负电子



of the  
ROYAL ASTRONOMICAL SOCIETY

MNRAS 485, 3869–3875 (2019)

Advance Access publication 2019 March 11

## Examining the Secondary Product Origin of Cosmic-Ray Positrons with the Latest AMS-02 Data

Zhi-Qiu Huang<sup>1,2</sup>, Ruo-Yu Liu<sup>1,2</sup> , Jagdish C. Joshi<sup>1,2</sup>, and Xiang-Yu Wang<sup>1,2</sup>

## Origin of cosmic ray electrons and positrons

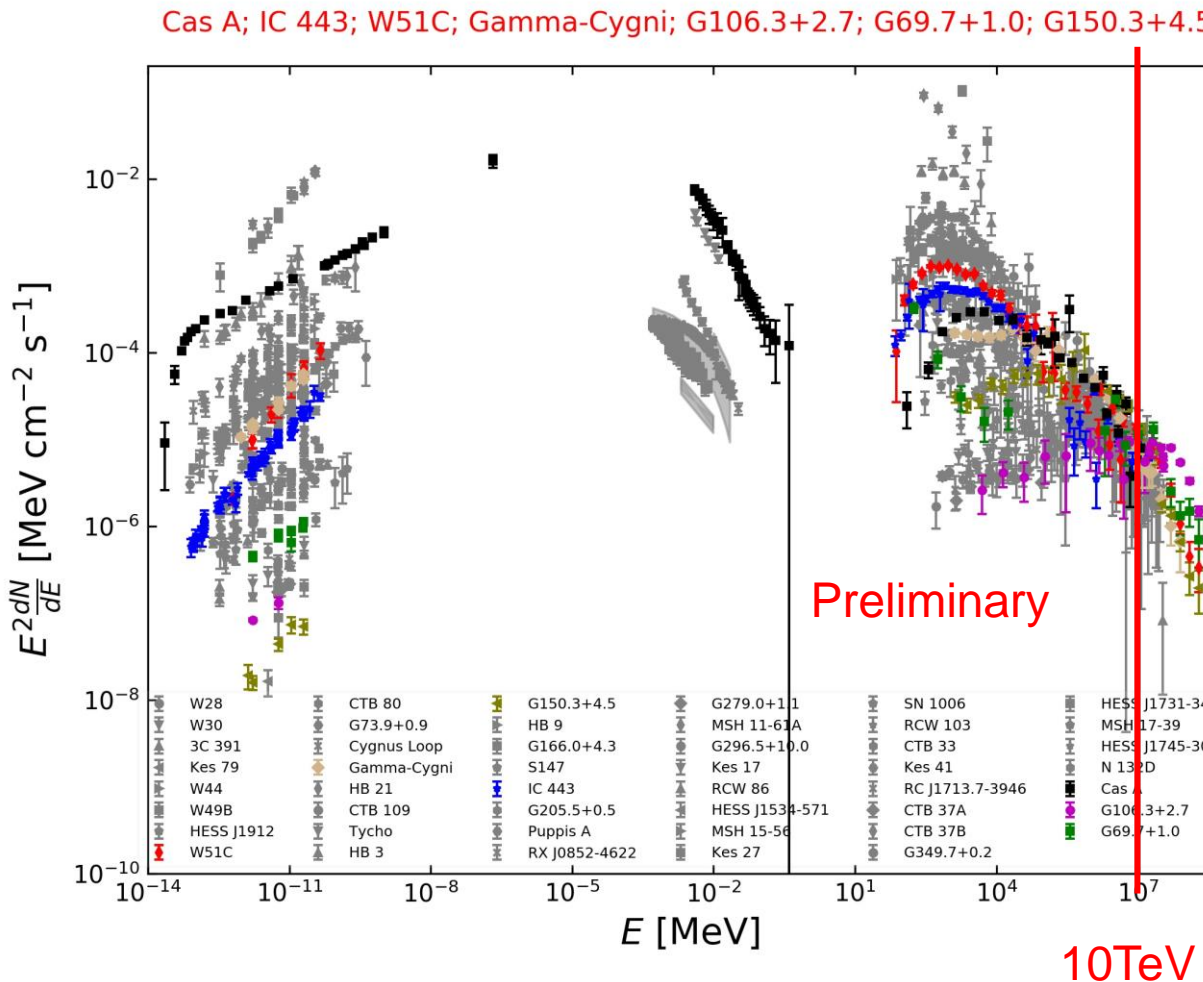
2023/9/1

Zhao-Dong Shi<sup>1,2</sup> and Siming Liu<sup>1,2</sup>

LHAASO合作组会议, 2023, 成都

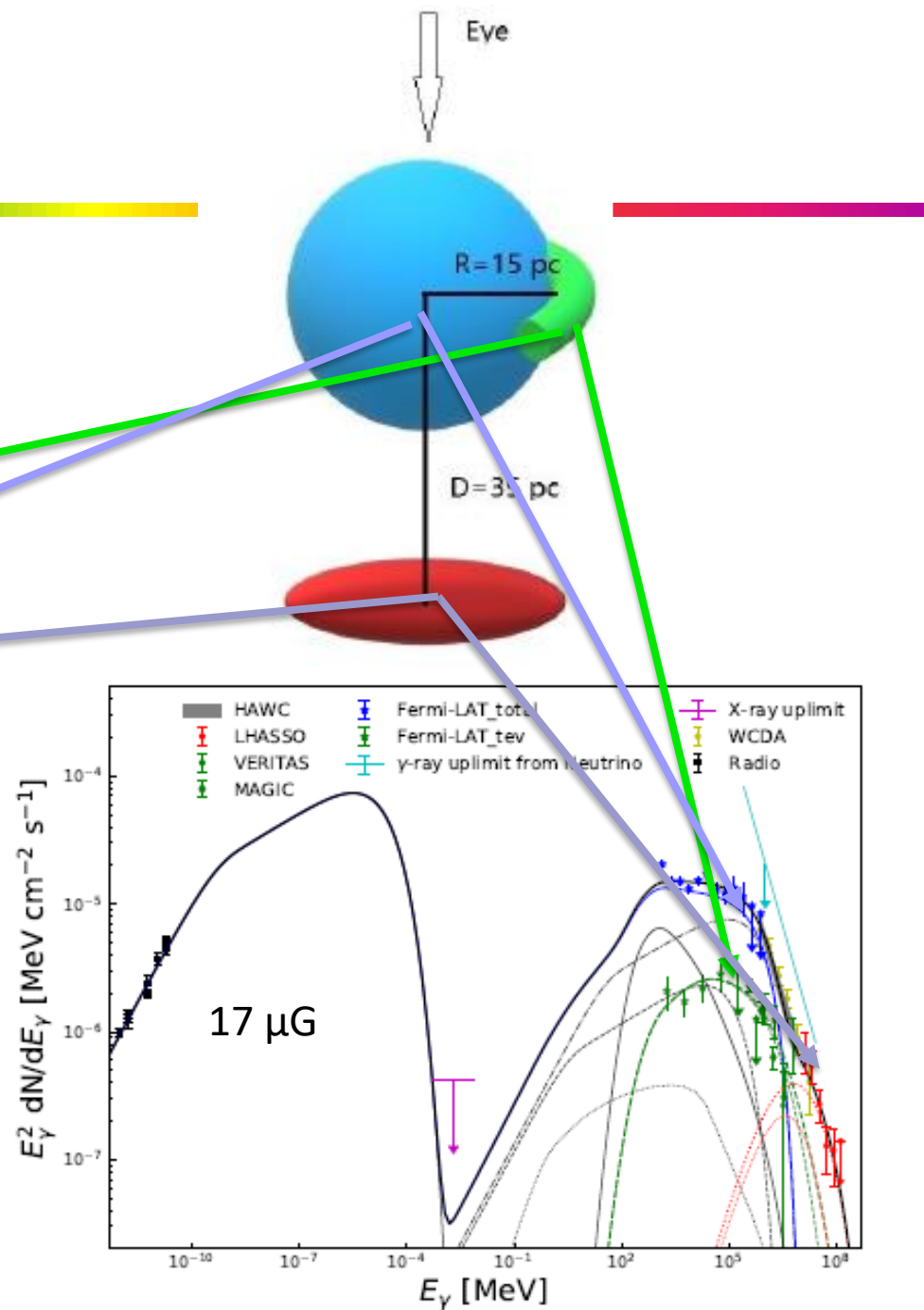
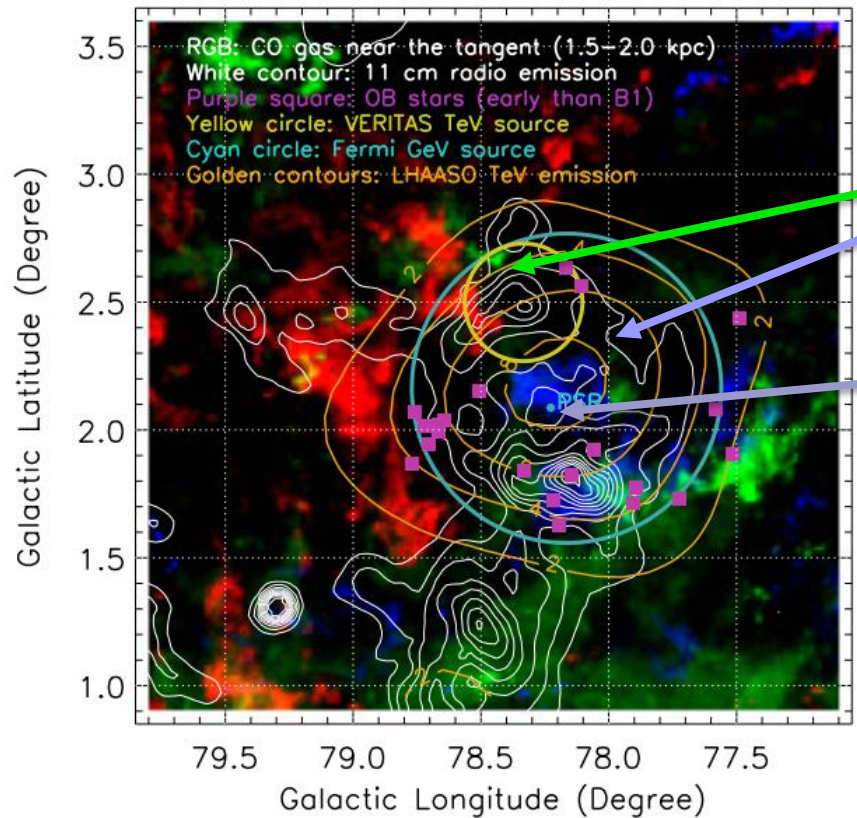
33

# >7 SNRs Detected by LHAASO



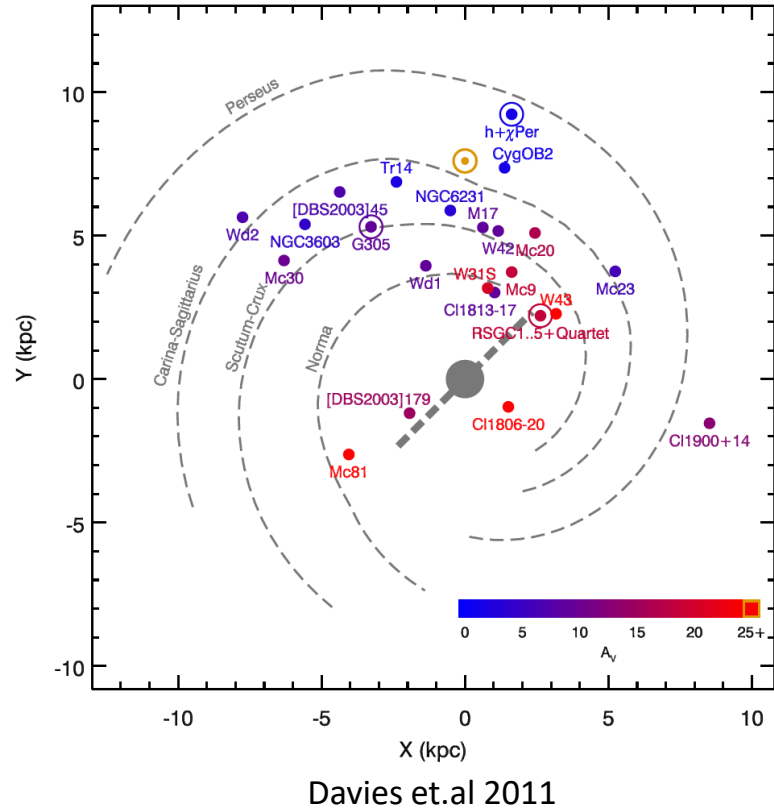
The higher energy spectra are softer (but harder than an exponential cutoff)

# Gamma Cygni



Considering the low density inferred from X-ray observations of  $0.2\text{--}0.3 \text{ cm}^{-3}$  and a high magnetic field

# YMSC IN OUR GALAXY

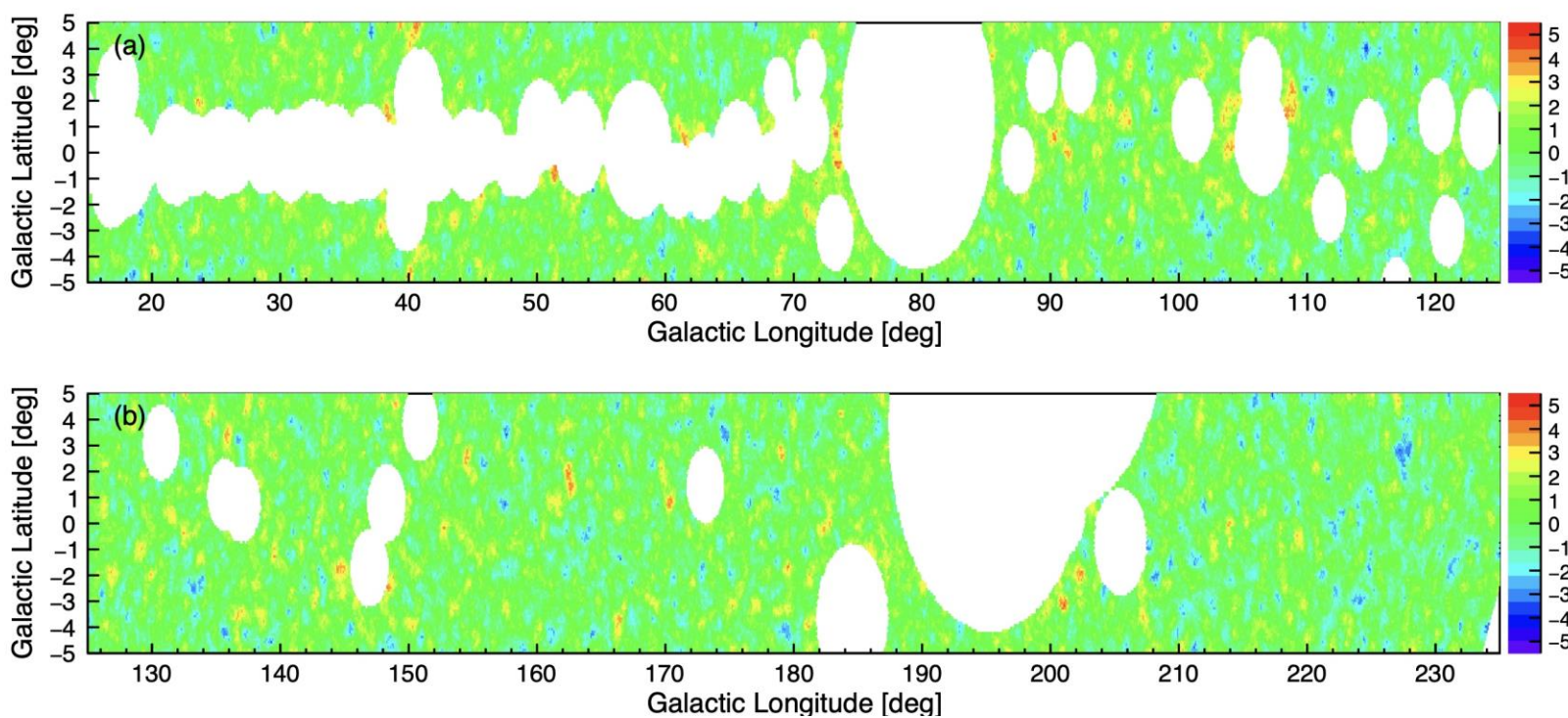


- ~20 in our Galaxy
- More to be discovered (high extinction in Galactic plane )

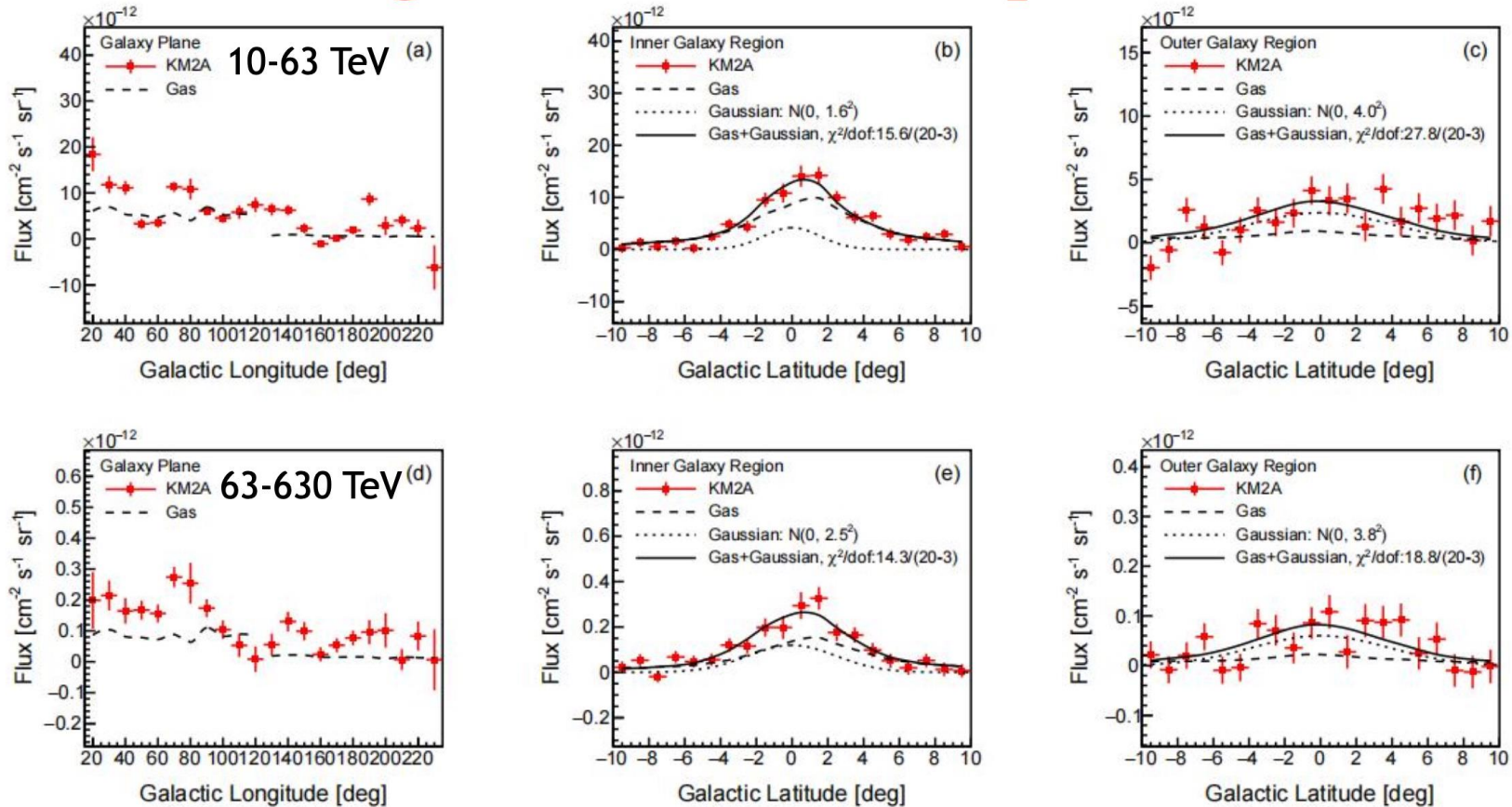
Stellar type	$\log[\dot{M}]$ $M_{\odot} \text{ yr}^{-1}$	$V_{\infty}$ $\text{km s}^{-1}$
WNL	-4.2	1650
WNE	-4.5	1900
WC6-9	-4.4	1800
WC4-5	-4.7	2800
WO	-5.0	3500
O3	-5.2	3190
O4	-5.4	2950
O4.5	-5.5	2900
O5	-5.6	2875

- The wind power of a single young star can be as high as  $1\text{e}37 \text{ erg/s}$

# 弥散伽马射线

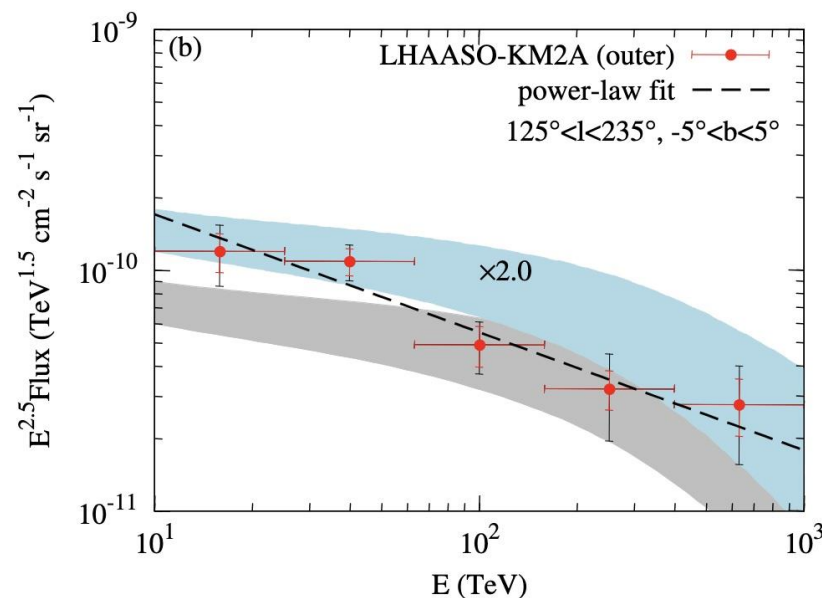
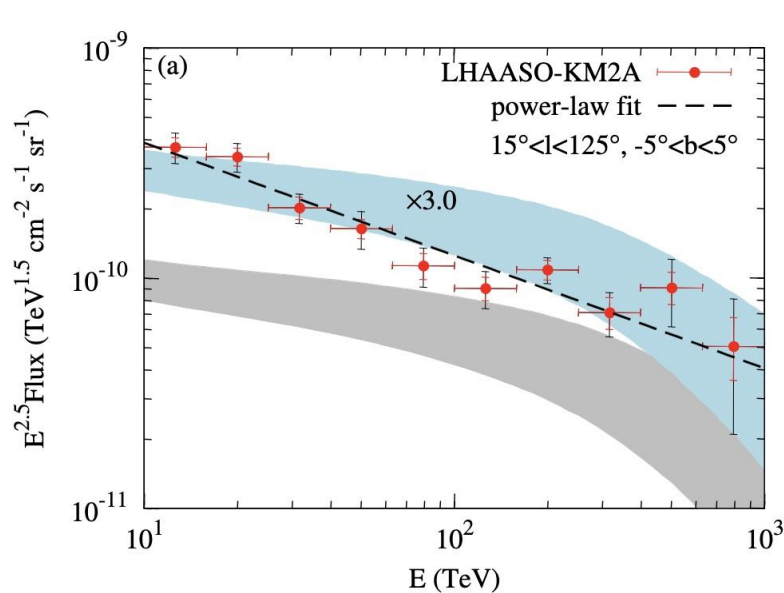


# Longitude and latitude profiles



Adding a Gaussian latitude template does not improve the fittings significantly

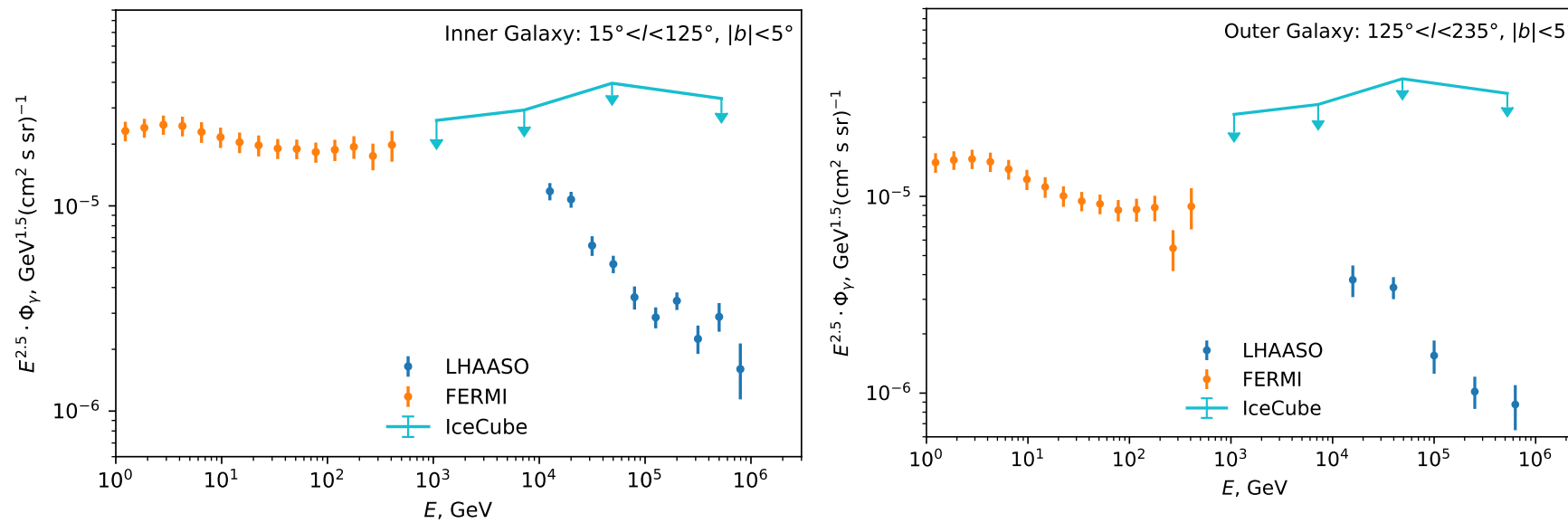
# LHAASO diffuse



$$\Xi^{A,A'}(E, l, b) = \int_0^\infty ds n_{\text{gas}}^{A'}(\mathbf{x}) I_{\text{CR}}^A(E, \mathbf{x})$$

$$I_\nu(E, l, b) = \sum_{A,A'} \int_E^\infty dE' \Xi^{A,A'}(E', l, b) \frac{d\sigma^{AA' \rightarrow \nu}(E', E)}{dE}$$

# Gamma-ray flux in inner and outer Galaxy



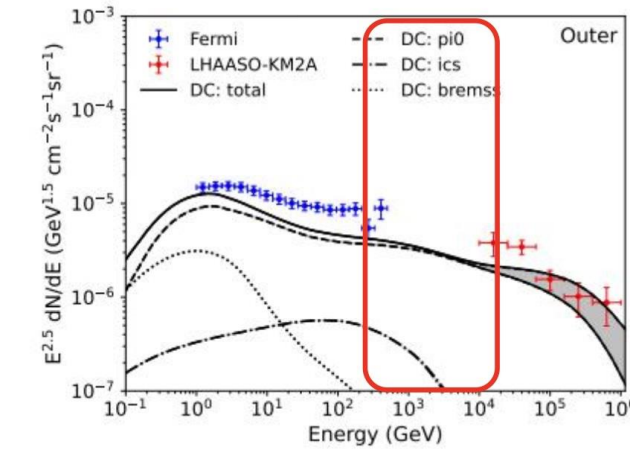
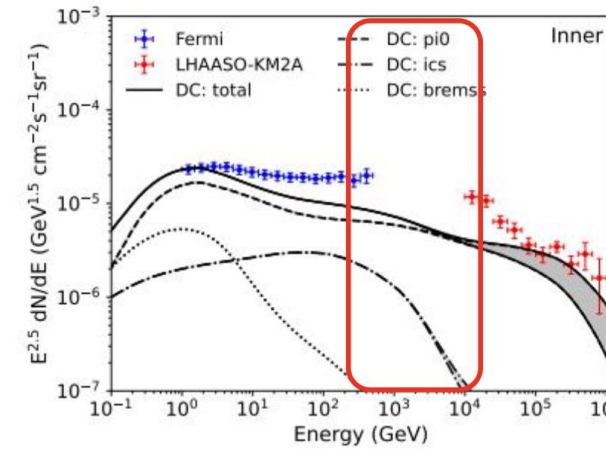
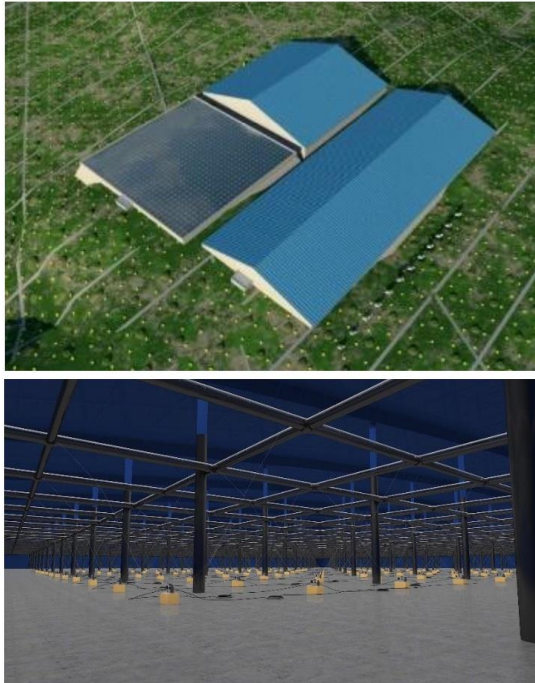
LHAASO data from  
LHAASO collaboration,  
2305.05372

Fermi from R. Zhang et al,  
2305.06948

IceCube data from IceCube 7 years limit on Kra-gamma model approximated to  $|b| < 5$

Gamma-ray flux in LHAASO is same  $1/E^3$ ,  
but combination with Fermi looks different.

# Energy coverage from sub-TeV to 10 TeV by WCDA



WCDA is expected to cover the energy range from sub-TeV to 10 TeV, and will perfectly bridge Fermi and KM2A.

# 结论

- 宇宙线起源问题是粒子天体物理的核心科学问题之一，也是LHAASO的主要科学目标之一
- 过去几十年从射电到甚高能伽马射线的天文多波段研究表明GeV宇宙线主要来自于高密度环境中的超新星遗迹激波加速而TeV宇宙线主要来自于低密度环境中的高速激波粒子加速
- LHAASO观测有望澄清PeV宇宙线的起源问题

# Summary

- Construction of LHAASO finished in September 2021. LHAASO operates with almost 100% duty cycle. It's one year sensitivity is better compared to 50 hours for present Cherenkov telescopes above few TeV. Above 20 TeV it is better compared to future CTA.
- LHAASO presented first catalog of 90 sources from about 2 first years of observation. 32 are new sources. Number of UHE gamma-ray sources above 100 TeV increased from 4 to 43 by LHAASO observations
  - 35 sources are PWN. Crab, Geminga, milisecond pulsar
  - 7 SNR, gamma-Cygni can not be explained by leptons
  - Star clusters Cygnus, w43
- Diffuse emission from Galaxy: new models required
- GRB 221009A: detailed properties of GRB afterglow from 60000 photons in LHAASO WCDA

# 1054年的客星

歷代名臣奏議卷之三百一

灾祥

宋仁宗至和二年侍御史趙抃上言曰臣伏見自去年五月已來。妖星遂見。僅及周稔。至今光耀未退。此谷永所謂馳騁驟芒炎長短所懸奸犯其為謫變甚可畏也。又去冬連令春京東西路及陝右川蜀諸郡旱曠不雨。麥苗焦死。既艱食寇攘必興。此京房所謂欲德不用。茲謂張厥災荒其為災沴復可懼也。邇來峽嶺山谷驚裂有聲。他郡數處地亦震動。此伯陽所謂陽伏而不能出。陰迫而不能升。蓋土失其性。其為災異益可駭也。夫燮調陰陽者三公之職。天戒若曰陛下左右輔弼當得忠賢剛正之人為之。乃可以召至和之氣。消未萌之釁。不然何以妖星謫變也。旱曠炎冷也。地震祥異也。三者咎應察明如是之著耶。臣愚伏望陛下謹天之戒。應天以實。取天下公議。察明如是之著耶。臣愚伏望陛下謹天之戒。應天以實。取天下公議。

奏議卷之三百一

與天下瞻望之所謂賢人君子者。除之使居廟堂之上。責以三公四輔之事業。委注而仰成之。若然則陰陽以和。災異以消。朝廷清明。夷狄畏服。太平之風可翹足引領而待之也。臣朝夕思慮。載惟擇賢命相。繫國家休戚治亂之本。伏願陛下慎重之。然後發聖斷力行而不疑。則宗廟社稷之福。天下生靈之幸。

起居舍人知諫院范鎮上奏曰臣伏見去冬多南風。今春多西北風。乍寒乍暑。欲雨不雨。又有黑氣蔽日。此皆人事之所感動也。黑氣陰也。小人也。日陽也。君象也。黑氣蔽日者。陰侵陽。人惑君也。欲雨不雨者。政事不決也。陳執中為相。不病而家居者百日矣。陛下以御史之言。決一婢死而欲退。宰相為是。即乞速退。執中以解天意。以御史之言為非。亦乞勅執中起視事。無使天意久不決也。寒暑者賞罰也。乍寒乍暑者不當賞而賞。當罰而不罰也。鄧保吉有過於法。不當為

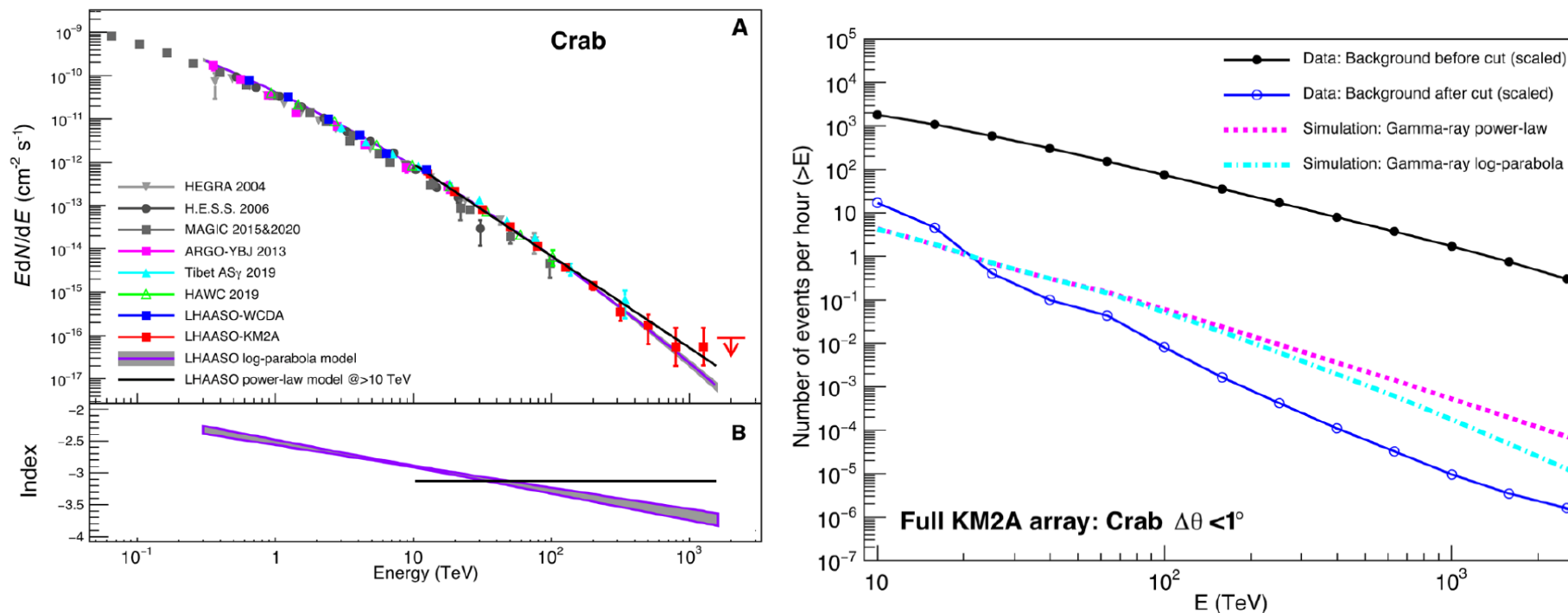
Cite as: The LHAASO Collaboration, *Science*  
10.1126/science.abg5137 (2021).

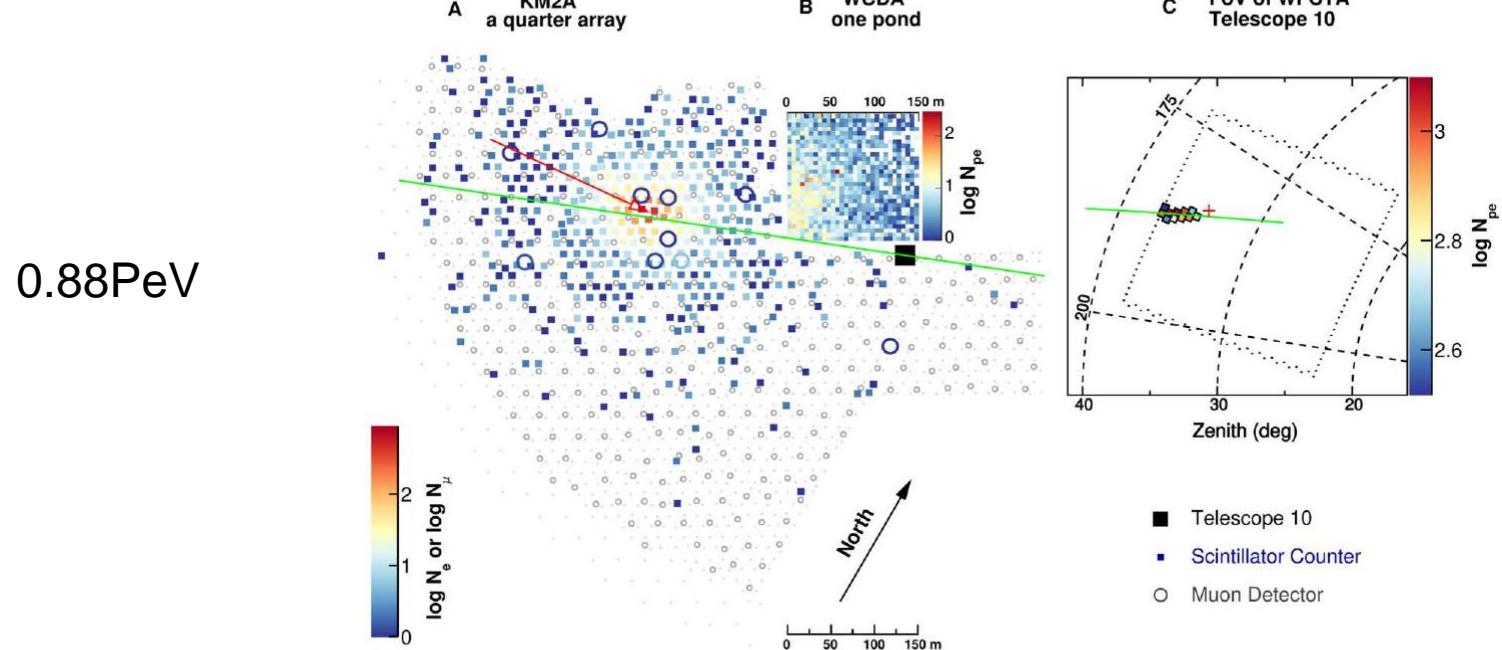
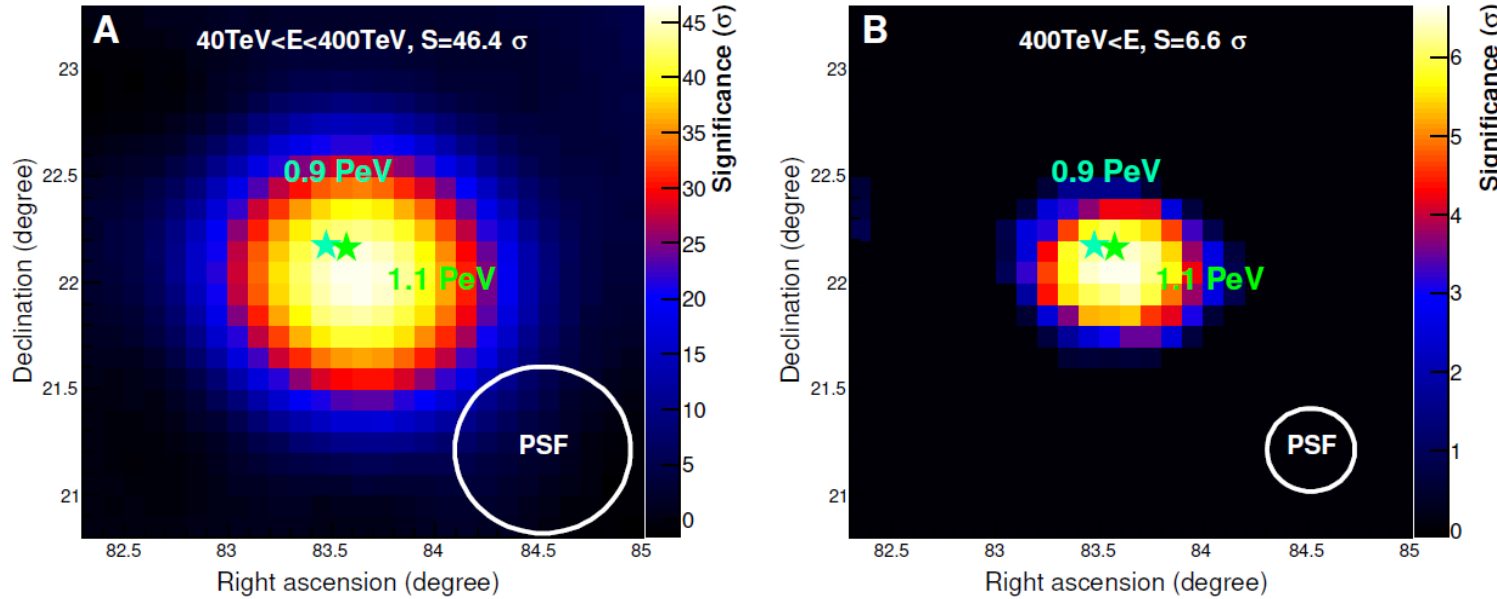
# PeV gamma-ray emission from the Crab Nebula

The LHAASO Collaboration\*†

\*Corresponding authors: Zhen Cao (caozh@ihep.ac.cn); S. Z. Chen (chensz@ihep.ac.cn); S. J. Lin (linsj6@mail.sysu.edu.cn); S. S. Zhang (zhangss@ihep.ac.cn); M. Zha (zham@ihep.ac.cn); Cong Li (licong@ihep.ac.cn); L. Y. Wang (wangly@ihep.ac.cn); L. Q. Yin (yinlq@ihep.ac.cn); F. Aharonian (felix.aharonian@mpi-hd.mpg.de); R. Y. Liu (ryliu@nju.edu.cn)

†The LHAASO Collaboration authors and affiliations are listed in the supplementary materials.



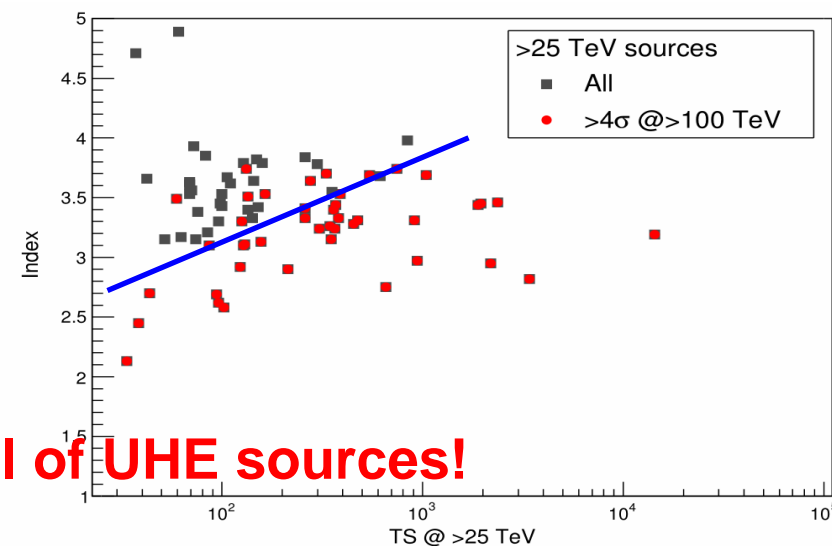
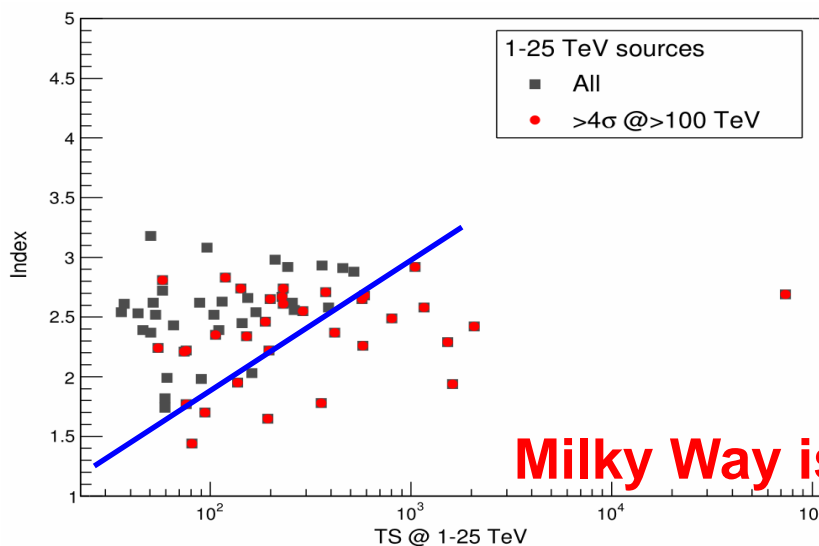


# 1<sup>st</sup> LHAASO source catalog

Source name	Components	$\alpha_{2000}$	$\delta_{2000}$	$\sigma_{p,95,stat}$	$r_{39}$	TS	$N_0$	$\Gamma$	TS <sub>100</sub>	Asso.(Sep.[°])
1LHAASO J0007+5659u	KM2A	1.86	57.00	0.12	<0.18	86.5	$0.33 \pm 0.05$	$3.10 \pm 0.20$	43.6	CTA 1 (0.12)
	WCDA						<0.27			
1LHAASO J0007+7303u	KM2A	1.91	73.07	0.07	$0.17 \pm 0.03$	361.0	$3.41 \pm 0.27$	$3.40 \pm 0.12$	171.6	CTA 1 (0.12)
	WCDA	1.48	73.15	0.10	<0.22	141.6	$5.01 \pm 1.11$	$2.74 \pm 0.11$		
1LHAASO J0056+6346u	KM2A	14.10	63.77	0.08	$0.24 \pm 0.03$	380.2	$1.47 \pm 0.10$	$3.33 \pm 0.10$	94.1	
	WCDA	13.78	63.96	0.15	$0.33 \pm 0.07$	106.1	$1.45 \pm 0.41$	$2.35 \pm 0.13$		
1LHAASO J0206+4302u	KM2A	31.70	43.05	0.13	<0.27	96.0	$0.24 \pm 0.03$	$2.62 \pm 0.16$	82.8	
	WCDA						<0.09			
1LHAASO J0212+4254u	KM2A	33.01	42.91	0.20	<0.31	38.4	$0.12 \pm 0.03$	$2.45 \pm 0.23$	30.2	
	WCDA						<0.07			
1LHAASO J0216+4237u	KM2A	34.10	42.63	0.10	<0.13	102.0	$0.18 \pm 0.03$	$2.58 \pm 0.17$	65.6	
	WCDA						<0.20			
1LHAASO J0249+6022	KM2A	42.39	60.37	0.16	$0.38 \pm 0.08$	148.8	$0.93 \pm 0.09$	$3.82 \pm 0.18$		LHAASO J0341+5258 (0.37)
	WCDA	41.52	60.49	0.40	$0.71 \pm 0.10$	53.3	$1.96 \pm 0.51$	$2.52 \pm 0.16$		
1LHAASO J0339+5307	KM2A	54.79	53.13	0.11	<0.22	144.0	$0.58 \pm 0.06$	$3.64 \pm 0.16$		LHAASO J0341+5258 (0.28)
	WCDA						<0.21			
1LHAASO J0343+5254u*	KM2A	55.79	52.91	0.08	$0.20 \pm 0.02$	388.1	$1.07 \pm 0.07$	$3.53 \pm 0.10$	20.2	LHAASO J0341+5258 (0.28)
	WCDA	55.34	53.05	0.18	$0.33 \pm 0.05$	94.1	$0.29 \pm 0.13$	$1.70 \pm 0.19$		

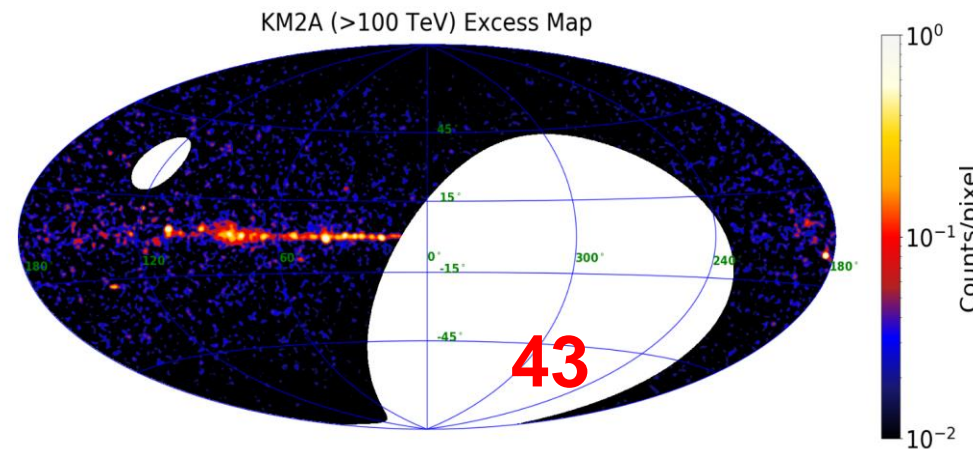
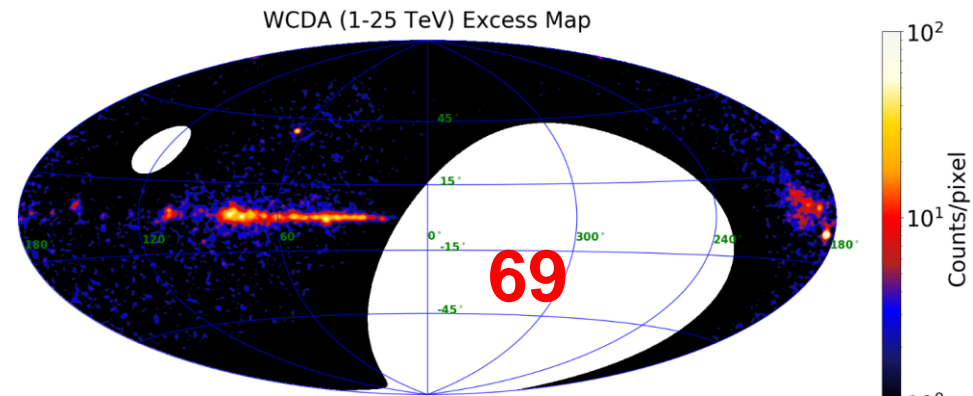
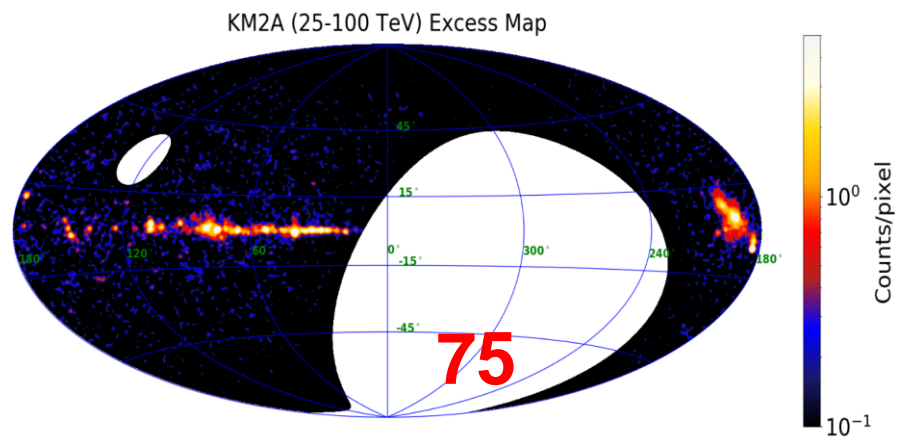
# PeVatrons

- 51% (35/69) 1-25TeV sources are UHE sources.
- 57% (43/75) >25TeV sources are UHE sources.
- 19% (8/43) UHE sources are not detected at 1-25TeV (**new class?**).

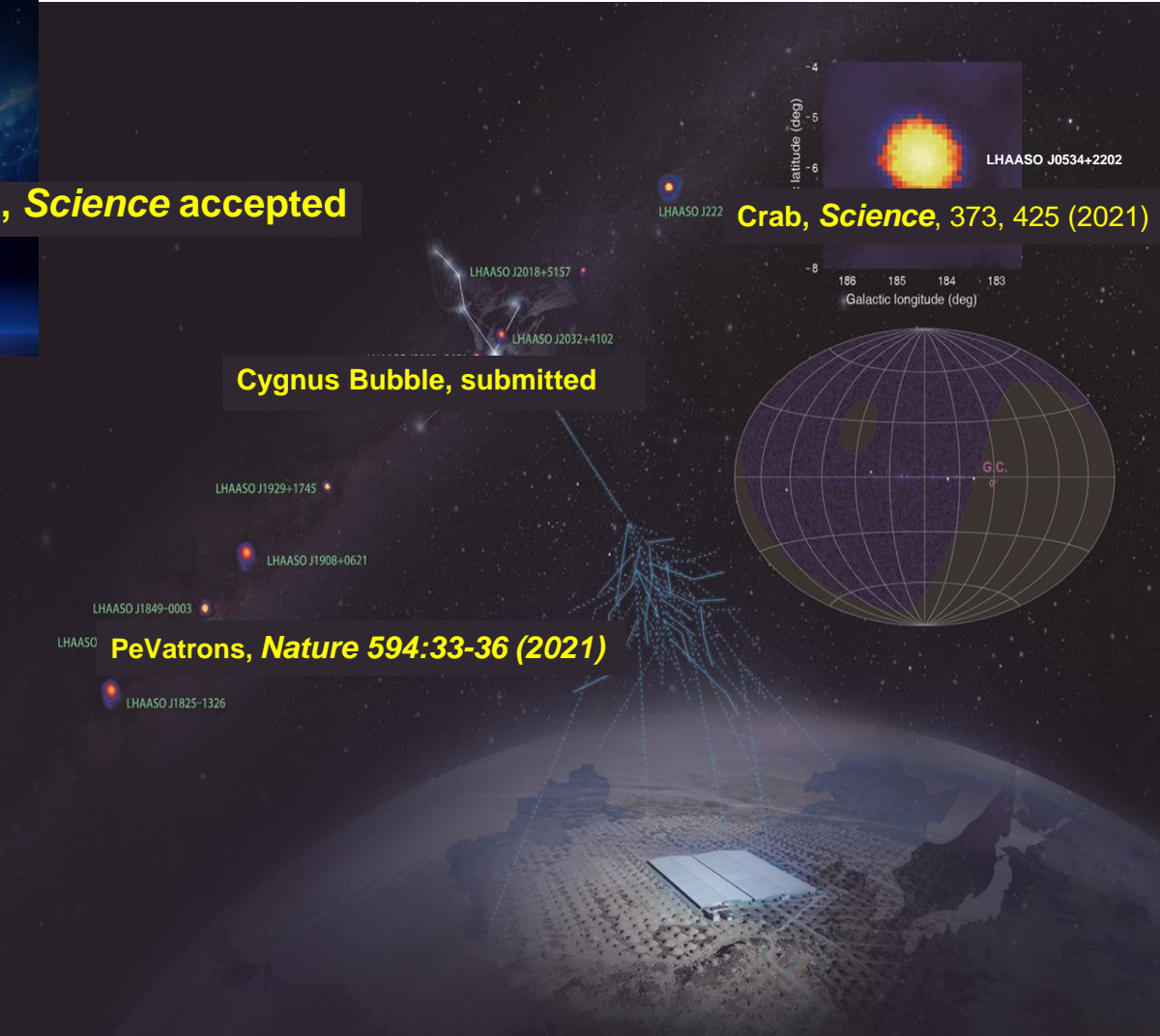


# LHAASO catalog

- **90 in 1<sup>st</sup> LHAASO sources.**
- **32 new discoveries**
- **43 UHE**

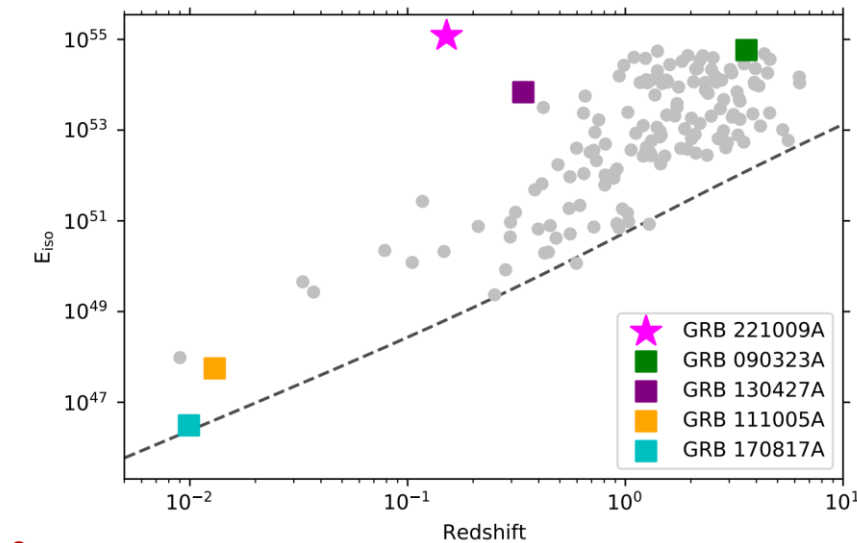
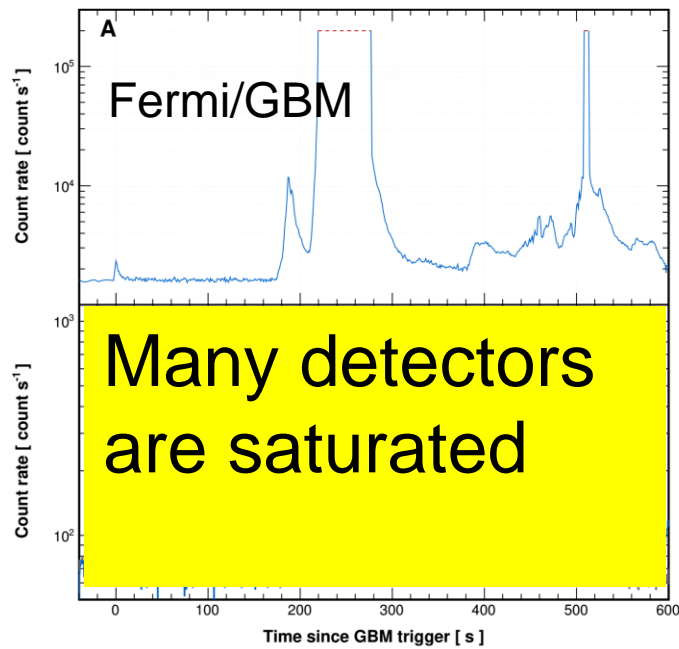


# Discovery Highlights



# GRB 221009A: brightest-of-all-time (BOAT) GRB

- Triggered on a weak precursor
- Fluence:  $>5\text{e-}2 \text{ erg/cm}^2$ , low redshift ( $z=0.151$ )
- deriving an enormous energy  $E_{\gamma,\text{iso}} \sim 10^{55} \text{ erg}$

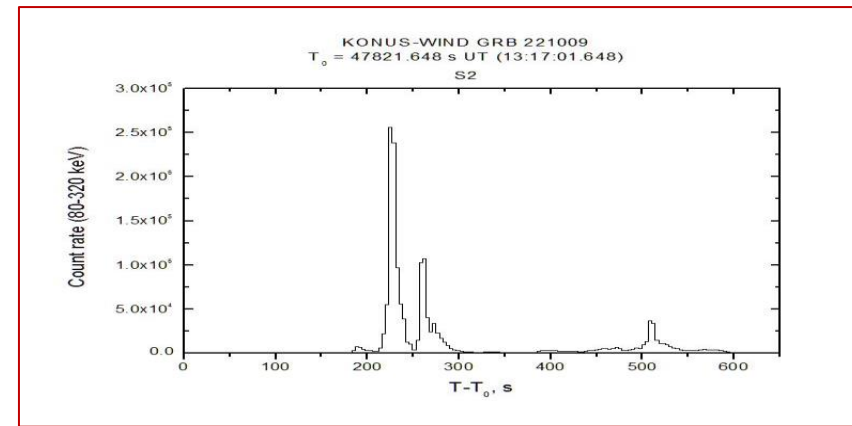
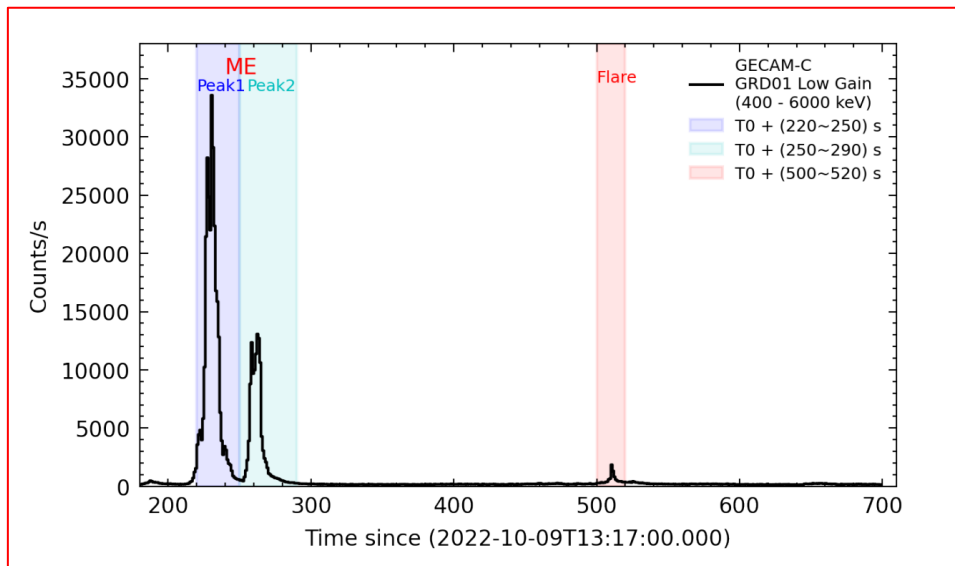


$R < 10^{-3} \text{ yr}$

$R_{\text{GRB}} \leq 6.1 \times 10^{-4} \text{ Gpc}^{-3} \text{ yr}^{-1}$

$z = 0.151$  volume  $\sim 1 \text{ Gpc}^3$

# GECAM/Konus-Wind Observations of GRB 221009A



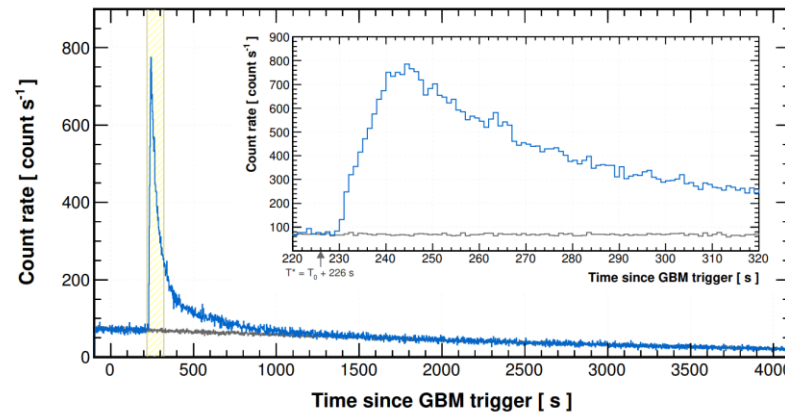
E<sub>iso</sub>~  $1.5 \times 10^{55}$  erg

Main peak 1 lasts ~10 s

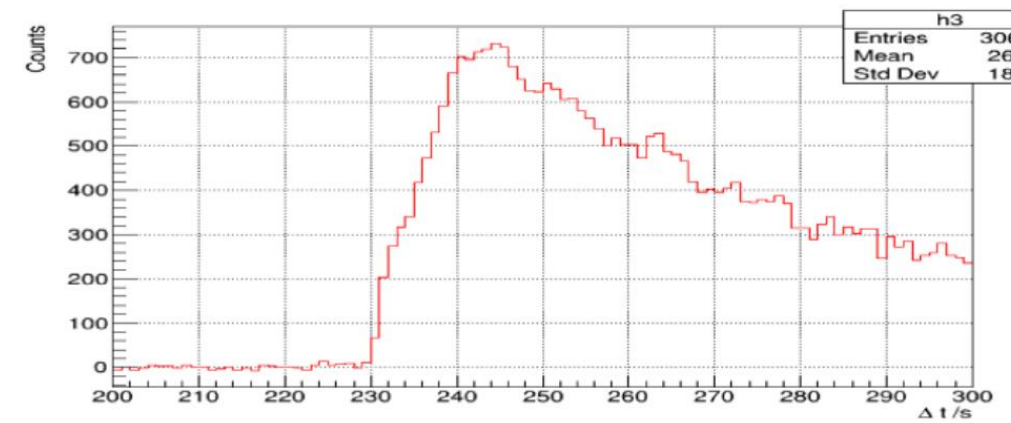
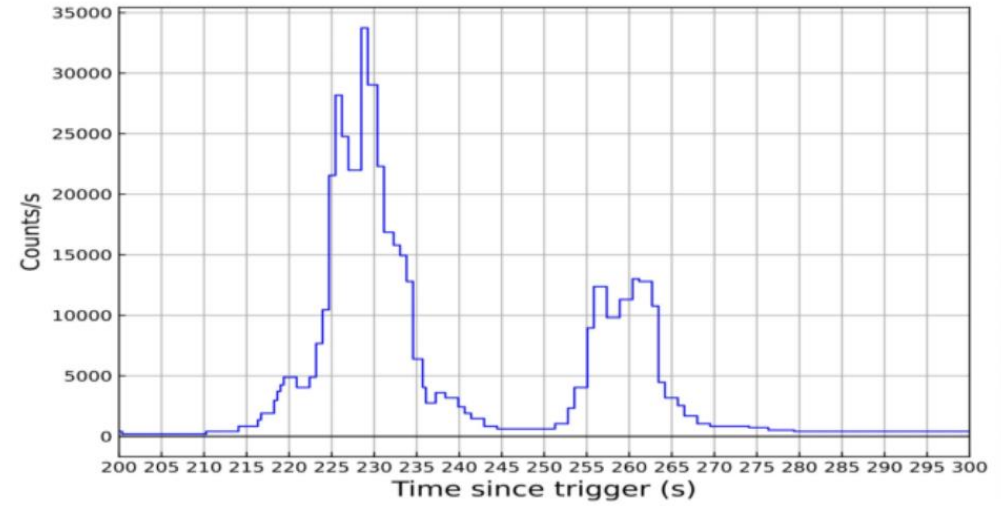
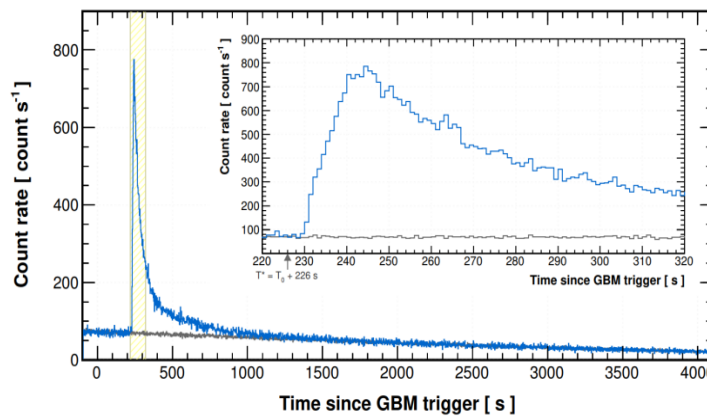
## LHAASO GRB221009A

- LHAASO detection of GRB 221009A: first GRB seen by a extensive air shower detector
- High statistics: >60,000 photons above 0.2TeV (LHAASO-WCDA)
- TeV count rate light curve:  
Smooth temporal profile –  
**external shock origin**

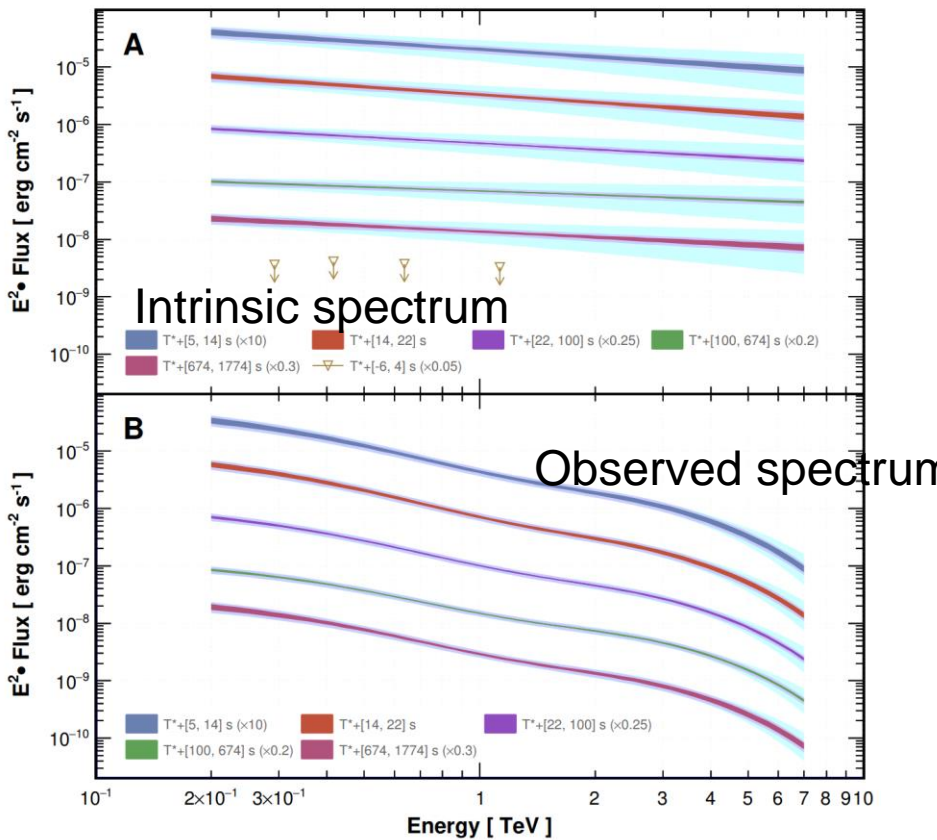
First time detection of the TeV afterglow onset !



# MeV vs TeV light curves: external shock origin



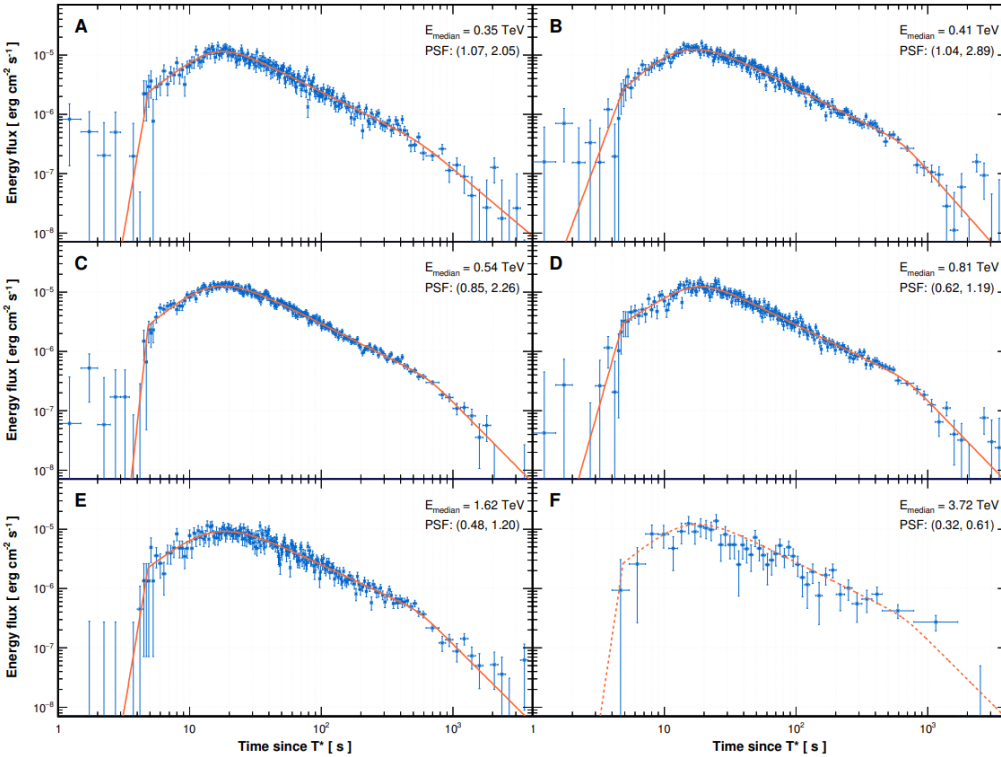
## SED measured by LHAASO-WCDA



- EBL model: A. Saldana-Lopez et al. (2021)

Time interval (seconds after $T_0$ )	$A$ ( $10^{-8} \text{ TeV}^{-1} \text{ cm}^{-2} \text{ s}^{-1}$ )	$\gamma$	$E_{\text{cut}}$ TeV	$\chi^2/\text{dof}$
Observed spectrum				
231–240	$42.9 \pm 2.7$	$2.983 \pm 0.061$	3.14 (fixed)	4.6/6
240–248	$70.1 \pm 3.8$	$3.006 \pm 0.052$	3.14 (fixed)	8.0/6
248–326	$39.9 \pm 1.0$	$2.911 \pm 0.028$	3.14 (fixed)	14.8/6
326–900	$7.35 \pm 0.16$	$2.788 \pm 0.026$	3.14 (fixed)	8.9/6
900–2000	$0.959 \pm 0.043$	$2.880 \pm 0.067$	3.14 (fixed)	2.9/5
Intrinsic spectrum, standard EBL				
231–240	$127.3 \pm 7.9$	$2.429 \pm 0.062$	＼	3.1/6
240–248	$208 \pm 11$	$2.455 \pm 0.054$	＼	6.5/6
248–326	$117.8 \pm 3.0$	$2.359 \pm 0.028$	＼	8.7/6
326–900	$21.77 \pm 0.47$	$2.231 \pm 0.026$	＼	3.4/6
900–2000	$2.84 \pm 0.13$	$2.324 \pm 0.065$	＼	2.2/5

# Fast decay phase



$$\alpha_3 = -2.21^{+0.30}_{-0.83}$$

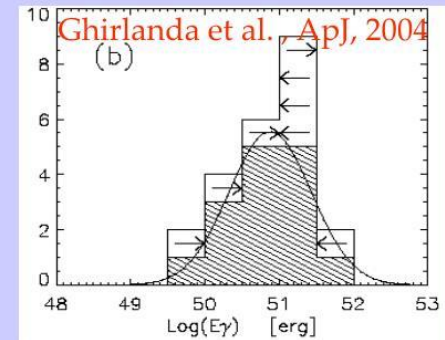
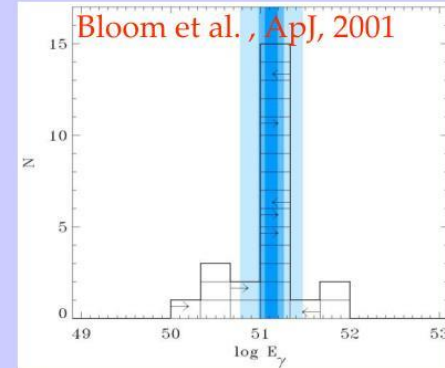
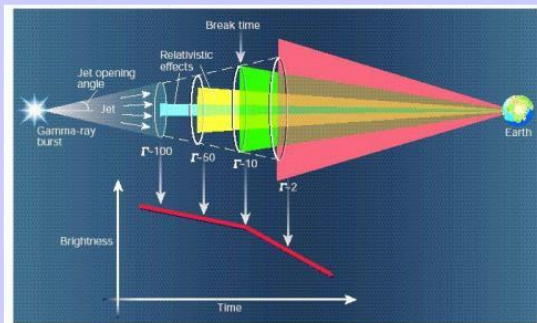
$$T_{b,2} = T^* + 670^{+230}_{-110} \text{ s}$$

Revealing a jet break at the earliest time.

## A narrow GRB jet

- Jet breaks have been seen in optical/X-ray bands
- First time seeing a jet break at TeV band
- Helps to understand the total energy of the GRB

➤ assuming jet angles derived from the break time of the optical afterglow light curve, the collimation-corrected radiated energy is clustered around  $\sim 10^{51}$  erg.

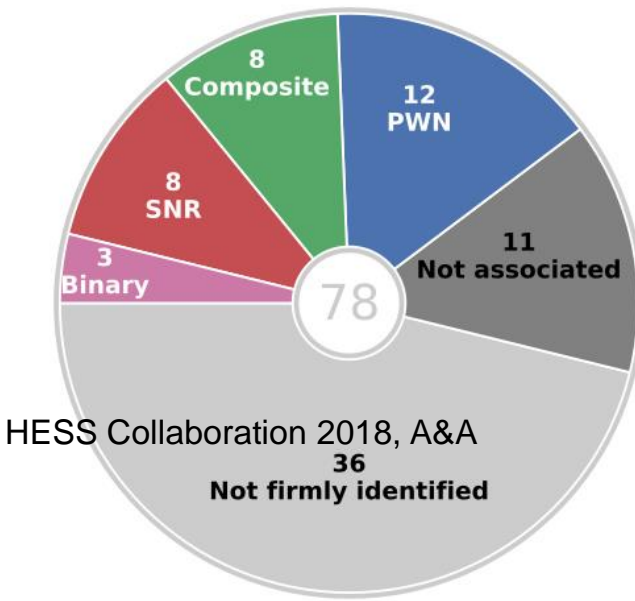


$$\theta_0 \sim 0.6^\circ E_{k,55}^{-1/8} n_0^{1/8} \left( \frac{t_{b,2}}{670 \text{ s}} \right)^{3/8}$$

$E_{\gamma,j} = E_{\gamma,\text{iso}} \theta_0^2 / 2 \sim 7.5 \times 10^{50} \text{ erg} E_{\gamma,\text{iso},55} (\theta_0 / 0.7^\circ)^2$

# Pulsars as Counterparts of VHE gamma-ray sources

Pulsars – the most commonly potential counterparts of detected VHE gamma-ray emitter



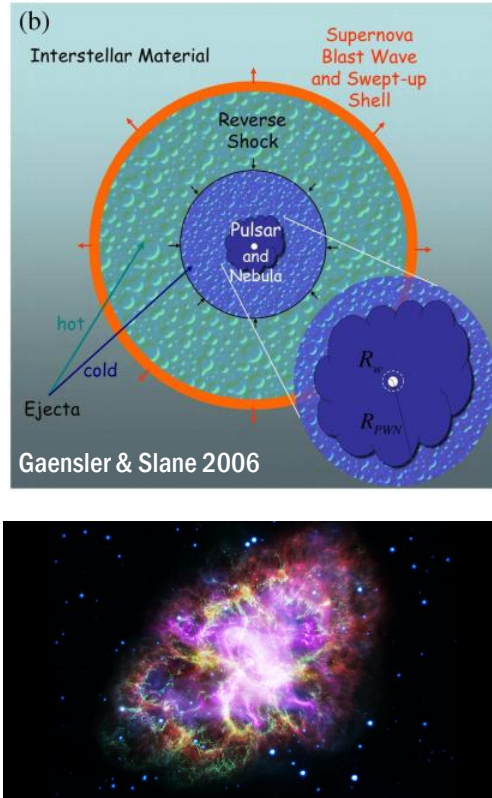
Among the 47 sources not yet identified, most of them (36) have possible associations with cataloged objects, notably PWNe and energetic pulsars that could power VHE PWN. — HGPS

## 14 firmly identified PWN by HESS

HGPS name	ATNF name	Canonical name	$\lg \dot{E}$	$\tau_c$ (kyr)	$d$ (kpc)	PSR offset (pc)	$\Gamma$	$R_{\text{PWN}}$ (pc)	$L_{1-10\text{TeV}}$ ( $10^{33} \text{ erg s}^{-1}$ )
J1813–178 <sup>1</sup>	J1813–1749		37.75	5.60	4.70	<2	2.07 ± 0.05	4.0 ± 0.3	19.0 ± 1.5
J1833–105	J1833–1034	G21.5–0.9 <sup>2</sup>	37.53	4.85	4.10	<2	2.42 ± 0.19	<4	2.6 ± 0.5
J1514–591	B1509–58	MSH 15–52 <sup>3</sup>	37.23	1.56	4.40	<4	2.26 ± 0.03	11.1 ± 2.0	52.1 ± 1.8
J1930+188	J1930+1852	G54.1+0.3 <sup>4</sup>	37.08	2.89	7.00	<10	2.6 ± 0.3	<9	5.5 ± 1.8
J1420–607	J1420–6048	Kookaburra (K2) <sup>5</sup>	37.00	13.0	5.61	5.1 ± 1.2	2.20 ± 0.05	7.9 ± 0.6	44 ± 3
J1849–000	J1849–0001	IGR J18490–0000 <sup>6</sup>	36.99	42.9	7.00	<10	1.97 ± 0.09	11.0 ± 1.9	12 ± 2
J1846–029	J1846–0258	Kes 75 <sup>7</sup>	36.91	0.728	5.80	<2	2.41 ± 0.09	<3	6.0 ± 0.7
J0835–455	B0833–45	Vela X <sup>7</sup>	36.84	11.3	0.280	2.37 ± 0.18	1.89 ± 0.03	2.9 ± 0.3	0.83 ± 0.11 <sup>*</sup>
J1837–069 <sup>8</sup>	J1838–0655		36.74	22.7	6.60	17 ± 3	2.54 ± 0.04	41 ± 4	204 ± 8
J1418–609	J1418–6058	Kookaburra (Rabbit) <sup>5</sup>	36.69	10.3	5.00	7.3 ± 1.5	2.26 ± 0.05	9.4 ± 0.9	31 ± 3
J1356–645 <sup>9</sup>	J1357–6429		36.49	7.31	2.50	5.5 ± 1.4	2.20 ± 0.08	10.1 ± 0.9	14.7 ± 1.4
J1825–137 <sup>10</sup>	B1823–13		36.45	21.4	3.93	33 ± 6	2.38 ± 0.03	32 ± 2	116 ± 4
J1119–614	J1119–6127	G292.2–0.5 <sup>11</sup>	36.36	1.61	8.40	<11	2.64 ± 0.12	14 ± 2	23 ± 4
J1303–631 <sup>12</sup>	J1301–6305		36.23	11.0	6.65	20.5 ± 1.8	2.33 ± 0.02	20.6 ± 1.7	96 ± 5

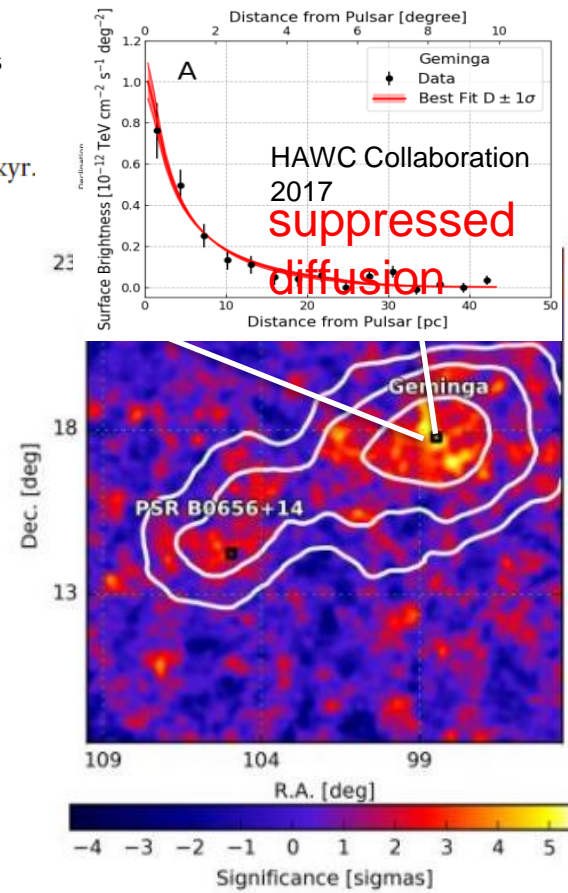
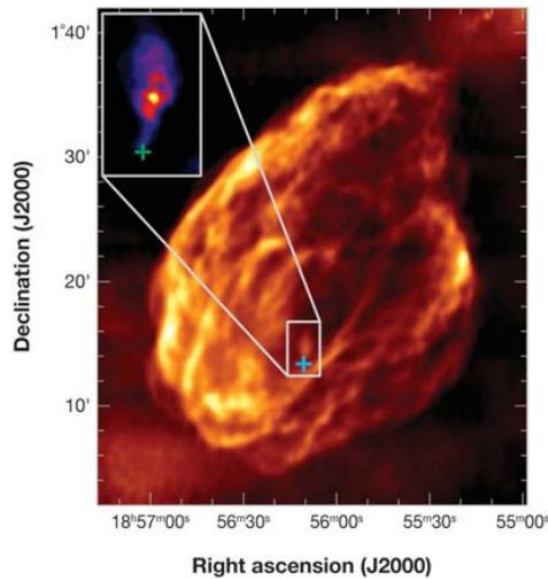
We have presented the third catalog of steady gamma-ray emitters detected by HAWC using 1523 days of data. The catalog consists of 65 sources, including two blazars. The most abundant source class among the potential counterpart of HAWC sources in the Galactic plane is pulsars (56). — 3HWC (HAWC Collaboration 2020, ApJ)

# From PWN to Pulsar Halos

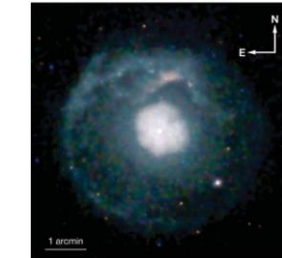
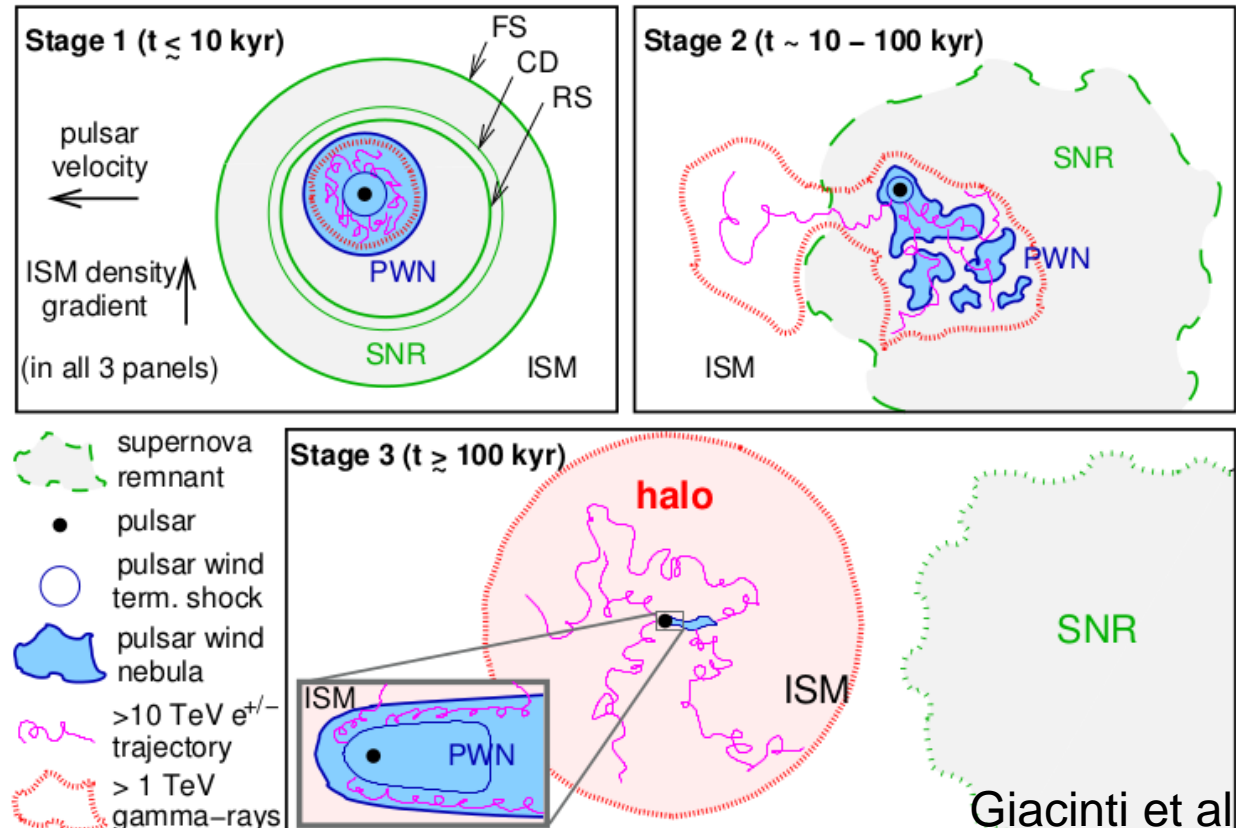


Conservation of Momentum: Natal kick velocity: 400-500 km/s

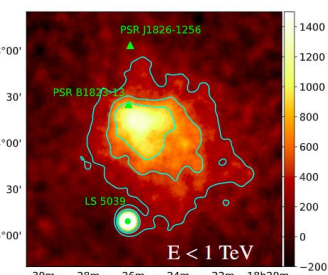
$$t_{cross} = 44 \left( \frac{E_{SN}}{10^{51} \text{ ergs}} \right)^{1/3} \left( \frac{n_0}{1 \text{ cm}^{-3}} \right)^{-1/3} \left( \frac{V_{PSR}}{500 \text{ km s}^{-1}} \right)^{-5/3} \text{ kyr.}$$



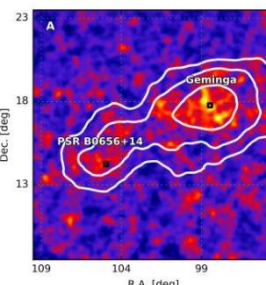
# Three Evolution Stages



SNR G21.5-0.9  
PSR J1833-1034

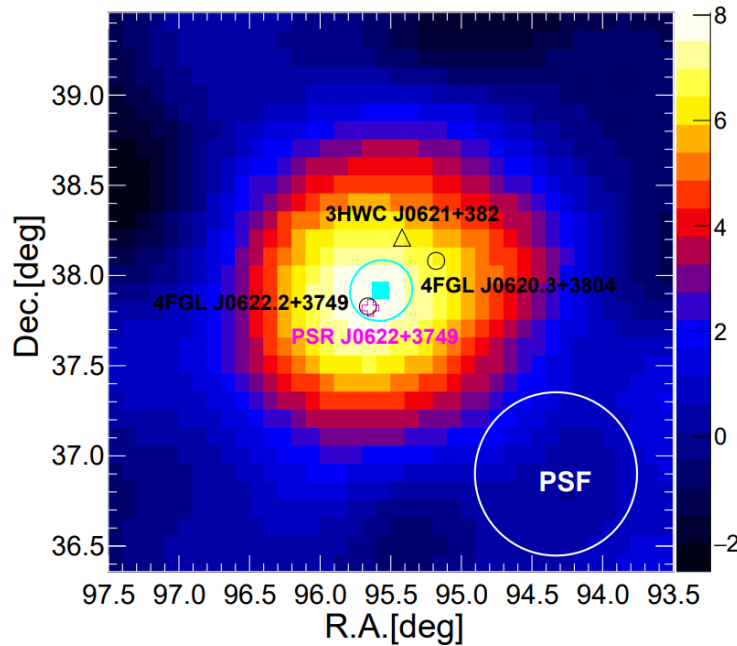


HESS J1825-137  
PSR J1826-1334



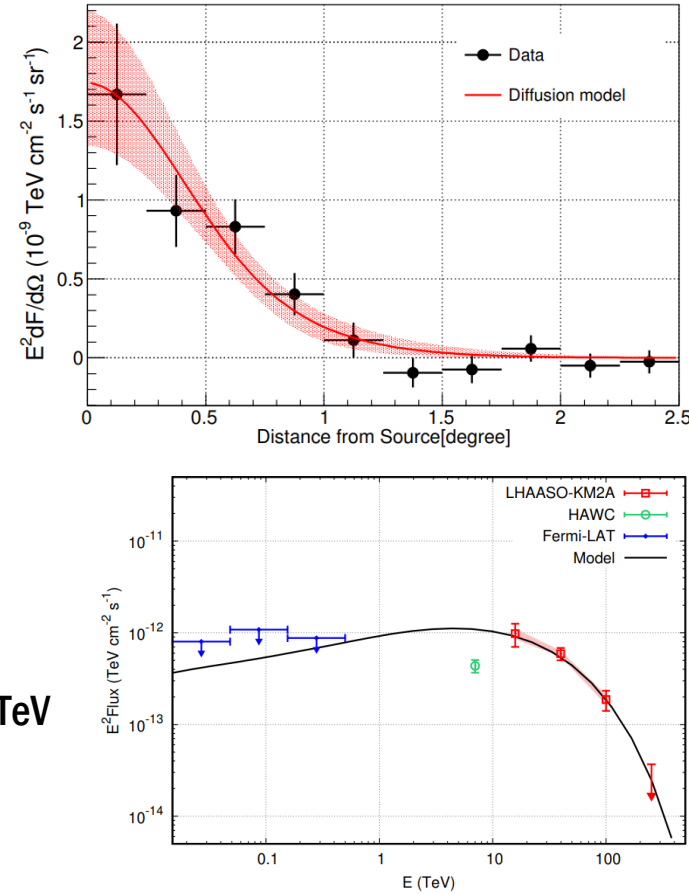
Geminga  
Monogem

# LHAASO J0621+3755



$$D \approx (8.9^{+4.5}_{-3.9}) \times 10^{27} (d/1.6 \text{ kpc})^2 \text{ cm}^2 \text{s}^{-1} \text{ for } E_e \sim 160 \text{ TeV}$$

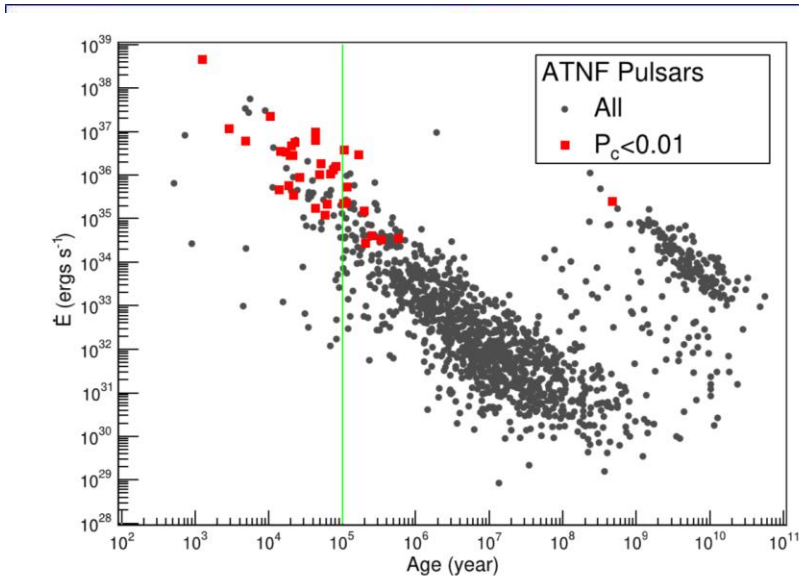
LHAASO Collaboration 2021, PRL



## 1LHAASO Catalogue

**35** sources associated with pulsars with  $\dot{E} > 10^{34}$ erg/s at a chance probablity  $<1\%$  (65 have  $\geq 1$  pulsar within 0.5 deg)

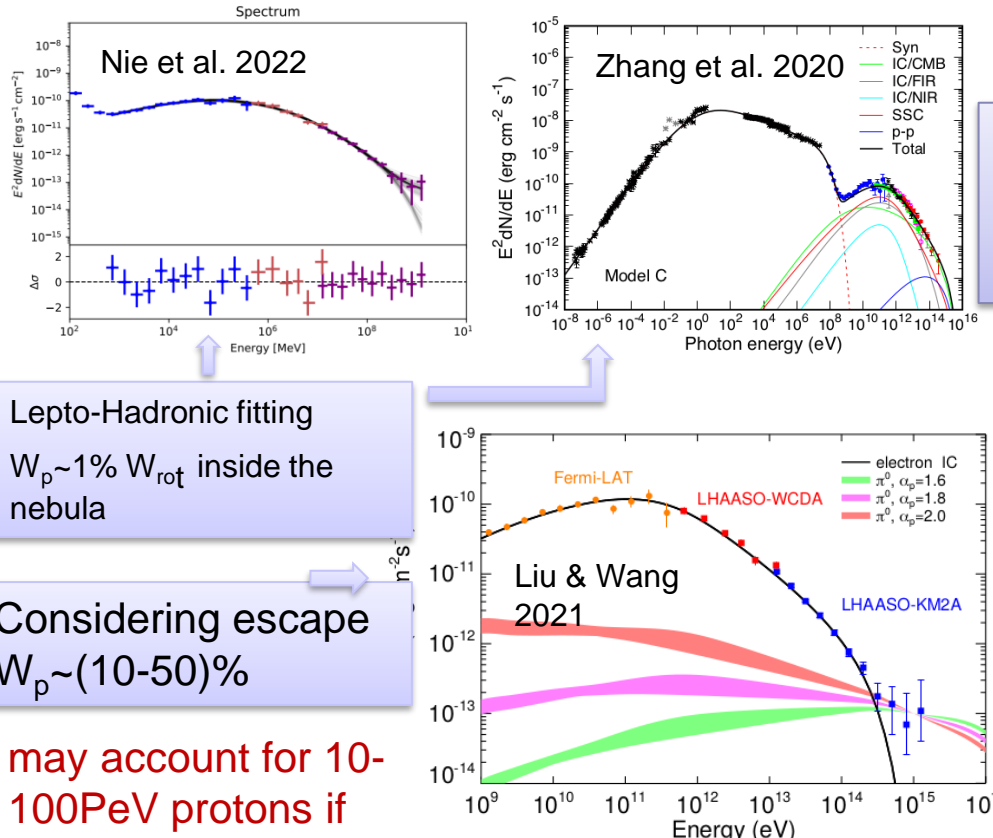
Source name	PSR name	dist.(°)	Distance (kpc)	$\tau_c$ (kyr)	$\dot{E}$ (ergs/s)	$P_c$	Identified type in TeVCat
1LHAASO J0007+7303u	PSR J0007+7303	0.05	1.40	14	4.5e+35	7.3e-05	PWN
1LHAASO J0216+4237u	PSR J0218+4232	0.33	3.15	476000	2.4e+35	3.6e-03	
1LHAASO J0249+6022	PSR J0248+6021	0.16	2.00	62	2.1e+35	1.5e-03	
1LHAASO J0359+5406	PSR J0359+5414	0.15	-	75	1.3e+36	7.2e-04	
1LHAASO J0534+2200u	PSR J0534+2200	0.01	2.00	1	4.5e+38	3.2e-06	PWN
1LHAASO J0542+2311u	PSR J0543+2329	0.30	1.56	253	4.1e+34	8.3e-03	
1LHAASO J0622+3754	PSR J0622+3749	0.09	-	208	2.7e+34	2.5e-04	PWN/TeV Halo
1LHAASO J0631+1037	PSR J0631+1037	0.11	2.10	44	1.7e+35	3.5e-04	PWN
1LHAASO J0634+1741u	PSR J0633+1746	0.12	0.19	342	3.3e+34	1.3e-03	PWN/Halo
1LHAASO J0635+0619	PSR J0633+0632	0.39	1.35	59	1.2e+35	9.4e-03	
1LHAASO J1740+0948u	PSR J1740+1000	0.21	1.23	114	2.3e+35	1.4e-03	
1LHAASO J1809-1918u	PSR J1809-1917	0.05	3.27	51	1.8e+36	6.2e-04	
1LHAASO J1813-1245	PSR J1813-1245	0.01	2.63	43	6.2e+36	6.3e-06	
1LHAASO J1825-1256u	PSR J1826-1256	0.09	1.55	14	3.6e+36	1.6e-03	
1LHAASO J1825-1337u	PSR J1826-1334	0.11	3.61	21	2.8e+36	2.8e-03	PWN/TeV Halo
1LHAASO J1837-0654u	PSR J1838-0654	0.12	6.60	23	5.6e+36	2.2e-03	PWN
1LHAASO J1839-0548u	PSR J1838-0537	0.20	-	5	6.0e+36	6.1e-03	
1LHAASO J1848-0001u	PSR J1849-0001	0.06	-	43	9.8e+36	1.2e-04	PWN
1LHAASO J1857+0245	PSR J1856+0245	0.16	6.32	21	4.6e+36	3.1e-03	PWN
1LHAASO J1906+0712	PSR J1906+0722	0.19	-	49	1.0e+36	5.9e-03	
1LHAASO J1908+0615u	PSR J1907+0602	0.23	2.37	20	2.8e+36	6.8e-03	
1LHAASO J1912+1014u	PSR J1913+1011	0.13	4.61	169	2.9e+36	1.5e-03	
1LHAASO J1914+1150u	PSR J1915+1150	0.09	14.01	116	5.4e+35	1.8e-03	
1LHAASO J1928+1746u	PSR J1928+1746	0.04	4.34	83	1.6e+36	1.6e-04	
1LHAASO J1929+1846u	PSR J1930+1852	0.29	7.00	3	1.2e+37	2.6e-03	PWN
1LHAASO J1954+2836u	PSR J1954+2836	0.01	1.96	69	1.1e+36	1.6e-05	PWN
1LHAASO J1954+3253	PSR J1952+3252	0.33	3.00	107	3.7e+36	6.7e-03	
1LHAASO J1959+2846u	PSR J1958+2845	0.10	1.95	22	3.4e+35	2.8e-03	PWN
1LHAASO J2005+3415	PSR J2004+3429	0.25	10.78	18	5.8e+35	9.9e-03	
1LHAASO J2005+3050	PSR J2006+3102	0.20	6.04	104	2.2e+35	9.2e-03	
1LHAASO J2020+3649u	PSR J2021+3651	0.05	1.80	17	3.4e+36	1.5e-04	PWN
1LHAASO J2028+3352	PSR J2028+3332	0.36	-	576	3.5e+34	8.0e-03	
1LHAASO J2031+4127u	PSR J2032+4127	0.08	1.33	201	1.5e+35	1.0e-03	PWN
1LHAASO J2228+6100u	PSR J2229+6114	0.27	3.00	10	2.2e+37	2.2e-03	PWN
1LHAASO J2238+5900	PSR J2238+5903	0.07	2.83	27	8.9e+35	3.0e-04	



$$P_c = 1 - e^{r^2/r_0^2} \quad r_0 = [\pi \rho(\dot{E})]^{-1/2}$$

$$|\mathbf{b} - \mathbf{b}_c| < 2.5^\circ \text{ & } |\mathbf{l} - \mathbf{l}_c| < 10^\circ$$

# Crab: PWN as a Super-PeVatron of protons?



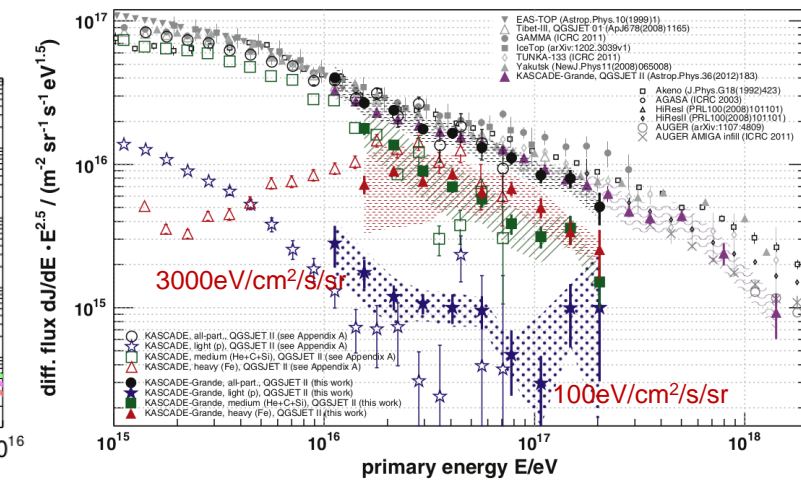
may account for 10-100PeV protons if each pulsars can accelerate protons >10PeV when they were young

Estimation  
with a  
leaky box  
model

$$F(E_p) = \frac{c}{4\pi} \frac{\eta_p L_{s,tot} t_{esc}}{2\pi R_{Gal}^2 H_{CR} \ln(E_{p,max}/E_{p,min})}$$

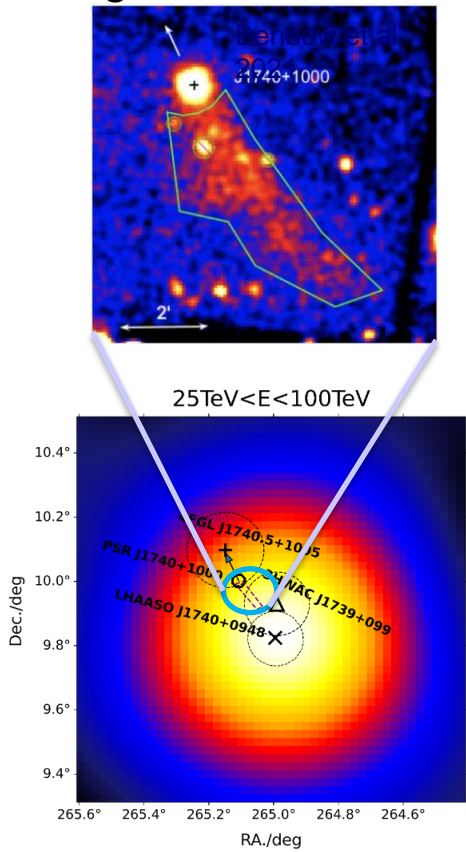
$$\approx 2 \times 10^3 \left( \frac{f_{pul} \eta_p L_{s,tot}}{10^{39} \text{ erg s}^{-1}} \right) \left( \frac{E_p}{10 \text{ PeV}} \right)^{-1/3}$$

$$\times \left( \frac{H_{CR}}{4 \text{ kpc}} \right) \left( \frac{R_{Gal}}{15 \text{ kpc}} \right)^{-2} \text{ eV cm}^{-2} \text{s}^{-1} \text{sr}^{-1}$$

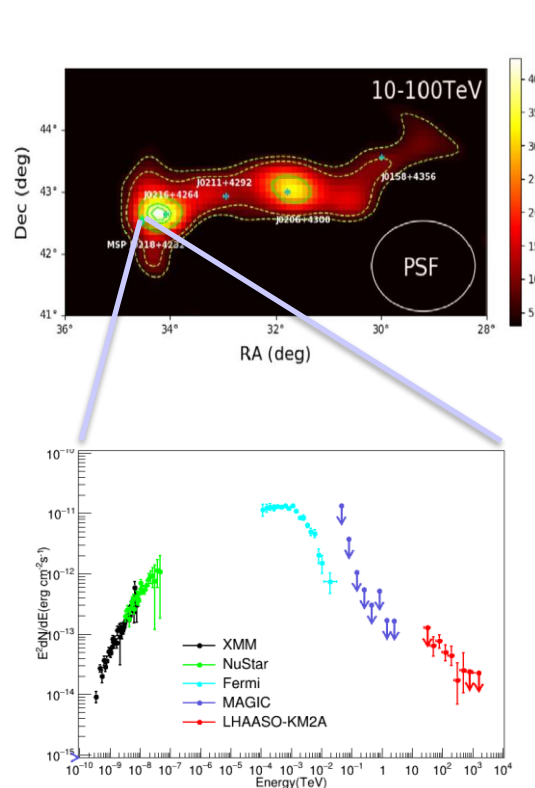


# Highlight Talks in PWN/Pulsar Halos by LHAASO

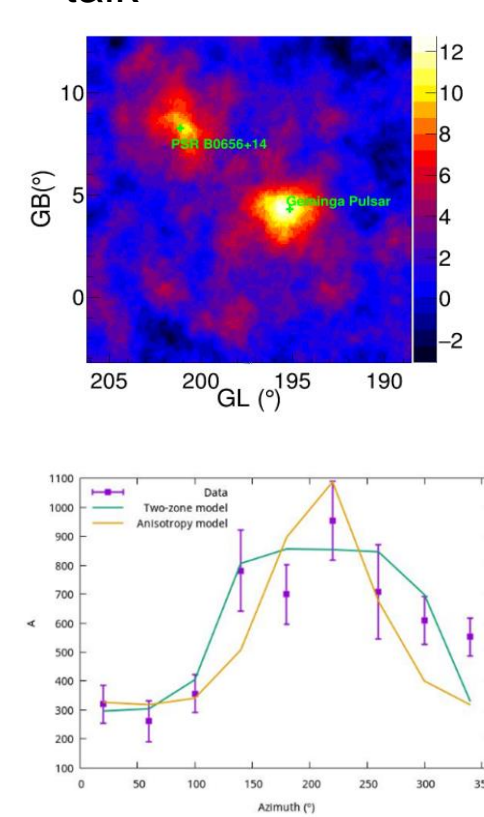
Renfeng Xu's talk



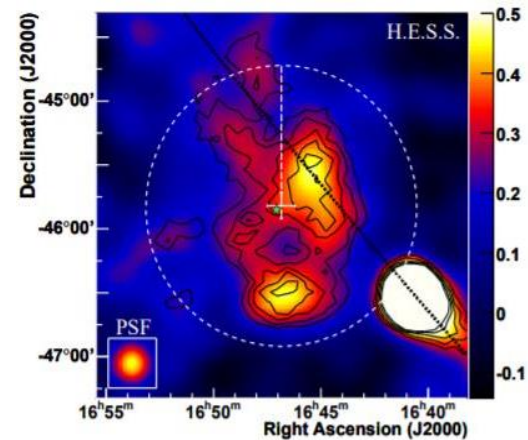
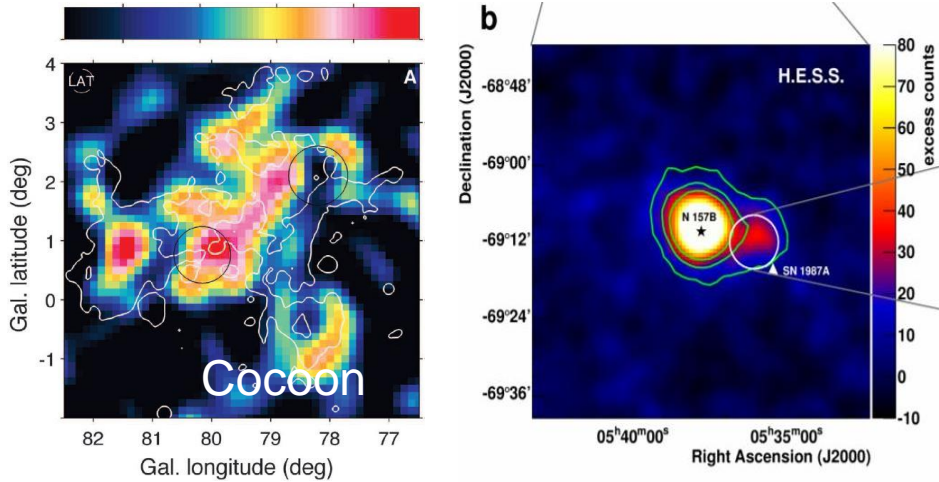
Dr. Zhe Li's talk



Dr. Yingying Guo's talk



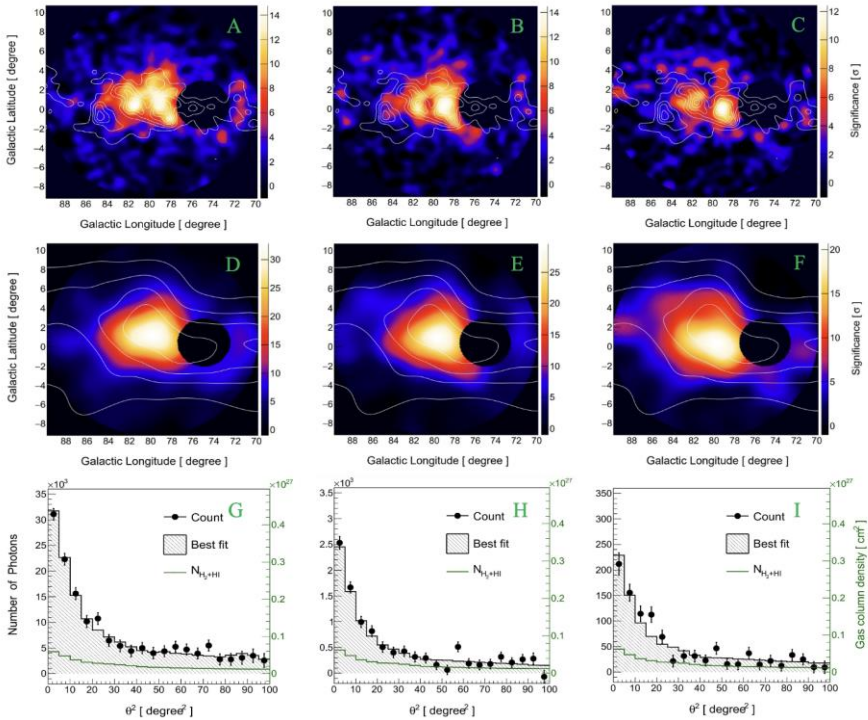
# Gamma-ray emitting YMSc



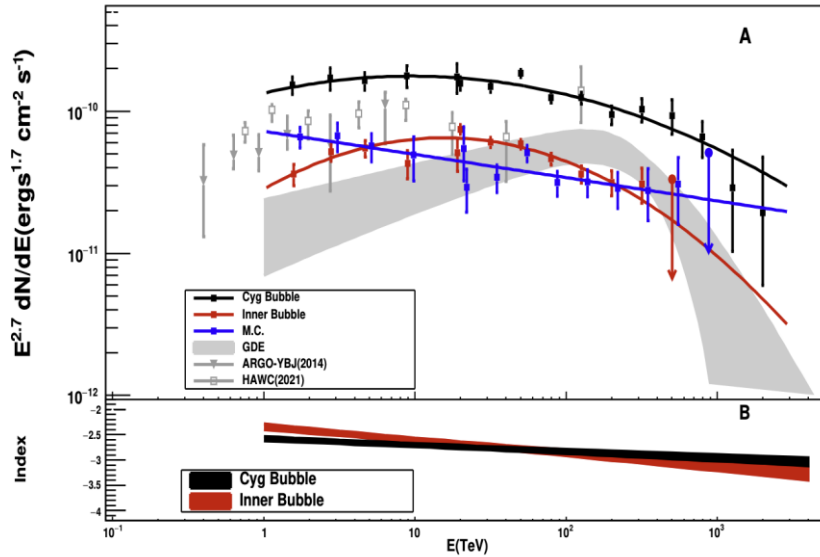
New GAMMA-RAY  
Source population:

Cygnus Cocoon(GeV-  
TeV)[Fermi 2012,  
HAWC2022]  
Westerlund 1 (TeV)  
[HESS collaboration]

# LHAASO VIEW ON CYGNUS

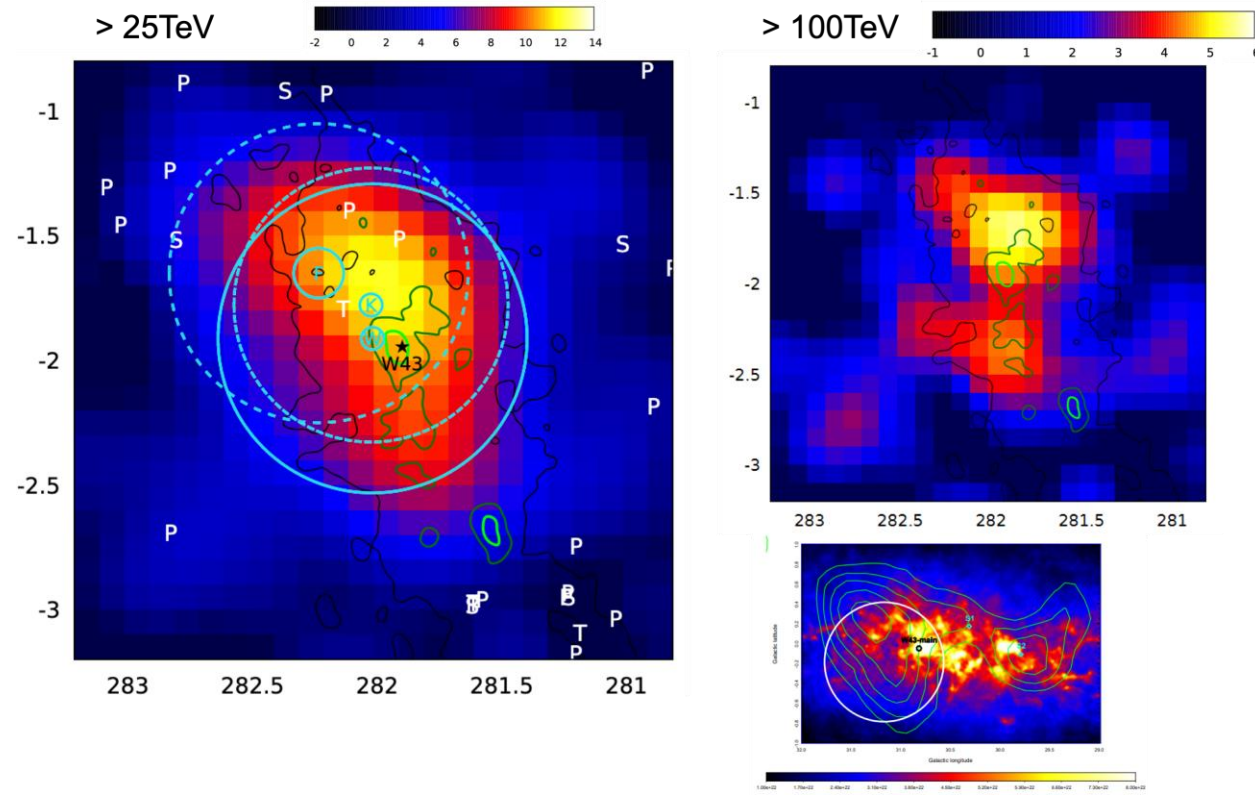


Huge bubble beyond ~10 degrees (200 pc)



Curved and uniform spectral shape  
 inner bubble:  $r \sim 3$  degrees, similar to “cocoon”  
 cygnus bubble:  $r \sim 10$  degrees

# LHAASO view on w43



- UHE gamma-ray emission reveal good correlation with dense gas
- Spectrum up to PeV